UNITED STATES DEPARTMENT OF COMMERCE

ALEXANDER B. TROWBRIDGE, *Secretary*,

NATIONAL BUREAU OF STANDARDS · A. V. ASTIN, *Director*

Hydrogenation of Ethylene on Metallic Catalysts

Juro Horiuti* and Koshiro Miyahara*

Hokkaido University
Sapporo, Japan

*Prepared under contract at the
Hokaido University
Sapporo, Japan

NSRDS–NBS 13
National Standard Reference Data Series-
National Bureau of Standards 13
(Category 6 — Chemical Kinetics)

Issued

**For Sale by the Superintendent of Documents, U.S. Government Printing Office
Washington, D.C. 20402–Price $1.00**

Foreword

The National Standard Reference Data System is a Government-wide effort to provide for the technical community of the United States effective access to the quantitative data of physical science, critically evaluated and compiled for convenience, and readily accessible through a variety of distribution channels. The System was established in 1963 by action of the President's Office of Science and Technology and the Federal Council for Science and Technology.

The responsibility to administer the System was assigned to the National Bureau of Standards and an Office of Standard Reference Data was set up at the Bureau for this purpose. Since 1963, this Office has developed systematic plans for meeting high-priority needs for reliable reference data. It has undertaken to coordinate and integrate existing data evaluation and compilation activities (primarily those under sponsorship of Federal agencies) into a comprehensive program, supplementing and expanding technical coverage when necessary, establishing and maintaining standards for the output of the participating groups, and providing mechanisms for the dissemination of the output as required.

The System now comprises a complex of data centers and other activities, carried on in Government agencies, academic institutions, and nongovernmental laboratories. The independent operational status of existing critical data projects is maintained and encouraged. Data centers that are components of the NSRDS produce compilations of critically evaluated data, critical reviews of the state of quantitative knowledge in specialized areas, and computations of useful functions derived from standard reference data. In addition, the centers and projects establish criteria for evaluation and compilation of data and make recommendations on needed modifications or extensions of experimental techniques.

Data publications of the NSRDS take a variety of physical forms, including books, pamphlets, loose-leaf sheets and computer tapes. While most of the compilations have been issued by the Government Printing Office, several have appeared in scientific journals. Under some circumstances, private publishing houses are regarded as appropriate primary dissemination mechanisms.

The technical scope of the NSRDS is indicated by the principal categories of data compilation projects now active or being planned: nuclear properties, atomic and molecular properties, solid state properties, thermodynamic and transport properties, chemical kinetics, colloid and surface properties, and mechanical properties.

An important aspect of the NSRDS is the advice and planning assistance which the National Research Council of the National Academy of Sciences-National Academy of Engineering provides. These services are organized under an overall Review Committee which considers the program as a whole and makes recommendations on policy, long-term planning, and international collaboration. Advisory Panels, each concerned with a single technical area, meet regularly to examine major portions of the program, assign relative priorities, and identify specific key problems in need of further attention. For selected specific topics, the Advisory Panels sponsor subpanels which make detailed studies of users' needs, the present state of knowledge, and existing data resources as a basis for recommending one or more data compilation activities. This assembly of advisory services contributes greatly to the guidance of NSRDS activities.

The NSRDS–NBS series of publications is intended primarily to include evaluated reference data and critical reviews of long-term interest to the scientific and technical community.

A. V. ASTIN, *Director.*

Contents

Hydrogenation of Ethylene on Metallic Catalysts

Juro Horiuti and Koshiro Miyahara

Reaction rate data for the catalyzed hydrogenation of ethylene, primarily in the presence of unsupported metallic catalysts, are cirtically reviewed. Reaction mechanisms are discussed in detail, and a statistical mechanical treatment of the reaction is given, according to the generalized theory of reaction starting from the well-known procedure of Glasstone, Laidler, and Eyring. Data for single-element catalysts and alloys are included and interpreted, as are data illustrating differences due to the physical form of the catalyst (film, foil, wire, powder, and some supported systems). Problems are discussed concerning reproducibility of experimental results over repeated runs, and as a function of catalyst pretreatment. The data is analyzed in 29 graphs and 29 tables, some of which are very extensive. The bibliography includes 141 references.

Key Words: Critical data, ethylene, hydrogenation, metallic catalysts, reaction mechanisms, reaction rates.

1. Introduction

The catalyzed hydrogenation of ethylene in the presence of metallic catalysts, especially nickel, has been a subject of intensive investigations, as a prototype of catalyzed hydrogenations of the sort, since its discovery by Sabatier and Senderens [1].[1] The catalyzed hydrogenation was found to be associated with parahydrogen conversion [2], which turned out to be a useful profile of the reaction. In 1932 deuterium appeared as a powerful tool for revealing further profiles of the reaction. These profiles were traced in the early days by following the parahydrogen content as well as deuterium content in hydrogen by means of the thermal conductivity method developed by Farkas, Eley, and others [3, 4]; the deuterium content was at that time also determined by measuring the density of water to which the hydrogen of samples in question was converted [5]. The research work has been substantially facilitated since 1950 when the infrared and mass spectrometers came into daily use for investigations of adsorbed states and for the determination of deuterium content as well as the relative amounts of different deutero-compounds.

Notwithstanding this progress in experimental techniques, there remained a serious, unresolved difficulty in exploring the catalyzed hydrogenation of ethylene. Rates of the catalyzed hydrogenation as well as of the associated reactions decline markedly and apparently uncontrollably on repetition of the runs over the same sample of catalyst. Few data are thus available, as they stand, for analysis of the catalyzed hydrogenation. It has been found, so far, that the decline in rate is caused, not only by impurities in the reactants, e.g., mercury vapor, or in catalysts which have escaped their pure preparation, but also by products of a side reaction of ethylene, i.e., its polymerization or dehydrogenated adsorption on the catalyst.

The character of catalyzed hydrogenation depends further on the form and condition of the catalyst, i.e., differs for evaporated films, powders, wires, and plates or catalyst supported on some dispersed medium, e.g., alumina or silica gel. For instance, ethylene is polymerized over nickel catalyst supported on kieselguhr but not over unsupported nickel powder. Moreover, some alloy catalysts are considerably more active than either of their components.

Films of various metals evaporated on glass walls were introduced by Beeck [6] in 1945 for the investigation of catalyzed hydrogenation. The evaporated film had been accepted at that time as the cleanest possible surface, and this piece of work hence raised lively hopes of correlating the catalytic activity and the characteristics of catalyst metals in view of the associated difficulty mentioned above. For this reason, more emphasis should be laid on unsupported catalysts than on supported catalysts, which might be associated with additional complications.

We deal in this monograph mainly with the catalyzed hydrogenation in the presence of unsupported catalysts, especially of evaporated films of pure metals, and shall refer to supported catalysts just for reference. Experimental data on the decline of catalytic activity are first reviewed, describing relevant methods of the experimental investigation. Summaries are then given of the observed kinetics of the catalyzed hydrogenation and of the different phases of profiles of the reaction. Attempts to formulate a mechanism of the phenomena in question are next reviewed, and finally the experimental results are accounted for systematically on the basis of the associative mechanism [7–11].

References are often made to the *optimum*, i.e., the point of maximum rate of the catalyzed hydrogenation with respect to temperature at given partial pressures of ethylene and hydrogen. For the sake of clear and concise presentation, protium and deuterium atoms are denoted by ^{1}H and D when they are discriminated. When they are not, either of

[1] Figures in brackets indicate the literature references at the end of this paper.

them or their mixture is denoted by H and called hydrogen atom. Likewise, any of $^1H_2$, ^1HD, and D_2 or their mixture is then denoted by H_2 and called hydrogen. $C_2{}^1H_{4-n}D_n$ is called *deuteroethylene* where $n \neq 0$, or *ethylene-d_n* inclusive of light ethylene for which $n=0$; any of them or their mixture is denoted by C_2H_4 and called ethylene, where no discrimination is made. A similar terminology is used for ethane. The catalyzed additions of $^1H_2$ and D_2 to ethylene are called *hydrogenation with light hydrogen* and *deuteration*, respectively, when discriminated, and both of them are called *hydrogenation* when not discriminated.

2. Reproducibility of Observations

The catalytic activity declines, as mentioned in the introduction, when a run of catalyzed hydrogenation of ethylene is repeated with the same sample of metallic catalyst. This effect is especially pronounced in case of unsupported catalysts. It is prerequisite for a reasonable study of the catalyzed hydrogenation to elucidate the nature of this decline. The present knowledge about it is reviewed in the following in terms of experimental results and comments upon or inference from them; experimental results are numbered as 2.1, 2.5.1, etc., and comments or inferences are denoted similarly except that the second figure of the mark is replacec by a Roman capital letter, e.g., as 2.A, 2.D.1, etc.

2.1. Beeck [6] used metal films evaporated on a glass wall kept at -183 °C and showed that, when the films were contacted preliminarily with ethylene, the rate of the catalyzed hydrogenation at 0 °C decreased, on the metals indicated in parentheses, to 10 percent (Ta), 20 percent (W), 40 percent (Ni), or 95 percent (Pt, Rh) of the rates without the preliminary contact in the respective cases.

2.2. The rate of the catalyzed hydrogenation depends on the sequence in which reactant gases are introduced over the catalyst. Toyama [12] observed the rates of three consecutive runs conducted over a sample of nickel powder reduced from its oxide (termed reduced nickel in what follows), introducing in the first run hydrogen and ethylene simultaneously, in the second hydrogen in advance and in the third ethylene in advance; each run was conducted after evacuating the product of foregoing run. In the second and third runs, the catalyst was left overnight at room temperature in contact with the reactant gas introduced in advance before the other was admitted. The second run gave a rate higher than the first, while the third run gave a rate lower than both the first and second.

2.A. The third run of 2.2 confirms 2.1 in the case of nickel, whereas the second run of 2.2 indicates a regeneration of catalytic activity by the hydrogen treatment. The features of the decline may be gathered from the results described next.

2.3.1. The following qualitatively coincident results were obtained when admitting repeatedly small doses of ethylene over films of Ni [6, 13, 14], Pd [15], W [16], or Ir [17] evaporated on a glass wall of a vessel kept at room temperature [18]. No gas whatever was detected inside the vessel until the total sum, Q, of the number of molecules of ethylene admitted exceeded a certain value A, when ethane alone began to appear with further increase of Q. When Q exceeded a certain other value B ($>A$), ethylene began to appear in the gas phase. Now, both the number of ethane molecules and the number, Q', of adsorbed ethylene molecules (Q minus the total number of ethylene and ethane molecules in the gas) increased until Q exceeded a certain third value, C ($>B$), beyond which both Q' and the number of ethane molecules remained, respectively, constant.

Number A corresponded to 30 percent coverage of the surfaces at room temperature provided that the number of hydrogen atoms adsorbed at -183 °C [13] equaled the number of their adsorption sites and each ethylene molecule occupied two such sites. The number of ethane molecules formed at $Q=B$ approximately equaled Q' at that point. The above results are shown in figure 1 [18], where the respective values, of Q, A, B, and C, are indicated with vertical broken lines.

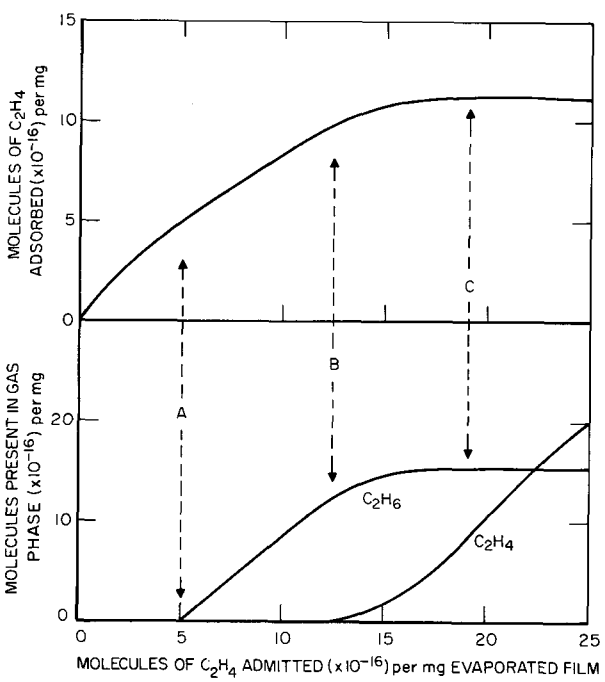

FIGURE 1. *Behavior of ethylene on evaporated nickel films [18].*
C_2H_4 adsorbed: C_2H_4 admitted minus $C_2H_4+C_2H_6$ in gas.

2.3.2. Mckee [19] found by the use of reduced nickel of 1.41 m^2 BET area that the number A in 2.3.1 increased with fall of temperature from

2×10^{17} C_2H_4 molecules at -22 °C to 13×10^{17} C_2H_4 molecules at -78 °C, which corresponded to the increase of coverage from ca. 3 to 20 percent of the surface.

2.4. Ethylene in contact with a metal film left on it compounds of a composition which varied with the temperature during contact, the extent of evacuation after contact and the sort of metal. The composition of the compounds was $C_2H_{0.8}$ at 25 °C [14] and C at 170 °C [13] on nickel film and $C_2H_{3.6\sim3.9}$ at 100 °C on Ir [17]. This process is called *dehydrogenated adsorption* and the compound termed *adsorbed complex* in what follows.

TABLE 1. *Rates of removal of adsorbed complex from evaporated metal films by treatment with hydrogen [18]*

Metal	Temp. °C	Reaction time, min	% Removed	Authors
Rh	23	1	60	Beeck [14]
Rh	23	long	100	Beeck [14]
Pd	0	5	50 ~ 60	Stephens [15]
Ni	20	60	20	Beeck [14] Jenkins and Rideal [13]

The product of the treatment in case of Rh was almost exclusively ethane, while in case of Ni 90 percent of the product were saturated hydrocarbons of carbon number 4 to 8.

2.5. The adsorbed complex can be removed from the surfaces by hydrogen treatment around room temperature as shown in table 1. The adsorbed complex is not so readily removed from nickel as it is from iridium. The removal from nickel is, on the other hand, appreciably slower than the catalyzed hydrogenation on the same metal, by a factor of several hundreds [13]. This aspect contrasts with that of preadsorbed acetylene which cannot by hydrogenated off nickel at 23 °C, whereas 40 percent of it can be hydrogenated off rhodium at the same temperature in 1 hr [14].

2.6. Thomson and Wishlade [20] saturated an evaporated nickel film with radioactive $^{14}C_2H_4$ at 20 °C, evacuated it subsequently a little while and followed its removal by different treatments with radioactivity measurements. 2 percent of the radioactivity were thus lost by contacting the saturated film with nonradioactive ethylene, another 10 percent were lost by allowing this film to catalyze the hydrogenation of 10 cm Hg nonradioactive ethylene with equimolar hydrogen, and the radioactivity still remaining was further diminished by 30 percent by a hydrogen treatment. The 58 percent radioactivity thus left could not be reduced further when allowing the film once again to catalyze the hydrogenation of nonradioactive ethylene of partial pressure around 9 cm Hg with equimolar hydrogen.

These results contrast with those obtained by Cormack, Thomson, and Webb [21] for alumina-supported catalysts of Ni, Rh, Pd, Ir, and Pt saturated with $^{14}C_2H_4$ which lost, respectively, 36.5 percent (Pd), 76 percent (Ni), 77.5 percent (Rh), 84 percent (Ir), and 93.5 percent (Pt) of the radioactivity as they catalyzed the hydrogenation of nonradioactive ethylene.

2.B. Results 2.1, 2.2, and 2.3.1 are accounted for by assuming that adsorbed complex poisons the catalyst, and hydrogen atoms formed by the dehydrogenated adsorption of ethylene are combined with ethylene from ethane. The number of ethane molecules at $Q=B$ would then approximately equal Q' as in 2.3.1, if the adsorbed complex is of composition C_2H_2, i.e., an *acetylenic complex* [6], in other words ethylene subjected to dehydrogenated adsorption gives off equimolar hydrogen which is combined with another ethylene molecule to form ethane.

Result 2.3.2 indicates that at lower temperatures the quantity of adsorbed ethylene has to be enhanced in order to provoke the dehydrogenated adsorption coupled with the hydrogenation.

Result 2.4 shows that ethylene is stripped of its hydrogen to a far greater extent over nickel than it is over iridium, while 2.5 and 2.6 show that the adsorbed complex is less readily removed with hydrogen treatment from nickel than from iridium. This great difference in ease of removal is compared with the contrasts in results 2.1, viz., that the adsorbed complex is more inhibitive of the catalyzed hydrogenation on nickel than on platinum metals.

2.C. Ethylene molecules may exchange their hydrogen atoms by way of the hydrogen atoms given off by dehydrogenated adsorption according to the associative mechanism [7–11] (cf. sec. 9.2) through the half-hydrogenated state $C_2H_5(a)$ attained by the step

$$C_2H_4(a)+H(a)\rightarrow C_2H_5(a),$$

where (a) signifies an adsorbed state. The hydrogen atom which has combined with $C_2H_4(a)$ to form $C_2H_5(a)$ shares, according to the associative mechanism, chemically equivalent positions with two hydrogen atoms from a methylene group of $C_2H_4(a)$, and each of the latter two gains, therefore, the probability 1/3 to become H(a) in the reverse of the above step, and hence to find its way into another ethylene molecule, as evidenced by the following result.

2.7. A rapid exchange between ethylene-d_4 and light ethylene was observed by Miyahara [22] on a freshly evaporated nickel film even at -23 °C, contrary to a negative result reported by Conn and Twigg [23]. Flanagan and Rabinovitch [24], tracing the experiment of Conn and Twigg [23], were able to observe an exchange reaction at 60 °C by using much more nickel wire than Conn and Twigg.

2.8. Results given next show that the dehydrogenated adsorption of ethylene occurs even in the pres-

ence of hydrogen, i.e., under the normal condition of the catalyzed hydrogenation.

2.8.1. Jenkins and Rideal [13] observed the catalyzed hydrogenation of 20 mm Hg ethylene with equimolar hydrogen at 20 °C over evaporated nickel film for 10 min, evacuated the product and repeated the experiment consecutively. The rates of total pressure decrease found were 3.50 mm Hg/min in the first run, 1.90 mm Hg/min in the second run and 1.30 mm Hg/min steadily in the third and several subsequent runs. When they contacted the evaporated film preliminarily with ethylene, the steady value (1.30 ~ 1.60 mm Hg/min) was obtained throughout from the first run on.

2.8.2. The catalytic activity of metal films is appreciably reduced by impurities, especially mercury [25] and oxygen [22, 27]; the former also diminishes the adsorption of hydrogen on metal films. Mercury is liable to be introduced into a reaction vessel along with reactant gases [26] and in consequence accumulates on the metal film. A trace of oxygen amplifies the decline of catalytic activity when the run of catalyzed hydrogenation is repeated [22], creating, besides, an induction period as seen in figure 2(a) [22]. Figure 2(b) [22] shows that a nearly reproducible rate of hydrogenation is secured by removing the impurities.

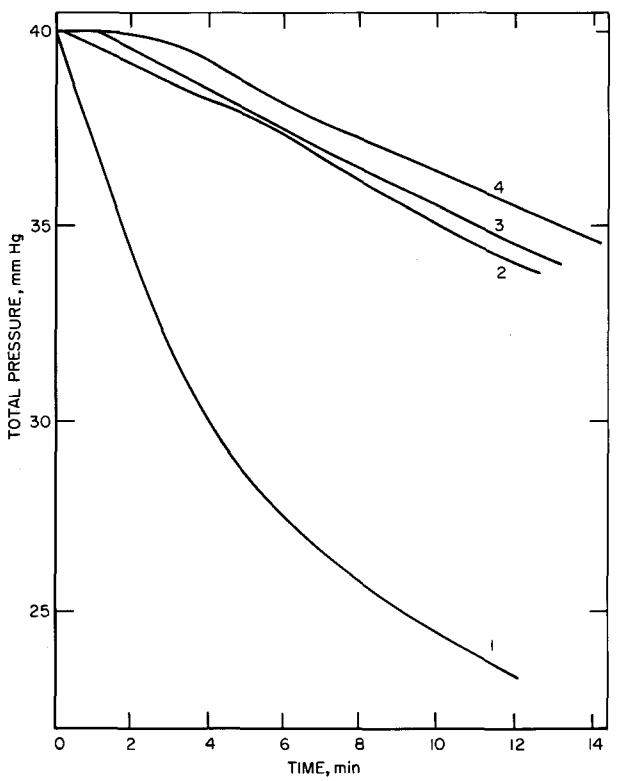

FIGURE 2(a). *The courses of repeated hydrogenations of ethylene with ca. equimolar hydrogen contaminated with oxygen at 50 °C over evaporated nickel film [22]; mercury excluded.*

2.8.3. Miyahara [26] determined, under the pure conditions attained in 2.8.2, the quantities, Q_E and Q_H, of ethylene and hydrogen adsorbed, respec-

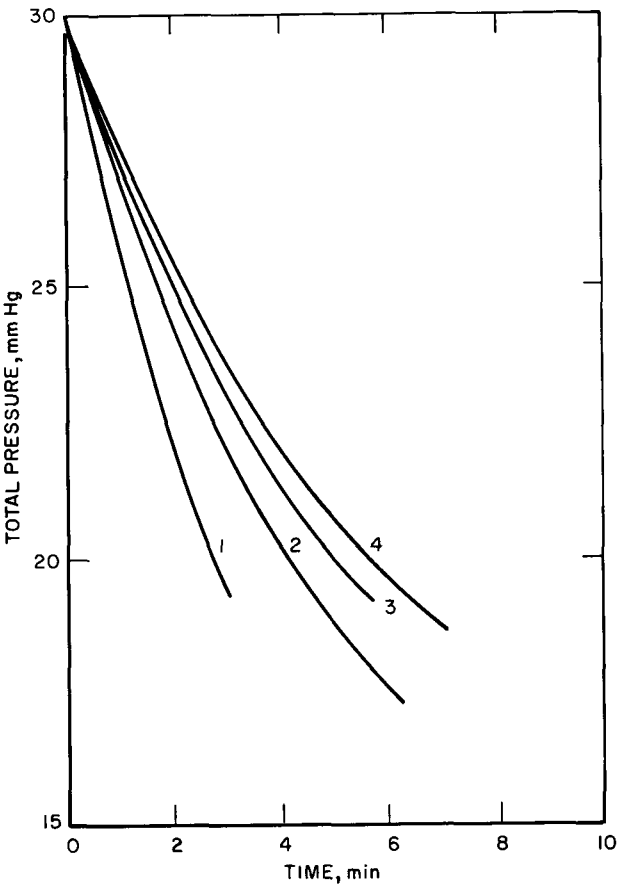

FIGURE 2(b). *The courses of repeated hydrogenations of ethylene with ca. equimolar pure hydrogen at 50 °C over evaporated nickel film [22]; mercury excluded.*

TABLE 2. *Number of moles of ethylene (Q_E) and hydrogen (Q_H) adsorbed on evaporated nickel films in course of hydrogenation of ethylene by equimolar hydrogen* [26].

Initial total pressure: ca. 0.1 mm Hg

Temp. °C	Surface of evaporated Ni film	$Q_E \times 10^8$	$Q_H \times 10^8$
0	F	17.1	5.5
	F	16.8	4.5
	S	15.4	6.5
	S	17.6	3.3
	C	13.1	1.7
101	F	15.6	1.3
	F	10.0	2.7
	S*	9.8	−8.8
	S	11.6	2.2
	C	9.5	0.5
145	F	9.6	−9.6
	S	11.4	0.8
	C	10.0	0.0

A given run of catalyzed hydrogenation were conducted over nickel films evaporated on the wall, kept at 200 °C, of a reaction vessel of 120 cm^3 capacity, by admitting the reactant gas mixture into the reaction vessel. Such a run was followed in some cases by another on evacuation of the product of the foregoing run. The films thus used were kept at 500 °C in H_2 of few mm Hg for an hour, evacuated at the same temperature to 10^{-7} mm Hg and then coated with new evaporation of nickel, and one or two runs were similarly conducted over the newly coated films. The sur-

face of a film either freshly evaporated or freshly coated is signified by F, and that used once as above by S; C refers to a surface used several times consecutively at 200 °C, each such run was preceded by an evacuation at the same temperature, until the rate decreased from that over F by a factor of several tens.

Q_E and Q_H were determined, as the excess of the number of moles of ethylene and hydrogen initially introduced into the reaction vessel over that of ethylene and hydrogen remaining in gas plus that combined in ethane, on the basis of the experimental result [61] that the adsorption of ethane is inhibited by ethylene. Gas mixtures were sampled for Q_E- and Q_H-determinations immediately after the measurement of the initial rate of total pressure decrease, which lasted a few seconds just after the introduction of the reactant gas mixture, except in a run marked with asterisk; gas mixture was sampled in the latter case toward the end of the run, when the total pressure decreased no longer perceptibly.

tively, in course of the progress of catalyzed hydrogenation, as shown in table 2. F and S in the table refer to the surfaces of freshly evaporated films or those once used for a run of hydrogenation, and C refers to surfaces used several times consecutively at 200 °C until the rate of hydrogenation over them decreased from that over F by a factor of several tens. C exhibited every characteristic of the "carbided surface" [13] which was obtained by exposing a freshly evaporated film to ethylene at 200 °C for 10 min.

2.D. The dehydrogenated adsorption of ethylene in the presence of hydrogen is evidenced by the negative value of Q_H in table 2, which indicates a net evolution of hydrogen, its absolute value being a lower limit to the amount of hydrogen evolved by dehydrogenated adsorption. A negative Q_H was observed over F as well as over S surfaces at temperatures above the optimum temperature, 30 °C, as seen in the table [26]. It follows that dehydrogenated adsorption occurs side by side with the catalyzed hydrogenation above the optimum both over F and S surfaces.

2.9. The following further data on the dehydrogenated adsorption of ethylene are available.

2.9.1. Miyahara [26] observed the distribution of deuterium in ethylene and hydrogen in the initial stage of catalyzed deuteration of light ethylene as shown in table 3 under the pure conditions established in 2.8.2. The optimum temperature for an equimolar mixture of ethylene and deuterium of 0.1 mm Hg initial total pressure was found 50 °C in this case. $^1H_2$ was evolved in case of F but not of S at temperatures below the optimum (−45 and −23 °C), whereas $^1H_2$ was evolved above the optimum in both the cases.

2.9.2. Formation of ethane from ethylene caused by its dehydrogenated adsorption on reduced nickel was almost suppressed, according to Hirota and Teratani [28], by a preliminary adsorption of CO_2, which covered 30 percent of the BET area of the reduced nickel, whereas the same preliminary adsorption on the same catalyst was almost ineffective with respect to catalyzed hydrogenation.

TABLE 3. *Relative amounts of ethylenes-*$d_n \equiv E_n$ *and hydrogens-*$d_n \equiv H_n$ *in the product of deuteration of light ethylene over evaporated nickel films* [26]

React. temp. °C	State of film surface	Deuterated % C_2H_4	Deuterated % C_2H_4 min^{-1}	Relative amounts								Deuterium atom fraction in	
				E_n in C_2H_4, %					H_n in H_2, %				
				E_0	E_1	E_2	E_3	E_4	$^1H_2$	^1HD	D_2	C_2H_4	H_2
−45	F	4	9.7	63	31	7	0	0	8.5	22.5	69	0.112	0.803
	S	2	3.5	93	7	0	0	0	0	1.6	98.4	0.017	0.992
−23	F	15	31.8	57	34	9	0	0	10	25	65	0.130	0.775
	S	10	18.2	90	10	0	0	0	0	1.6	98.4	0.025	0.992
0	F	35	74.3	44	36	18	2	0	11	26	63	0.195	0.760
	S	20	56.9	64	30	6	0	0	0	6	94	0.105	0.970
28	F	40	110.3	45	38	14	2	0	11	30	59	0.180	0.740
	S	43	98.0	66	28	5	1	0	2	10	88	0.103	0.930
32	F	45	129.7	49	34	11	7	0	11	22	67	0.165	0.780
	S	41	107.1	40	36	20	4	0	10	19	71	0.220	0.805
75	F	40	102.1	21	35	28	13	3	30	42	28	0.355	0.440
	S	38	97.0	29	38	24	7	2	30	29	41	0.263	0.695
110	F	18	54.0	16	32	32	16	4	11	39	50	0.400	0.695
	S	21	50.2	21	29	37	10	2	14	39	47	0.340	0.665

"Deuterated percent C_2H_4" in the third column represents the percentage decrease of the sum of the numbers of moles of $C_2H_4 = \sum_{n=0}^{4} E_n$ from the sum at the beginning of the catalyzed hydrogenation, when C_2H_4 is practically exclusively $C_2{}^1H_4$. F denotes the surface of freshly evaporated film and S that used once for a run; cf. legend of table 2.

2.E.1. The dehydrogenated adsorption will lead to an evolution of $^1H_2$ as in 2.9.1, if it consists simply of a release of hydrogen molecules into the gas. If it supplies, on the other hand, hydrogen in an intermediate state of the catalyzed hydrogenation, e.g., H(a) directly, then $^1H_2$ will also appear in the gas as a product of conversion of this intermediate, unless steps consuming it are rapid enough to suppress the conversion, e.g., to inhibit the recombination of the H(a)'s by lowering their activity. It follows now from the observed absence of $^1H_2$ evolution over S surfaces below the optimum that dehydrogenated adsorption occurs neither under immediate release of hydrogen molecules nor to evolve them through the intermediate state. Under the latter conditions the dehydrogenated adsorption, if any, may be traced by a deviation from the stoichiometry of normal hydrogenation; the total pressure would not then decrease, in case of catalyzed hydrogenation of ethylene with excess hydrogen in a constant volume, as far as corresponding stoichiometrically to the exhaustion of the ethylene. On account of absence of such a deviation (cf. 4.1), the dehydrogenated adsorption is concluded to be practically suppressed on S surface.

The validity of the above arguments rests upon the postulate that the hydrogenation and the dehydrogenation of ethylene are exclusively reactions occurring on metallic catalysts. This is assumed throughout in what follows.

2.E.2. It follows from the preferential inhibition of dehydrogenated adsorption observed in 2.9.1 that the two reactions do not occur on the same site, insofar as both reactions on their respective sites are admitted to be blocked solely by the product, adsorbed complex, of dehydrogenated adsorption. It is induced from this conclusion and 2.9.2 that the nickel catalyst's surface consists of two parts, (d) and (h), which catalyze the dehydrogenated adsorption and hydrogenation, respectively;[2] the former remains poisoned by adsorbed complex if it is on an S surface below the optimum (2.9.1) and also by CO_2 (2.9.2) [28].

2.10. Experimental results are reviewed next from which diverse theories are derived on the state of catalyst's surface.

2.10.1. Crawford, Roberts, and Kemball [29] annealed nickel films, evaporated on glass walls kept at -195 °C, at different temperatures from 0 to 400 °C and observed their activity in catalyzing both the hydrogenation with $^1H_2$ and the deuteration of light ethylene. The rate of hydrogenation with $^1H_2$ decreased when the runs were repeated on the same surface but their rates per unit BET area remained constant for a definite annealing temperature and decreased only with rise of the annealing temperature. Both the activation heat of hydrogenation with $^1H_2$ and the deuterium distribution in the ethane formed by the deuteration remained unchanged throughout [29].

2.10.2. The BET area referred to in 2.10.1 decreased by a little over 40 percent when contacting the film with ethylene as shown in table 4, irrespective of the annealing temperature.

TABLE 4. *Change of BET area of evaporated nickel film by adsorption of* C_2H_4 *at* -80 *°C* [29]

Annealing temp. °C	Volume of C_2H_4 adsorbed cm^3 (S.T.P.) $\times 10^3$	BET area $cm^2 \times 10^{-2}$		$\frac{\mathscr{A}_2}{\mathscr{A}_1}$
		Before adsn., $\mathscr{A}_1$	After adsn., $\mathscr{A}_2$	
0	20	23.2	12.8	0.55
25	12	19.6	11.0	0.56
100	8	13.4	7.8	0.58

2.10.3. Campbell and Duthie [30] found that the BET area of nickel film decreased to the same extent when allowing the film preliminarily to adsorb N_2O, O_2, or Hg.

2.10.4. Jenkins and Rideal [13] found that nickel surface covered by acetylenic complex and preliminarily evacuated, evolved hydrogen, amounting to be equimolar with the acetylenic complex, as temperature was raised gradually from 20 °C up to 170 °C in a closed space. On cooling it down to room temperature the evolved hydrogen was absorbed, but not completely.

2.10.5. Foss and Eyring [27] found the rates of consecutive runs of hydrogenation to be reproducible on a carbided nickel surface[3] when this was treated with 5 cm Hg hydrogen at 250 °C for 30 min before every run. The reproducible rate thus established was about one half that on a freshly evaporated film but was several tens of times larger than that on a carbided surface (see footnote 3) not treated with hydrogen.

2.10.6. A preliminary contact of the catalyst in 2.10.5 with ethylene retarded the hydrogenation in the beginning of its course, but did no longer so several minutes later [27].

2.F. Kemball et al. [29], attributed the decrease of BET area in 2.10.1 and 2.10.2 to a sintering of the catalyst's surface caused by the heat of hydrogenation or adsorption but did not take into account the effect of adsorbed complex. Campbell and Duthie [30] referred the effect, on the basis of 2.10.3, to the adsorbed complex, which was suggested to decrease the quantity of krypton adsorbed in BET measurements, thus simulating a reduction in BET area, although their reason why it should decrease the adsorption of krypton does not appear clear.

Result 2.9.1 speaks definitely against sintering as responsible for the rate decrease. The decrement

[2] The two parts may be attributed to different lattice planes exposed on the catalyst surface; cf. 2.11.1.

[3] Cf. 2.8.3.

of the rate between F and S in 2.9.1 becomes monotonously smaller with rise in temperature; it falls from 64 percent at −45 °C to 8 percent at 110 °C, as seen in table 3. If sintering was responsible for the decline in rate, its extent and in consequence the rate decrement ought to be the greater, the higher the reaction temperature and the greater the rate of heat evolution, i.e., the reaction rate times reaction heat per mole. The reaction rate increases from −45 to 32 °C monotonously by a factor of more than ten, as seen in the same table, and the reaction heat per mole, though slight, increases as well. The decrement of rate should hence increase monotonously with rise of temperature. This is quite contrary to the experimental result, and the sintering can, therefore, not be responsible for the decrease in rate.

It appears, however, necessary to regard 2.10.1, 2.10.2, and 2.10.3 with caution, in view of 2.8.2, because of a possible intrusion of mercury, which has been positively evidenced under similar experimental conditions [31].

Jenkins and Rideal [13] attributed the result of 2.10.4 to the migration of carbon atoms from the surface into the bulk of metal so that a clean metallic surface, available for adsorption of hydrogen, was regained. However, results 2.10.5 and 2.10.6, backed by 2.5 and 2.6, indicate the substantial effect of hydrogen in recovering a catalytically active metallic surface from the carbided surface. These results lead to the view, amplifying upon 2.E.2, that the treatment before every run in 2.10.5 released part (h) from the poisoning due to the foregoing run, leaving part (d) steadily poisoned so as to secure the reproducibility of the results.

2.11. The following results might provide further informations relative to the dual catalyst surface advanced.

2.11.1. Cunningham and Gwathmey [32] observed the activity of individual lattice planes of nickel single crystal in catalyzing the hydrogenation of ethylene from 50 to 200 °C, preliminarily treating the lattice planes with hydrogen at 500 °C. They found that $(321) > (111)$ and $(110) > (100)$ as shown in figure 3, where the *Miller indices* represent the relevant activities. They also observed that lattice planes other than (111) and (100) lost their metallic luster by contact with ethylene at 450 °C, which they termed carbon deposition.

2.11.2. Farnsworth and Woodcock [33] observed effects of heating in high vacuum, bombardment with Ar^+ ions etc., on the activity of nickel and platinum plates in catalyzing the hydrogenation of ethylene with equimolar hydrogen at 0.1 to 1.0 mm Hg total pressure. The results are shown in table 5, where the catalytic activity is given in terms of the first order rate with respect to hydrogen partial pressure. The table shows the enhanced activity due to heating in high vacuum and bombardment in treatments (1) and (3), which is all but lost again by annealing at 550 °C as seen in treatments (2), (4), and (5).

TABLE 5. *Rates of hydrogenation of ethylene over catalysts of diverse pretreatments* [33].

Pretreatments	Activity (arbitrary units)	
	Ni catalyst	Pt catalyst
(1) Heat-treated and quenched.....	45 ± 5	2400 ± 200
(2) Heat-treated, quenched, and annealed.	17 ± 2	750 ± 30
(3) Bombarded with positive argon ions.	700 ± 100	2200 ± 200
(4) Bombarded and annealed.....	8 ± 2	200 ± 30
(5) Bombarded, heat-treated, quenched, and annealed.	7 ± 2	225 ± 30

Approximate temperature of: heat-treatment of nickel, 850°; annealing nickel, 500 to 550 °C; heat-treatment of platinum, 1050 to 1350°; annealing platinum, 700°. Quenching was always preceded by an induction heat-treatment of at least one-half hour to insure uniformity in surface structure of the catalyst preceding the quenching. The quenching was accomplished by suddenly stopping the induction heating current and allowing the catalyst to cool in vacuum to room temperature.

Farnsworth and Woodcock attributed the enhanced activity to lattice defects created by the treatments (1) and (3) in table 5 [33].

2.G. The following are general conclusions regarding the reproducibility of observations on the catalyzed hydrogenation.

The decline of catalytic activity, though considerably reduced by purification of reactants, persists, even in the case where purest reactants are used, which is attributed to a poison produced by dehydrogenated adsorption of ethylene, i.e., adsorbed complex, termed acetylenic complex [6], carbide [13], coke [34], or polymer [34]. It is induced from experimental results that the catalyst surface consists of two parts: one part (d) causes the dehydrogenated adsorption of ethylene, is readily poisoned by adsorbed complex and is not readily recoverable; the other part (h) catalyzes the hydrogenation, is but slowly poisoned and readily recoverable.

The carbided surface [13] shows no decline of catalytic activity at all, which might hence appear pertinent to the investigation of the catalyzed hydrogenation. The carbided surface might, however, be substantially degenerated from the genuine metallic surface, on account of the considerable differences in their properties as discussed in section 8. To the best of our present knowledge it appears that catalyzed hydrogenation on a genuine metallic surface is observed with an S surface below the optimum, provided that the reactant gases are rigorously freed from impurities, especially mercury and oxygen. Above the optimum, where hydrogenation and dehydrogenated adsorption are simultaneously going on, it would be necessary for the elucidation of the catalyzed hydrogenation to find a reasonable way to analyze the observed overall reaction with respect to the two individual reactions.

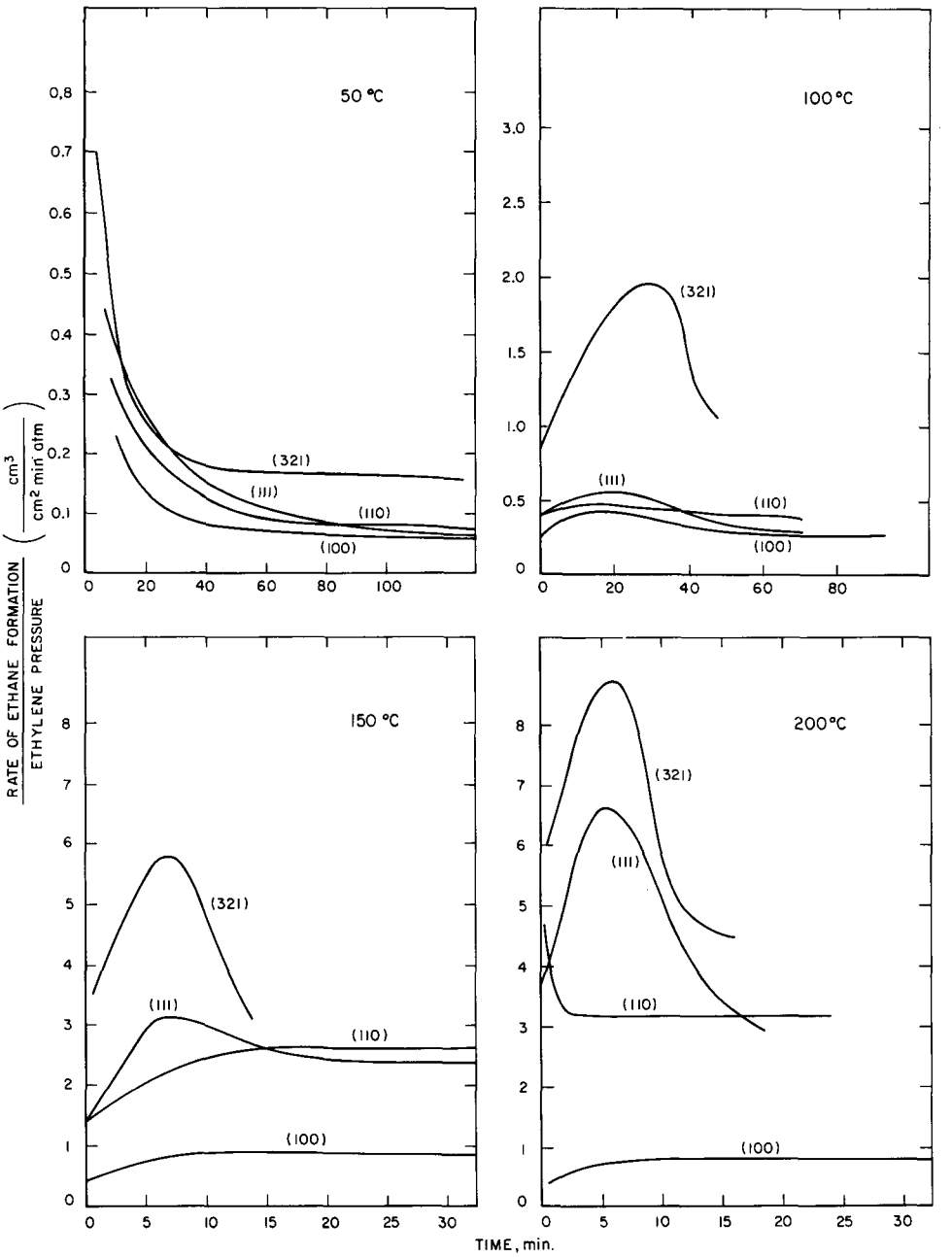

FIGURE 3. *Activities of crystal planes of* Ni *in catalyzing the hydrogenation of ethylene* [32].

Much more work will be necessary before hydrogenation which is associated with dehydrogenated adsorption can be reasonably discussed on the level of lattice planes and lattice defects of catalysts.

3. Catalytic Activity of Various Pure Metals and Alloys

The rate of catalyzed hydrogenation of ethylene is very sensitive to the preliminary treatment of the catalyst metal, apart from the working conditions as reviewed in 2, and this treatment must be precisely specified, should the informations gained be of any significance. Informations on catalytic activities which are more or less significant in this sense are reviewed next, if not immediately assignable to intrinsic properties of the catalyst material.

3.1. Beeck observed the activity of evaporated films of various metals in catalyzing the hydrogenation of ethylene comparatively at 0 °C [6, 14]. The rates

were strictly proportional to hydrogen pressure and independent of ethylene pressure, according to Beeck, although no data are given [6, 14] of their absolute magnitude. The results are shown in figure 4 and table 6 in terms of activity λ, percent *d*-character of metallic bonds and adsorption heat of reactants on the metals. The quantity λ is the ratio between the first order rate with respect to hydrogen per unit BET area on a given metal and that on rhodium. Figure 4(a) shows that the activity increases generally with the percent *d*-character of metals and that the activity of a Ni film with the preferred orientation of the (110) lattice plane parallel to the glass base, marked with (110), is ca. four times as large as that of a Ni film with random orientation of crystallites. Figure 4(b) shows that Rh is the metal at the maxima of both the activity and percent *d*-character and at the minima of the adsorption heats of both ethylene and hydrogen.

The results obtained by Beeck [6, 14] have been commented upon from a variety of aspects as below.

3.1.1. Phenomenologically, a linear relation was advanced by Schuit [35] between $\log_{10}\lambda$ observed by Beeck [6, 14] and the product of percent *d*-character and the valency of metals according to Pauling [36], as shown in figure 5.

3.1.2. The closest distance between two Rh atoms is 2.69 Å in its f.c.c. crystal of lattice constant 3.80 Å indicated in figure 4(b). This closest distance is nearly coincident with the ideal metal-metal distance, 2.73 Å, for the associative adsorption [4] of ethylene without strain as calculated by Twigg and Rideal [37] assuming the carbon-metal distance to be that in nickel carbonyl, 1.82 Å. Notwithstanding this nice agreement, our present theoretical equipment appears not replete enough to afford a consistent explanation of the maximum activity at rhodium in this way.

3.1.3. Beeck [14] suggested that the rate of catalyzed hydrogenation was controlled by the process of hydrogenated desorption, e.g., the reversal of dehydrogenated adsorption, of the adsorbed complex which makes room for adsorption of hydrogen. This can hardly be the case, however, since the catalyzed hydrogenation is progressively poisoned by adsorbed complex in its course as elucidated in section 2., and moreover, the hydrogenated desorption is far slower than the catalyzed hydrogenation [13] as mentioned in 2.5.

3.1.4. Ethylene is subject to the dehydrogenated adsorption as concluded in 2.4 and 2.B and, as seen from tables 1 and 6, the less active catalyst is that which is not easily rid by hydrogenated desorption of the adsorbed complex thus formed and associated with a high initial heat of adsorption [14].

3.1.5. The activation heat of the catalyzed hydrogenation over different metals amounts uniformly to 10.7 kcal, except in the case of tungsten where it is 2.4 kcal/mole [6]. It follows that the catalytic activity is proportional to the preexponential factor for all these metals except tungsten [6, 14].

3.1.6. An exception similar to that in 3.1.5 is found in case of tungsten by a statistical-mechanical analysis of kinetic data [38]. We obtain 10^{15} cm^{-2} as an order of magnitude for the number of sites of the critical complex [5] per unit area of the catalyst's surface from an analysis of kinetic data of the reaction involving no hydrocarbon over tungsten, which is in the line with the number derived from almost all available date of more than 60 cases of reactions over other metallic catalysts; but the number was found exceptionally low, around 10^6 cm^{-2}, in case of the exchange reaction between methane and deuterium over tungsten.

3.1.7. The above results, 3.1.4, 3.1.5, and 3.1.6, are accounted for on the basis of the following theoretical results. Toya [39] has shown by first principles of quantum mechanics that hydrogen adatoms exist in *r*- and *s*-states and that the hydrogen adsorbed first on nickel exists predominantly in the *r*-state, adatoms in the *s*-state increasing with further increase of the adsorbed amount. The *r*-state is that of adatoms in the usual sense, whereas

[4] Ethylene is assumed [37] to be held by two adjacent metal atoms breaking its π-bond and forming two carbon-metal bonds, and all bonds of the carbon atoms are tetrahedrally disposed like those of ethane.

[5] The critical complex is the system of a step, i.e., the set of particles involved in the step, at a particular configuration with its representative point on the critical surface. The critical surface partitions the configuration space appropriate to the initial system of the step from that to the final system and is situated so as to minimize the rate of transit of representative points of the relevant canonical ensemble in either direction; the initial or final system is the same set of particles at the state before or after the occurrence of the step, respectively. The critical complex includes as its special case the activated complex as defined by Eyring et al. [H. Eyring, J. Chem. Phys. **3**, 107 (1935); W. F. K. Wynne-Jones and H. Eyring, ibid. **3**, 492 (1935); M. C. Evans and M. Polanyi, Trans. Faraday Soc. **31**, 875 (1935); **33**, 448 (1937); M. Polanyi, J. Chem. Soc. 629 (1937)] with special reference to the saddle point of the potential energy of the system of the step. In cases where there exist interactions between systems of the step and other particles, the appropriate configuration space and the relevant canonical ensemble should be those of the assembly comprising all the interacting species [cf. J. Horiuti and T. Nakamura, Advances in Catalysis **17**, (1966), section II.A.].

TABLE 6. *Catalytic activities in hydrogenation of ethylene, adsorption heats of light ethylene,* $-\Delta H_E$, *adsorption heat of light hydrogen,* $-\Delta H_H$, *and percent* d-*character of metals [6, 14]*

λ is the ratio between the value of $k_h \equiv v_h/P_H$ at 0 °C of a given metal catalyst and that of Rh.

	Rh	Pd	Pt	Ni	Fe	W	Cr	Ta
$\log_{10}\lambda$	0	−0.8	−1.65	−2.6	−3.0	−4.0	−4.2	−4.4
$-\Delta H_E$ kcal/mole	50			58	68	102	102	138
$-\Delta H_H$ kcal/mole	26	27	28	29 ~ 32	32 ~ 36	45 ~ 52	45	45
% *d*-character	50	46	44	40	39.7	43	39	39

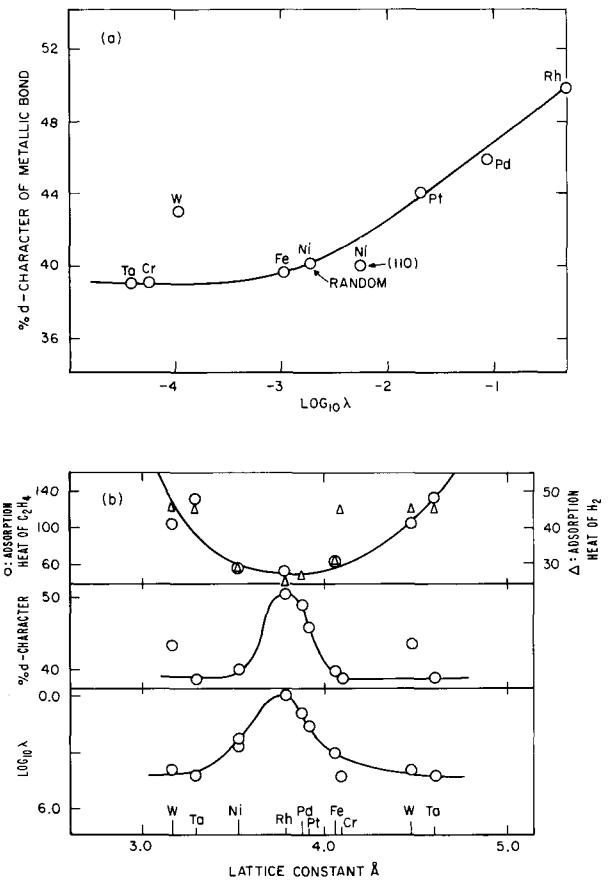

FIGURE 4. *Catalytic activity, λ, of evaporated metal films and the properties of the metals [14].*

Films were evaporated in high vacuum and in case of Ni, in 1 mm Hg N_2 as well on glass wall kept at −183 °C; "Random" and "110" refer to the random orientation of crystallites and a preferred orientation of (110)-lattice planes parallel to the basic wall, respectively, as observed by electron diffraction of the Ni film evaporated in high vacuum or in 1 mm Hg N_2. λ is the ratio between the first order rate at 0 °C with respect to hydrogen pressure per unit BET area of a given metal and that of Rh.

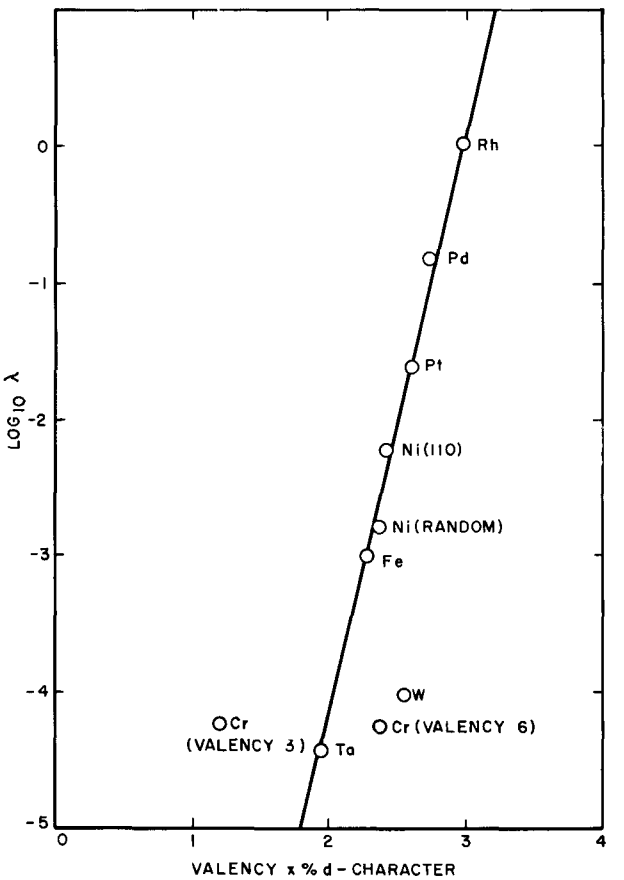

FIGURE 5. *Linear relation between $\log_{10}$ λ and valency (Pauling) × percent d-character [35].*

λ is the ratio between the first order rate at 0 °C with respect to hydrogen pressure per unit BET area of a given metal and that of Rh; cf. Beeck [14].

the *s*-state is that of H atoms dissolved in the metal but retained between the electronic surface of metal and a plane through the centers of the metal atoms in the first layer. Observed variations of electric resistance [40] and work function [41, 42] with amount of hydrogen adsorbed have been adequately explained on this basis, and it was inferred that [43] the *r*-state on tungsten is of an extremely low energy so that the *s*-state does not practically exist on tungsten, that hydrogen is irreversively adsorbed [44], and that hydrocarbons are stripped of hydrogen atoms to leave carbon deposit on tungsten. Methane will thus diminish the number of sites of the critical complex as in 3.1.6.

It would be of some interest to decide whether adatoms of *r*- or *s*-state partake in the hydrogenation reaction. Takeuchi and Asano [45] allowed nickel oxide reduced at 200 °C to adsorb one after the other small quantities of tritium and protium. Then, ethylene was admitted over the catalyst. The ethane thus formed was found less radioactive when protium was admitted first: hence, that decided which the initially adsorbed hydrogen was active in hydrogenation. It would follow from this experimental result, with reference to Toya's theory, that only hydrogens in the *r*-state were catalytically active. Since nickel might not, however, be sufficiently reduced and evacuated at 200 °C, it is desirable to confirm the result with nickel reduced and evacuated at higher temperature or with a clean surface of evaporated nickel film.

3.2. The close correlation of the catalytic activity with properties of metals as seen in figures 4(a) and 4(b) would suggest an investigation of alloys whose properties vary continuously with composition. The theory of catalysis of Dowden [46] predicts, in particular, that Ni alloyed with more than 60 percent Cu has its *d*-holes filled by electrons from Cu and is deprived of its catalytic activity. A lively interest has been aroused by this state of affairs in the catalytic activity of alloys for ethylene hydrogenation which has, however, been earlier explored by Rienäcker and his co-workers [47–51].

3.2.1. Rienäcker's work provides the following information.

3.2.1.1. Alloys of transition elements with Cu, i.e., Ni-Cu [47], Pd-Cu [48], and Pt-Cu [48, 50], were prepared in the form of thin plates, which by means of x-ray analysis were confirmed to be disordered when flashed or flashed and quenched but ordered with a superlattice when alloys of the appropriate atomic ratio were annealed. In their experiments runs were conducted by allowing an equimolar mixture of ethylene and hydrogen of 1 atm total pressure to flow through a catalyst bed and by analyzing the effluent gas for the ethane-yield; the absence of methane in the effluent gas was therewithal confirmed. The results are shown in figure 6 in comparison with the extent of parahydrogen conversion effected by the same catalysts. The following comments are remarked [50, 51, 48].

The activity of these alloys in catalyzing the hydrogenation increases, as seen from figure 6 with their content of Ni, Pd, or Pt only up to a certain small value of the content and the remains constant, closely in parallel with their activity in catalyzing parahydrogen conversion [50].

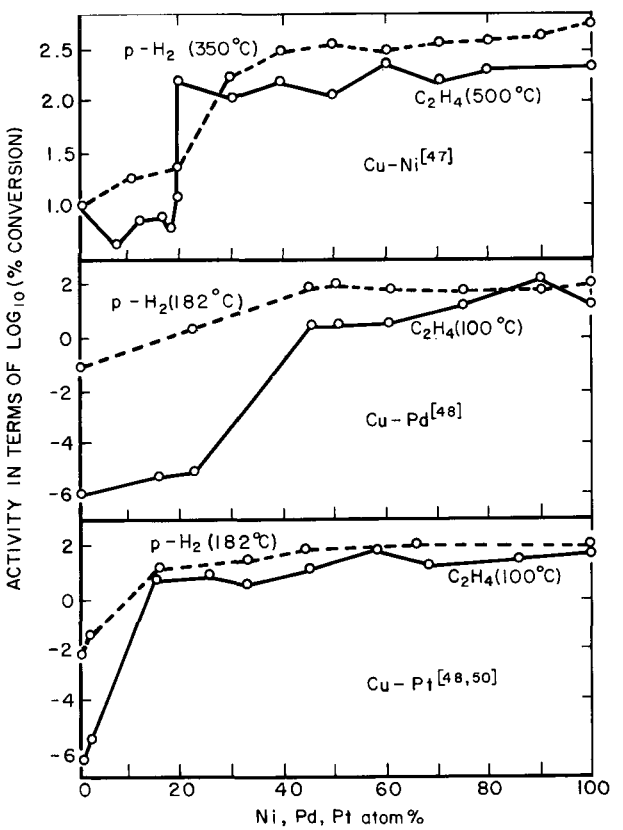

FIGURE 6. *Activity of alloys in catalyzing the hydrogenation of ethylene in comparison with that in catalyzing parahydrogen conversion [51].*

An equimolar mixture of C_2H_4 and H_2 was allowed to flow with a rate of 20 cm^3/min and 50 cm length at 1 atm total pressure. The catalyst was conditioned at 650 to 800 °C in a flow of hydrogen for several dozens of hours before every run. The content of ethane in the effluent gas was determined, hence the percentage conversion. Parahydrogen conversion was observed with the same catalysts statically at 235 mm Hg hydrogen pressure by means of the thermal conductivity method.

Alloys with superlattice have lower activation heats, although their activity is much the same as that of disordered alloys [47, 48, 49].

3.2.1.2. The catalytic activity of Cu-Ag alloy was observed by Rienäcker and Bommer [49] at 550 and 700 °C, but its dependence on composition was found imperceptible.

3.2.2. *Further data are provided on the dependence* of the activity of alloys on their composition.

3.2.2.1. Kowaka [52] observed at 100 °C a pronounced activity of Ag-Pd alloys of Pd content above 40 atom percent in hydrogenation of ethylene but practically none below 40 atom percent.

3.2.2.2. Best and Russell [53] have observed the activity of Cu-Ni alloys in catalyzing the hydrogenation of ethylene from −70 to above 100 °C; the results indicate that the activity of the alloys outweigh that of any pure component, in contrast with the results at 500 °C shown in figure 6.

3.2.2.3. Farnsworth et al. [54, 55], observed the hydrogenation of ethylene over Cu-Ni alloy plates subjected to bombardment with Ar^+. Figure 7 shows the results obtained at 40 °C in terms of the first order rate with respect to hydrogen pressure. The activity of these alloys attained a maximum at a certain value of bombarding current, whereas such is not the case with pure nickel. The figure shows the maximum exaltation of activity at 60.5 percent Cu content. Figure 8 shows the relative activity at 40 °C of catalyst plates bombarded and then annealed at different temperatures. The activity of pure nickel decreases gradually with increase of annealing temperature, whereas the activity of alloys keeps constant until the annealing temperature attains 400 °C, beyond which it decreases steeply. Farnsworth et al. [54, 55], attributed the latter, steep decrease to the migration of copper atoms from inside the alloy to the part of surface, which originally is rich in nickel and lattice defects created by the bombardment.

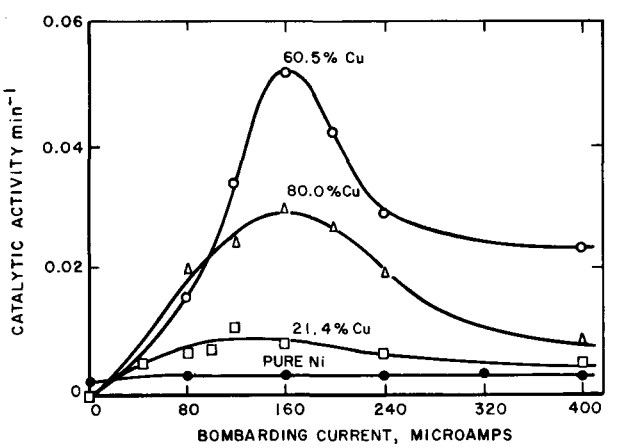

FIGURE 7. *Catalytic activity at 40 °C of* Cu-Ni *alloys bombarded with* Ar^+ *ion versus bombarding current [54].*

Catalytic activity is given in terms of first order rate with respect to hydrogen pressure. Alloy plates were preliminarily evacuated to 10^{-8} mm Hg at 900 °C.

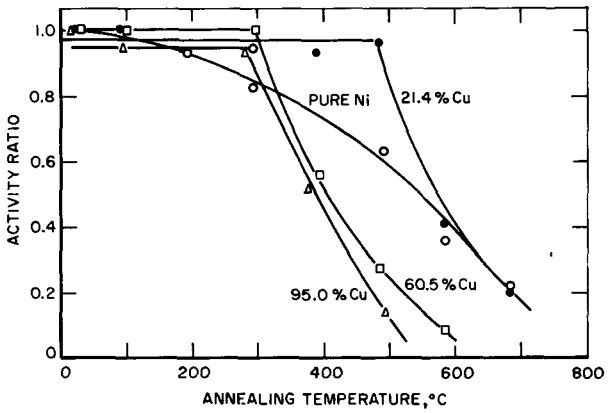

FIGURE 8. *Effect of* Ar^+ *ion bombardment and subsequent annealing on the catalytic activity of* Cu-Ni *alloy in hydrogenation of ethylene* [54].

Activity ratio is the value of the catalytic activity at 40 °C of plates of the alloy bombarded with Ar^+ and subsequently annealed, divided by that of the same plates similarly bombarded but not annealed. The catalysts were pretreated similarly to those of figure 7 and bombarded with 120 μA current at 500 V for 10 min.

3.3. Important contributions have recently been made by application of the microcatalytic method [56] developed by Emmett's school to the studies of promotion and poisoning effects of preadsorbed hydrogen on the hydrogenation of ethylene, para-hydrogen conversion and $^1H_2$–D_2 equilibration over Cu-Ni alloy catalysts. In the microcatalytic method, helium is allowed to flow, as a carrier, through a differential reactor packed with 5 cm^3 catalyst which is directly connected with a gas chromatograph. A slug of reactant gas mixture, 60 percent H_2 + 40 percent C_2H_4, was passed over the catalyst and then directly through the chromatographic column.

3.3.1. Hall et al. [57, 58, 59], observed the above mentioned reaction at 200 °K with the catalysts pretreated in two ways, i.e., "H_2-treated" and "He-treated," with a view to find the expected effect of preadsorbed hydrogen diminished in case of "He-treated," as compared with that of "H_2-treated." The catalysts were reduced in a flow of hydrogen overnight at 350 °C and, in case of "H_2-treated," cooled in the same flow down to the reaction temperature or, in case of "He-treated," kept in a flow of helium at 350 °C for 30 to 45 min and then cooled in the same flow of helium down to the reaction temperature. Figure 9 shows the catalytic activity of the alloys against their composition; the "H_2-treated" catalyst is more active for hydrogenation of ethylene than the "He-treated" one except for pure nickel, where the reverse is the case. Hall and Emmett [58] thus found that the conversion (i.e., formation of ethane) over pure nickel was increased from 50 percent for "H_2-treated" to 95 percent for "He-treated." "H_2-treated" copper was found 12 times as active as the "He-treated' one. Figure 9 shows the results of Hall and Emmett [58] side by side with the new results of Hall and Hassel [57].

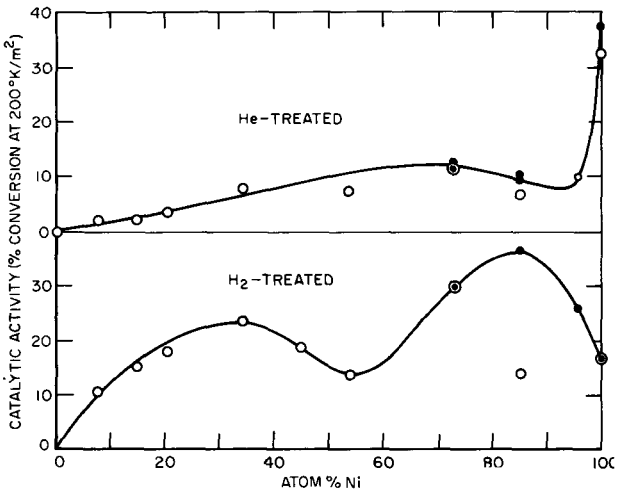

FIGURE 9. *Catalytic activity of* Cu-Ni *alloys in hydrogenation of ethylene at 200 °C* [57, 58].

○: Hall and Emmett (1959) [58]. ⊙: Hall and Hassel (1963) [57].

The catalysts were reduced at 350 °C in a flow of hydrogen overnight and then, in case of "H_2-treated," cooled in the same flow down to the reaction temperature, or, in case of "He-treated," kept in a flow of helium at 350 °C for 30 to 45 min and then cooled in the same helium flow down to the reaction temperature. The catalytic activity is given in terms of percent hydrogenation at 200 °K per m^2 BET area as observed by passing a 8 cm^3 NTP slug of 60 percent H_2 + 40 percent C_2H_4 in the helium carrier of 50 cm^3/min flow rate.

The conversion over "He-treated" nickel was reduced to 82 percent by passing slugs of the same composition 16 times consecutively. In case of Cu-Ni alloys, Hall and Emmett [58] found that the conversion over "H_2-treated" (cf. legend of fig. 10) catalyst was unchanged by passing slugs repeatedly, whereas that over the "He-treated" one (cf. legend of fig. 10) thus gradually increased.

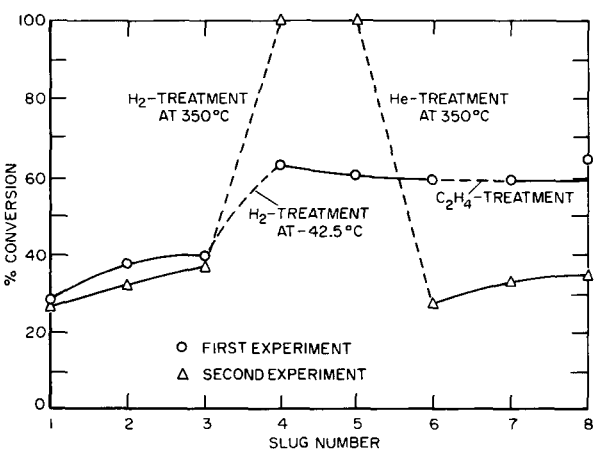

FIGURE 10. *Effect of pretreatments on* Cu-Ni *alloy of 34.3 atom percent* Ni [58].

Both in the first and the second experiment the catalyst was preliminarily He-treated as described in 3.3.1. and slugs of 60 percent H_2 + 40 percent C_2H_4 were passed over the catalyst at −42.5 °C successively. After the third slug had passed over the catalyst in the first experiment, the hydrogen stream was turned back over the catalyst at −42.5 °C for 30 min, following which it was swept out with helium carrier gas and the catalytic activity redetermined with the next three consecutive slugs. The catalyst was treated similarly after the sixth slug with purified ethylene and its effect was observed with the seventh and eighth slugs.

In the second experiment the catalyst was kept in hydrogen flow at 350 °C for 30 min. (H_2-treatment in the figure) after the third slug and kept in helium flow at 350 °C (He-treatment in the figure) after the fifth slug, respectively. The first and second experiment were conducted with the same charge of catalyst successively with the He-treatment described in 3.3.1 applied inbetween. Reproducible results were obtained as shown in figure 9.

They hence concluded [58] that the poisoning by absorbed complex referred to by Beeck [6, 14] and Jenkins and Rideal [13] is a relatively minor as compared with that of preadsorbed hydrogen.

Hall and Emmett [58] found that the activity of "He-treated" alloys in terms of log (% conversion at 200 °K per m^2) increased monotonously with the mean valency of metal atoms in the alloy according to the valence bond theory of Pauling [36] as well as with percent *d*-character over the region of its composition, where the catalytic activity varied linearly with atom percent of nickel as seen from the curve "He-treated" in figure 9.

The activation heat of catalyzed hydrogenation at temperatures around 200 °K was found [58], irrespective whether "He-treated" or "H_2-treated," to be 8 kcal for pure Cu, ca. 5 kcal for a Cu-7.8 percent Ni alloy and 4 kcal for Cu-alloys of Ni contents of 14.7 percent and above, including pure nickel.

3.3.2. Hall and Hassel [57] observed in the case of other catalysts the ratio between the activities of "H_2-treated" and "He-treated" samples in the hydrogenation of ethylene as below:

G-Fe-51 (pure iron catalyst from M. K. Research & Development Co., Pittsburgh, Pa.)	0.1
G-Co-51 (cobalt oxide catalyst from the same company as above)	0.4
P-2007 (singly promoted iron-synthetic ammonia catalyst containing 3 weight % Al_2O_3, from U.S. Bureau of Mines)	0.4
89 EE (cobalt-thoria-magnesia-Kieselguhr catalyst of the composition 100 : 6 : 12 : 200 in weight, from U.S. Bureau of Mines)	>1
and	
Ni(0104) (nickel-kieselguhr catalyst containing 59 wt % Ni, from Harshaw Chem. Co.)	<1

The "H_2-treated" catalysts are thus less active than the "He-treated" ones with the exception of 89 EE.

3.3.3. Hall, Lutinski, and Hassel [59] have investigated comparatively the effects of an alternative set of pretreatments, i.e., "outgassed" and "H_2-cooled," on the catalytic activity in hydrogenation of ethylene, parahydrogen conversion and $^1H_2-D_2$ equilibration at 200 °K with Cu-Ni alloys. The catalysts were reduced at 350 °C for 2 hr, at 500 °C for 2 hr and then again at 350 °C for 12 hr. In the pretreatment "outgassed," the reduction at 350 °C overnight was followed by evacuation at the same temperature and then by cooling down to the reaction temperature. The pretreatment "H_2-cooled" is the "H_2-treated" one followed by an evacuation at the reaction temperature for 30 min. The amount of preadsorbed hydrogen is expected to be diminished in case of "outgassed" relative to that of "H_2-cooled." It was thus found that the activity of "H_2-cooled" Cu-Ni alloys was two to three times that of "outgassed" alloys uniformly for all three reactions, while the reverse was again the case with pure nickel.

It is remarkable that parahydrogen conversion as well as $^1H_2-D_2$ equilibration over a Cu-Ni alloy of 72.4 atom percent Ni is accelerated severalfold by the preliminary passage of a slug of ethylene in both cases of pretreatment, although the reactions are retarded by coexistent ethylene. The activation heat of parahydrogen conversion was found 4.2 kcal in either case of pretreatment, whereas the preliminary passage of an ethylene slug reduced it to 3.9 kcal for the "outgassed" and 3.0 kcal for the "H_2-cooled" catalyst, respectively. The activation heat of $^1H_2-D_2$ equilibration was 5 kcal in either case of pretreatment.

3.4. Ru-Pt binary catalysts of 20–40 percent Ru content being not specified whether being alloyed or not, are known to exhibit an activity 2 ~ 6 times larger than that of pure platinum [60] in catalyzing the hydrogenation of such polar compounds as nitrobenzene, cyclohexanone, maleic acid, and methyl butynol, whereas no contribution appears to have been made toward the study of its catalytic activity in hydrogenation of ethylene.

4. Reaction Kinetics of Catalyzed Hydrogenation

The reaction kinetics of the catalyzed hydrogenation was extensively investigated over a variety of simple metals as catalyst, whereas work on alloys was limited so far to studies on the dependence of kinetic parameters, e.g., rate and activation heat, upon the composition of alloys under suitably selected conditions as reviewed in section 3. A detailed account of the reaction kinetics is hence given next, with special reference to catalysts of simple metals for hydrogenation of ethylene.

4.1. The rate v_h of the hydrogenation is determined on the basis of the material balance in accordance with the stoichiometric equation

$$C_2H_4 + H_2 = C_2H_6. \tag{4.1}$$

The applicability of the material balance has been verified by Rienäcker and Bommer [47] at 596 °C by a flow method. Miyahara, Teratani, and Tsumura [61] has shown mass-spectrometrically that the equimolar gas mixture of reactants of 0.1 mm initial total pressure over evaporated nickel film was converted exclusively to a mixture of ethylene, hydrogen, and ethane. Miyahara [22] observed that

the total pressure of a 0.93:1 mixture of ethylene and hydrogen decreased from its initial value of 30.0 mm Hg ultimately down to 15.6 mm Hg in a constant volume over evaporated nickel film coincidently at 91, 114, and 129 °C, which verified the conclusion from the material balance of eq (4.1) that the final total pressure should be 30.0 mm Hg $\times 1/(1+0.93) = 15.6$ mm Hg. We have seen, on the other hand, in section 2, that a small amount of ethylene is subjected to dehydrogenated adsorption, which may cause a deviation from the above material balance (cf. 2.E.1); it is inferred from these results that the disturbing effects of the dehydrogenated adsorption are negligible for sufficient amounts of reactant gases.

4.2. Table 7 shows the kinetic parameters of the catalyzed hydrogenation in the presence of metallic catalysts. The first row shows the kinetic parameters of the uncatalyzed homogeneous hydrogenation in gas as observed by Pease [62] for reference, which ought to be excepted from the following illustration of columns referring to the catalyzed heterogeneous hydrogenation. Every blank indicates the lack of relevant description in the original paper, whereas "none" means that an appropriate process is not applied according to the original paper.

The column I gives the isotopic specification of the hydrogenation of ethylene, protium, deuterium and their mixture which are denoted by ^{1}H, D, and H, respectively, in accordance with the symbolism noted in section 1.[6]

The column II indicates the species of metal used as catalyst and the column III the form (and/or condition) of the catalyst, i.e., powder, foil, plate, wire, thimble, evaporated film or supported; when supported, the description is given, e.g., as 1 percent on SiO_2, indicating the weight percent of the catalyst metal and the material of supporter.

The column IV gives the procedures of preparation of the catalyst in order of their application. The column V presents, in distinction from the "preparation" in column IV, the pretreatment of the catalyst for conditioning the catalyst in order to secure reproducibility. "None" means that no such treatment is applied except the evacuation of the product of the foregoing run, in cases where the reaction is followed in a closed space as commented upon below.

The column VI gives temperature and column VII shows the initial values, $P_{E,0}$ and $P_{H,0}$, of partial pressures of C_2H_4 and H_2, P_E and P_H, respectively.

The column VIII gives three points of specification of the "modes of measurement." The first point specifies whether the "static," "stir," "circulation," "thermal siphon," "flow" or "flow-circulation" method of following the reaction was used. In the "static" or "stir" method, the reactant gas mixture is kept statically or stirred by means of a stirrer in a closed vessel over the catalyst, while in "circulation" the reactant gas mixture is driven by a circulation pump through a closed circuit over the catalyst. In the "thermal siphon" method, the circulation is effected by thermal siphon instead by means of a circulation pump. In the "flow" method, the reactant gas mixture is allowed to pass through a catalyst bed toward an open space. In the "flow-circulation" method, the gas mixture is rapidly circulated over the catalyst through a circuit, which is fed slowly with reactant gas mixture at one spot while the circulating gas is led out from the opposite spot of the circuit. The second point specifies that "hydrogen" or "ethylene" is brought into contact first with the catalyst, and the other reactant subsequently, or else that a homogeneous "mixture" of reactants is admitted over the catalyst. The third point specifies the modes of following the rate law. In case of "static," "stir," "circulation," or "thermal siphon," where the whole gas mixture is kept in a closed space, the rate law is determined either by measuring the "initial" rate, i.e., the rate of reaction at the moment of contact of reactant gas mixture with the catalyst at different partial pressures of reactant gases, or by following the "course" of the reaction by decrease of reactants or increase of products or both. In the former case, enough accuracy of measurements and reproducible experimental conditions have to be secured, whereas in the latter case it should be guaranteed that the course is not associated with such an advance of poisoning that distorts the coherence of data. The coincidence of the rate laws deduced by these alternative methods is a necessary condition for them being reality. The "initial" rate and the "course" method with the whole gas mixture kept in a closed space correspond, respectively, to the differential rate measurement by means of differential reactor [111] and the analysis of integral-conversion data [112] in case of the flow method, which are denoted in the Table by "differential" and "integral," respectively. In the "flow-circulation" method the conditions of differential reactor is secured by the rapid circulation.

The column IX shows the rate law, $v_h \propto P_E^m P_H^n$ of the catalyzed hydrogenation in terms of $m \equiv \partial \ln v_h / \partial \ln P_E$ and $n \equiv \partial \ln v_h / \partial \ln P_H$, where v_h is the rate. Attached figures, if any, indicate the range of application of the rate law. The column X gives the optimum temperature referred to in section 1, if observed at all.

In case of the "static," "stir," "circulation," or "thermal siphon" methods, where the whole gas mixture is confined in a closed space, v_h of reaction (4.1) is determined, either by change of the total pressure in the closed space or by the C_2H_6-yield, whereas in case of the flow method the rate is determined preferentially by C_2H_6-yield rather than by the decrease of C_2H_4 or H_2.

[6] Hydrogen atoms of approximately 99 percent D content is denoted by D, light hydrogen with natural D content by ^{1}H, respectively, but hydrogen gas of intermediate D content is denoted by H in this table.

TABLE 7. *Reaction kinetics of catalyzed hydrogenation of ethylene.*—Continued

The reactant gas mixture was either confined in a close space over the catalyst or allowed to flow through a catalyst bed toward an open space. "Modes of measurement" in the respective cases are as follows.

In the former case, the gas mixture was kept either "static" or dynamic by "stir" with a stirrer, by "thermal siphon," or by "circulation" through a close circuit with a circulation pump, respectively. "Mixture," "ethylene" and "hydrogen" mean that at the beginning of a run in the measurements, a homogeneous mixture of reactant gases, ethylene or hydrogen, respectively, were first admitted into the closed space and allowed to contact with the catalyst. "Initial" and "course" refer to the mode of observing the kinetics of the reaction by measuring the initial rate at different partial pressures of reactant gases or by following the change of composition of a charge of reactant gas mixture with time, respectively.

The latter case, signified by "flow," is classed as "differential" or "integral." In the differential method the conversion through the catalyst bed is restricted to practically infinitesimal an extent, so that the observed rate can be directly referred to practically unchanged partial pressures. In the "integral" method finite changes in partial pressures are observed as functions of flow rates to analyze them for the rate as a function of the partial pressures. In the "flow-circulation" method a gas mixture reacting over a catalyst bed is rapidly circulated through a circuit, which is steadily supplied with reactants while the circulating mixture is constantly led out for analysis; the results give directly coherent data of rate and partial pressures.

I	II	III	IV	V	VI	VII	VIII	IX			X	XI	XII
								Rate law					
Reaction	Metal	Form	Preparation	Pretreatment	Reaction temp. °C	Initial pressures of ethylene ($P_{E,0}$) and hydrogen ($P_{H,0}$) mm Hg	Modes of measurement	$\frac{\partial \ln v_h}{\partial \ln P_E} \equiv m$	$\frac{\partial \ln v_h}{\partial \ln P_H} \equiv n$	Given by the authors	Optimum temp. t_X °C ($=T_X$ °K -273)	Activation heat kcal · mole^{-1}	Authors
	Homogeneous reaction				475 ~ 550	$P_{H,0}/P_{E,0} = 1, 2, 3$ total pressure = 760, 380, 190	In Pyrex glass vessel	1	1			43.15	[62]
$C_2{}^1H_4 + {}^1H_2$	Ni	Foil	Nitrate formed on the surface decomposed by heating and reduced in H_2 at 270 °C	Evac. to less than 0.1 mm Hg	73 ~ 200	$P_{E,0} = 30$ $P_{H,0} = 730$	Static, mixture, course		1		137	1.8 ($T < T_X$)	[63]
			.....do.....	.....do.....	100 ~ 192	$P_{E,0} = 730$ $P_{H,0} = 30$	.....do.....	1					[63]
				700 °C in H_2 for 24 hr	400 ~ 600	$P_{E,0} + P_{H,0} = 760$ $P_{E,0} : P_{H,0} = 1 : 1$	Flow, differential					5.0 (400 ~ 500 °C)	[47]
			Reduced at 200 °C		−10 ~ 130	$P_{E,0} = 0.03$ $P_{H,0} < 0.04$	Static, ethylene, course	0 ($T < T_X$) 1 ($T > T_X$)	1 1		60	4.6 ($T < T_X$)	[64]
		Plate		Outgassed at 900 °C in ultra-high vacuum	35 ~ 85	$P_{H,0} > P_{E,0}$ $= 0.02 \sim 21.7$	Static, hydrogen, course	0 ~ −1	1		120 ($P_E = 2 \sim 4$)	11.0 ± 0.3 (Ar^+ ion bombardment) 10.7 ± 0.2 (Outgassing and annealing) 9.0 ± 0.6 (Outgassing and quenching) 7.9 ± 0.5 (Ar^+ ion bombardment and annealing) 6.0 ± 0.4 (Contamination at elevated temp.)	[65]
		Wire	600 °C in air and 300 °C in H_2	300 °C in H_2 for 20 hr	50	$P_{E,0} = P_{H,0} = 11.3$	Circulation, mixture, course		0.8 (initial) 1.0 (final)				[66]
			600 °C in air and 330 °C in H_2	200 °C in H_2	0 ~ 200	$P_{E,0} = 1 \sim 5$ $P_{H,0} = 2 \sim 8$	Static, mixture, course			$\frac{\partial \ln v_h}{\partial \ln (P_E + P_H)} = 0$	140 ($P_E = 3$, $P_H = 5$)		[67]
$C_2{}^1H_4 + D_2$	Ni	Wire	.....do.....	.....do.....	.....do.....	.....do.....	.....do.....			.....do.....	160 ($P_E = 3$, $P_H = 5$)	8	
$C_2{}^1H_4 + {}^1H_2$	Ni	Wire	600 °C in air and 300 °C in H_2		20 ~ 155	$P_{E,0} = 7 \sim 20$ $P_{H,0} = 10 \sim 30$	Static, mixture, course			.....do.....			[2]
$C_2{}^1H_4 + D_2$	Ni	Wire	600 °C in air and 330 °C in H_2	None	70 ~ 207	$P_{E,0} = 20.5 \sim 113$ $P_{H,0} = 82.4 \sim 159$	Static, ethylene, initial	0 (156 °C)	1			14 (70 ~ 100 °C) 0 ~ −1 (207 °C)	[68]
			.....do.....	.....do.....	55 ~ 120		Static, ethylene, initial	0	1			8.2 ± 0.5	[69]
$C_2{}^1H_4 + {}^1H_2$	Ni	Wire	600 °C in air, 300 °C in H_2 and annealed at 600 °C	300 °C in H_2	−45 ~ 95	$P_{E,0} = 0.02 \sim 0.15$ $P_{H,0} = 0.02 \sim 0.15$	Static, mixture, {initial / course}	0 (−45 °C, 0 °C)	0.7		60 ($P_E = 0.03$, $P_H = 0.09$)	5.3 ± 0.2 ($T < T_X$)	[70]
			Red-heated in air and 360 °C in H_2	Outgassed at at 200 °C	99 ~ 165	$P_{E,0} = 10 \sim 130$ $P_{H,0} = 10 \sim 160$	Static, mixture, course			$v_h = k_1 \frac{P_H P_E}{1 + k_2 P_E}$		0 ($= RT^2 \partial \ln k_1 / \partial T$)	[71]

TABLE 7. *Reaction kinetics of catalyzed hydrogenation of ethylene.* — Continued

I	II	III	IV	V	VI	VII	VIII	IX			X	XI	XII
								Rate law					
Reaction	Metal	Form	Preparation	Pretreatment	Reaction temp. °C	Initial pressures of ethylene ($P_{E,0}$) and hydrogen ($P_{H,0}$) mm Hg	Modes of measurement	$\frac{\partial \ln v_h}{\partial \ln P_E} \equiv m$	$\frac{\partial \ln v_h}{\partial \ln P_H} \equiv n$	Given by the authors	Optimum temp. t_X °C ($=T_X$ °K − 273)	Activation heat kcal · mole^{-1}	Authors
$H_4 + {}^1H_2$	Ni	Wire	Heated in air and in H_2	300 °C in H_2 0.5 hr	83 ~ 190	$P_{E,0} = 20 \sim 360$ $P_{H,0} = 50 \sim 400$	Static, initial	1.2 ~ 0.5 (135 °C)	0.7		180 ($P_E = 1.1$, $P_H = 3.7$)	5	[72]
			850 ~ 1150 °C in air, 300 ~ 420 °C in H_2		62 ~ 201	$P_{E,0} = 380 \sim 3040$ $P_{H,0} = 380 \sim 6080$	Stir, hydrogen, initial	0 (135 ~ 188 °C)	0.97 ± 0.07			13.4 (Porous, active) 15.5 (Reactivated by reduction) 11.3 (Smooth)	[73]
		Powder	$Ni(NO_3)_2$ decomposed at 400 °C and 480 °C in H_2	Evac. 2 hr	−78 ~ 0	$P_{E,0} = 100 \sim 400$ $P_{H,0} = 100 \sim 400$	Static, mixture {initial course	−0.6	0.98	$v_h \propto \frac{P_E P_H}{(1 + kP_H + k'P_E)^2}$		6	[12, 74]
			NiO reduced at 350 °C in H_2	250 °C in H_2 overnight	−78 ~ 125	$P_{E,0} = 253$ $P_{H,0} = 507$	Flow, differential					4	[58]
			NiSi alloy refluxed (Raney Ni)	300 °C in H_2	0 ~ 180	$P_{E,0} + P_{H,0} = 50 \sim 250$	Thermal siphon, mixture, course	0.6 (Calculate by the rate law given by the author for $P_E = P_H = 100$ 128 °C)	0.55	$v_h \propto \frac{P_E P_H}{(1 + kP_H + k'P_E)}$ ($k = 0.030$, $k' = 0.027$ 128 °C)		18.7 ± 1 (100 ~ 150 °C)	[75]
			$Ni(NO_3)_2$ decomposed at 400 °C, 500 °C in H_2 10 hr and 350 ~ 500 °C in H_2 15 hr	100 °C in H_2 1 hr	53 ~ 123	$P_{H,0}/P_{E,0} = 1.2$ $P_{E,0} + P_{H,0} = 760$	Flow, differential					8.1	[53]
		Evaporated film		None	−80 ~ 150		Circul.	0	1			10.7	[6]
			190 °C in C_2H_4 0.5 hr	None	20 ~ 180	$P_{E,0} = 2 \sim 10$ $P_{H,0} = 2 \sim 10$	Circul., mixture, initial	0 (114 °C)	1	$v_h \propto \frac{P_E P_H}{1 + kP_E}$ (165 °C)	165 ($P_E = P_H = 50$)	10.2 ($T < T_X$)	[13]
			190 °C in C_2H_4 0.5 hr	250 °C in H_2 0.5 hr	0 ~ 96	$P_{E,0} + P_{H,0} = 0.03 \sim 300$	Static, mixture, course	0	1			8.0 ($P_E + P_H = 3$)	[27]
$^1H_4 + D_2$	Ni	Evaporated film		None	−120 ~ −100	$P_{E,0} = 2.7$ $P_{H,0} = 8.1$	Static, initial	0	0.5			7	[76]
$^1H_4 + {}^1H_2$	Ni	Evaporated film		None	−40 ~ 40	$P_{E,0} = 49$ $P_{H,0} = 98$	Static, mixture, course	0	1			9.1 ~ 10.3	[29]
			32.3 °C in 100 mm Hg C_2H_4, 0.5 hr	32.3 °C in 100 mm Hg H_2, 0.25 hr	30 ~ 80	$P_{E,0} = 10 \sim 300$ $P_{H,0} = 10 \sim 300$	Static, ethylene, initial	−0.4 (32.3 °C) −0.2 (80 °C)				10.0 ($P_E = 53$, $P_H = 55$)	[77]
							Static, mixture, initial		Decreases with P_H from 1 to 0.7			7.8 ($P_E = 48$, $P_H = 58$)	
							Static, mixture, course	Initially 0, then 2.3 and then 1 with decrease of $P_E (\ll P_H)$	Decreases from 1 to 0.7 with $P_H (\ll P_E)$				

TABLE 7. *Reaction kinetics of catalyzed hydrogenation of ethylene.*—Continued

I	II	III	IV	V	VI	VII	VIII	IX			X	XI	XII
Reaction	Metal	Form	Preparation	Pretreatment	Reaction temp. °C	Initial pressures of ethylene ($P_{E,0}$) and hydrogen ($P_{H,0}$) mm Hg	Modes of measurement	Rate law $\frac{\partial \ln v_h}{\partial \ln P_E} \equiv m$	Rate law $\frac{\partial \ln v_h}{\partial \ln P_H} \equiv n$	Given by the authors	Optimum temp. t_X °C (= T_X °K − 273)	Activation heat kcal · mole^{-1}	Authors
$C_2H_4 + H_2$	Ni	Evaporated film		250 ~ 300 °C in H_2 40 min, evac. at reaction temp.	−15 ~ 15	$P_{H,0}/P_{E,0} = 1$ $P_{E,0} + P_{H,0} = \sim 1.5$	Static, mixture					6 ~ 8	[78]
				335 °C in H_2 1.5 hr	−28.5 ~ 70	$P_{E,0} = 10 \sim 300$ $P_{H,0} = 10 \sim 300$	Static, mixture, initial	−0.5 (0 °C)	0.9			7($P_E = P_H = 45$)	[79]
				None	0 ~ 200	$P_{E,0} = 15$ $P_{H,0} = 15$	Circul., mixture, initial				130	5.6 ($T < T_X$) −9.5 ($T > T_X$)	[22]
				.....do.....	−45 ~ 200	$P_{E,0} = \sim 0.05$ $P_{H,0} = \sim 0.05$	Static, mixture, initial				35	5 ($T < T_X$)	[61]
				.....do.....	−40 ~ 220	$P_{E,0} = 0.03 \sim 100$ $P_{H,0} = 0.03 \sim 20$	Circul. Static } mixture, initial				$\frac{1}{T_X} = \frac{1}{5300}(14.5 - \log P_E)$	3.3 ~ 5.5 ($T < T_X$) −5 ~ −14 ($T > T_X$)	[80]
		Supported 2.94% on SiO_2		500 °C in H_2	−78 ~ 0		Circul., mixture, initial	−0.08 ± 0.12 (−40 °C)	0.67 ± 0.10			8.4 ± 0.5	[81]
		Supported on Al_2O_3	$Ni(NO_3)_2$ calcined at 400 °C 10 hr, reduced in H_2 at 250 °C 24 hr, 170 °C in H_2 + excess C_2H_4	None	32 ~ 80	$P_{E,0} = 137 \sim 2090$ $P_{H,0} = 326 \sim 3260$ $\frac{P_{H,0}}{P_{E,0} + P_{H,0}} = 0.40 \sim 0.90$	Flow, differential	0.33 (90 °C)	0.93			11.6($P_E = 550$, $P_H = 200$)	[82, 83]
			$Ni(NO_3)_2$ calcined, 700 °C in H_2 2 hr	Oxidized in air reduced at 500 °C 2 hr	80 ~ 140	$P_{E,0} + P_{H,0} = 760$	Flow, differential					8.2	[84]
	Pt	Platinized foil		None	0 ~ 236	$P_{E,0} = 20 \sim 111$ $P_{H,0} = 20 \sim 67$	Static, mixture: initial	< 0 (25 °C)	> 0		160 ($P_E = 40$, $P_H = 20$)	10 (0 ~ 78 °C)	[85]
							Static, mixture: course			$\partial \ln v_h / \partial \ln (P_E + P_H) = 1$			
				200 °C in H_2 12 hr	0 ~ 52	$P_{E,0} = 50 \sim 150$ $P_{H,0} = 50 \sim 150$	Static, ethylene, initial	−0.5 (0 °C)	1.2				[86]
		Foil		650 °C in H_2 12 hr	70 ~ 130	$P_{E,0} = P_{H,0} = 380$	Flow, differential					4.5	[48]
		Wire	400 °C in air 20 ~ 30 min, 400 °C in H_2 20 ~ 30 min, 200 °C in C_2H_4 30 min	300 °C in H_2 30 min		$P_{E,0} = 20 \sim 80$ $P_{H,0} = 20 \sim 100$	Circul., mixture, initial	−0.5 ($T < T_X$) 0 ($T > T_X$)	1.2 1		240 ($P_E = 26$, $P_H = 116$)	10 ($T < T_X$)	[87]

TABLE 7. *Reaction kinetics of catalyzed hydrogenation of ethylene.*—Continued

I	II	III	IV	V	VI	VII	VIII	IX			X	XI	XII
								Rate law					
Reaction	Metal	Form	Preparation	Pretreatment	Reaction temp. °C	Initial pressures of ethylene ($P_{E,0}$) and hydrogen ($P_{H,0}$) mm Hg	Modes of measurement	$\frac{\partial \ln v_h}{\partial \ln P_E} \equiv m$	$\frac{\partial \ln v_h}{\partial \ln P_H} \equiv n$	Given by the authors	Optimum temp. t_X °C ($=T_X$ °K − 273)	Activation heat kcal · mole^{-1}	Authors
$C_2{}^1H_4 + {}^1H_2$	Pt	Supported 1% on Al_2O_3	H_2PtCl_6 heated in vac. at 200 °C and reduced in H_2 at 200 °C 12 hr	Reduction for shorter time than in "preparation," as activity decayed	−18 ~ 52	$P_{E,0} = 50 \sim 200$ $P_{H,0} = 20 \sim 200$	Static, ethylene, initial	−0.5	1.2 (0 °C)			9.9 ± 0.5 (0 ~ 50 °C)	[88]
$C_2{}^1H_4 + D_2$	Pt	.....do.....	.....do.....	.....do.....	−18 ~ 52	$P_{E,0} = 50 \sim 200$ $P_{H,0} = 20 \sim 200$	.....do.....	−0.5	1.2 (0 °C)			10.9 ± 0.5 (0 ~ 50 °C)	[89]
$C_2{}^1H_4 + D_2$	Pt	Supported on Al_2O_3	H_2PtCl_6 reduced in H_2 at 400 °C, exposed to air at room temp., 200 °C in H_2 0.5 hr		−20 ~ 50	$P_{E,0} = 100 \sim 250$ $P_{H,0} = 50 \sim 100$	.....do.....	−0.3 ± 0.1	1.0 ± 0.1 (0 °C)			15 ± 2 (0 ~ 40 °C) ($P_E = P_H = 100$)	
$C_2{}^1H_4 + {}^1H_2$	Pt	Supported 1% on SiO_2	H_2PtCl_6 heated in vac. at 200 °C, reduced in H_2 at 200 °C 12 hr	Reduction for shorter time than in "preparation," as activity decayed	0 ~ 52	$P_{E,0} = 100 \sim 250$ $P_{H,0} = 50 \sim 100$	.....do.....	−0.5	1.2 (0 °C)				[88]
		Supported on SiO_2	"Davison" gel impregnated with H_2PtCl_6				Circul., mixture, initial	0.25 ± 0.07	0.77 ± 0.07 (−40 °C)			8.4 ± 0.4	[81]
		Supported 0.05% on SiO_2	H_2PtCl_6 calcined at 538 °C in air 1 hr, reduced in H_2 at 500 °C 3 hr	10 min in H_2-flow at reaction temp.	45 ~ 93	$P_{E,0} = 5.3 \sim 302$ $P_{H,0} = 11.4 \sim 760$	Flow, differential	0 (97°, 45 °C)	0.5 (77°, 45 °C)			16 ($P_E = 22.8$, $P_H = 152$)	[90]
		Supported 1% on SiO_2–Al_2O_3	H_2PtCl_6 reduced in H_2 at 400 °C, exposed to air at room temp., 200 °C in H_2 0.5 hr	Reduction for shorter time than in "preparation," as activity decayed	0 ~ 78	$P_{E,0} = 50 \sim 290$ $P_{H,0} = 50 \sim 160$	Static, ethylene, initial	−0.5	1.2 (0 °C)				[88]
		Supported 1% on pumice	H_2PtCl_6 reduced in H_2 at 400 °C, exposed to air at room temp., 200 °C in H_2 0.5 hr	.....do.....	−18 ~ 50	$P_{E,0} = 20 \sim 150$ $P_{H,0} = 20 \sim 100$	Static, ethylene, initial	−0.5	1.2 (0 °C)				[88]
	Pd	Plate		300° ~ 380 °C in air, 250 °C in H_2 8 hr	0 ~ 209	$P_{E,0} = 100 \sim 500$ $P_{H,0} = 100 \sim 500$	Flow-circulation	0 0.5	1 1 (22 °C) (176 °C)			10.6 (0 ~ 42 °C) 1.2 (102 ~ 209 °C)	[91]
		Foil	400 °C in air 20 ~ 30 min, 400 °C in H_2 20 ~ 30 min, 200 °C in C_2H_4 30 min	300 °C in H_2 30 min	100 ~ 300	$P_{E,0} = 20 \sim 80$ $P_{H,0} = 20 \sim 100$	Circul., hydrogen, initial	0 $T < T_X$ 1 $T > T_X$			230 ($P_E = 2.6$, $P_H = 117$)		[87]

TABLE 7. *Reaction kinetics of catalyzed hydrogenation of ethylene.*—Continued

I	II	III	IV	V	VI	VII	VIII	IX			X	XI	XII
								Rate law					
Reaction	Metal	Form	Preparation	Pretreatment	Reaction temp. °C	Initial pressures of ethylene ($P_{E,0}$) and hydrogen ($P_{H,0}$) mm Hg	Modes of measurement	$\frac{\partial \ln v_h}{\partial \ln P_E} \equiv m$	$\frac{\partial \ln v_h}{\partial \ln P_H} \equiv n$	Given by the authors	Optimum temp. t_X °C ($=T_X$ °K -273)	Activation heat kcal · mole^{-1}	Authors
$C_2{}^1H_4 + {}^1H_2$	Pd	Foil		650 °C in H_2 12 hr	70 ~ 130	$P_{E,0} = P_{H,0} = 380$	Flow, differential					10 ~ 14	[48]
			Annealed at 800 °C 2 hrs in vac.	400 °C in H_2 1 min	0 ~ 180	$P_{E,0} = 100$ $P_{H,0} = 100$	Static, mixture, course		1			5.3 ~ 5.8	[52]
		Thimble		Evac. 1 hr at 350 °C	0 ~ 98	$P_{E,0} = 100$ $P_{H,0} = 100$	Stir, hydrogen, course	0	1			5.1 (Pure Pd) 6.1 (H_2 treated) 7.3 (C_2H_4 treated)	[92]
		Powder	$PdCl_2$ reduced with KOH and HCHOaq.	200 °C in O_2 200 °C in H_2	70 ~ 120	$P_{E,0} = 1.7 \sim 11.0$ $P_{H,0} = 0.9 \sim 6.4$	Static, hydrogen, initial	1	1			−2.9	[93]
			.....do.....	200 °C in O_2 200 °C in H_2	75 ~ 105	$P_{E,0} = 49.2 \sim 151.0$ $P_{H,0} = 199 \sim 560$	.....do.....	~ 2.4	~ −2	$r_h = \frac{P_E}{P_H}$		11.4	[93]
		Supported on SiO_2	"Davison" gel impregnated with $PdCl_2$				Circul., mixture, initial	-0.03 ± 0.07	0.66 ± 0.55			8.4 ± 0.4	[81]
		Supported on Al_2O_3	Reduced from a convenient salt in H_2 at 400 °C, exposed to air at room temp., 200 °C in H_2 0.5 hr		−36 ~ 77	$P_{E,0} = 25 \sim 200$ $P_{H,0} = 25 \sim 350$	Static, ethylene, initial	0	1			11.4 ± 1.0 (50 ~ 77 °C) ($P_E = P_H = 100$)	[94]
$C_2{}^1H_4 + D_2$	Rh	Evaporated film		None	−120 ~ −100	$P_{E,0} = 2.7$ $P_{H,0} = 8.1$	Static, initial					7	[76]
$C_2{}^1H_4 + {}^1H_2$	Rh	Supported on SiO_2	"Davison" gel impregnated with $RhCl_3 \cdot 3H_2O$				Circul., mixture, initial	-0.74 ± 0.18	0.85 ± 0.11				[81]
$C_2{}^1H_4 + D_2$	Rh	Supported on Al_2O_3	Reduced from a convenient salt in H_2 at 400 °C, exposed to air at room temp., 200 °C in H_2 0.5 hr		−18 ~ 110	$P_{E,0} = 50 \sim 100$ $P_{H,0} = 26 \sim 250$	Static, ethylene, initial	0	1			12 ± 2 (73 ~ 110 °C) ($P_E = P_H = 100$)	[94]
$C_2{}^1H_4 + D_2$	Ru	Supported 5% on Al_2O_3	$RuCl_3 \cdot 3H_2O$ reduced in H_2 at 200 °C 5 hr		0 ~ 80	$P_{E,0} = 28 \sim 100$ $P_{H,0} = 54 \sim 165$	.....do.....	−0.2	1			8.7 ± 0.5 (32 ~ 80 °C) ($P_E = 75$, $P_H = 76$)	[95]

TABLE 7. *Reaction kinetics of catalyzed hydrogenation of ethylene.*—Continued

I	II	III	IV	V	VI	VII	VIII	IX			X	XI	XII
								Rate law					
Reaction	Metal	Form	Preparation	Pretreatment	Reaction temp. °C	Initial pressures of ethylene ($P_{E,0}$) and hydrogen ($P_{H,0}$) mm Hg	Modes of measurement	$\frac{\partial \ln v_h}{\partial \ln P_E} \equiv m$	$\frac{\partial \ln v_h}{\partial \ln P_H}$ n	Given by the authors	Optimum temp. t_X °C ($=T_X$ °K -273)	Activation heat kcal · mole^{-1}	Authors
$C_2{}^1H_4 + {}^1H_2$	Ru	Supported on SiO_2	"Davison" gel impregnated with $RuCl_3 \cdot 3H_2O$				Circul., mixture, initial	-0.95 ± 0.08	0.95 ± 0.05 (−70 °C)			8.4 ± 0.4	[81]
	Ir	Supported on Al_2O_3	Ammonium chloroiridate reduced in H_2 at 400 °C, exposed to air, 200 °C in H_2 0.5 hr		−20 ~ 150		Static, ethylene, initial	-0.4 ± 0.1	1.6 ± 0.1 (60 °C)			13.8 ± 1.0 (80 ~ 120 °C) ($P_E = 50$, $P_H = 100$)	[89]
$C_2{}^1H_4 + D_2$	Os	Supported 5% on Al_2O_3	Ammonium chloroosmate reduced in H_2 at 200 °C 5 hr		0 ~ 80	$P_{E,0} = 50$ $P_{H,0} = 27 \sim 203$	Static, ethylene, initial		1 (24 °C)			8.5 ± 0.5 (17 ~ 47 °C) ($P_E = P_H = 50$)	[95]
$C_2{}^1H_4 + {}^1H_2$	Cu	Foil		700 °C in H_2 24 hr	550 ~ 700	$P_{E,0} + P_{H,0} = 760$ $P_{E,0} = 76 \sim 380$	Flow, differential					19.5	[47]
		Evaporated film		250 ~ 300 °C in H_2 40 min, evac. at reaction temp.		$P_{H,0}/P_{E,0} = 1$ $P_{E,0} + P_{H,0} \sim 1.5$	Static, mixture, course	0	0.4			6 ~ 8	[78]
		Powder	Cu reduced and annealed at 250 °C 1 hr		150 ~ 275	$P_{E,0} = 340 \sim 440$ $P_{H,0} = 190 \sim 440$	Stir	1	1			12.0 (150 ~ 200 °C) 1.3 (200 ~ 250 °C) 0 (250 ~ 275 °C)	[96]
			Cu reduced in H_2 200 °C 30 ~ 40 hr, annealed at 450 °C 1.5 hr		0 ~ 20	$P_{H,0}/P_{E,0} = 0.5, 1.2$ $P_{E,0} + P_{H,0} = 380 \sim 760$	Static, mixture, initial	−0.4	0.8 (0 °C)			7.8	[97]
			CuO reduced in H_2 at 200 °C 30 40 hr, annealed at 500 ~ 550 °C		150 ~ 250	.....do.....	.....do.....	0.66	0.8 (200 °C)			10.8 (150 ~ 200 °C) 7 (200 ~ 250 °C) ($P_E = 507$, $P_H = 253$)	[98]
			$CuCO_3$ decomposed, reduced in H_2 at 350 °C	200 °C in H_2 overnight	−73 ~ 125	$P_{E,0} = 253$ $P_{H,0} = 507$	Flow, differential					8	[58]
			$Cu(NO_3)_2$ decomposed at 400 °C, in H_2 500 °C 10 hr, in H_2 350 ~ 500 °C 15 hr	100 °C in H_2 1 hr	−10 ~ 25	$P_{H,0}/P_{E,0} = 1.2$ $P_{E,0} + P_{H,0} = 760$	Flow, differential					7.9	[53]
		Powder mixed with 50 mole % MgO	CuO, MgO mixture reduced in H_2 at 250 °C		9 ~ 79	$P_{E,0} = 36 \sim 512$ $P_{E,0} + P_{H,0} = 760$	Flow, integral	0	1			13.32	[99]

TABLE 7. *Reaction kinetics of catalyzed hydrogenation of ethylene.* – Continued

I	II	III	IV	V	VI	VII	VIII	IX			X	XI	XII
								Rate law					
Reaction	Metal	Form	Preparation	Pretreatment	Reaction temp. °C	Initial pressures of ethylene ($P_{E,0}$) and hydrogen ($P_{H,0}$) mm Hg	Modes of measurement	$\frac{\partial \ln v_h}{\partial \ln P_E} \equiv m$	$\frac{\partial \ln v_h}{\partial \ln P_H} \equiv n$	Given by the authors	Optimum temp. t_X °C ($= T_X$ °K − 273)	Activation heat kcal · mole^{-1}	Authors
$C_2{}^1H_4 + {}^1H_2$	Cu	Supported on brick	$Cu(NO_3)_2$ decomposed at 200 °C in H_2, annealed at 500 °C 8 hr		0 ~ 100	$P_{E,0} = 95 \sim 570$ $P_{H,0} = 95 \sim 570$	Static, mixture, initial	0	1 (100 °C)			13.4 (not annealed 0 ~ 60 °C) 13.2 (annealed 60 ~ 100 °C) ($P_E = P_H = 380$)	[100]
		Supported on glass beads	Cuprous hydroxides reduced		194 ~ 220	$P_{E,0} = 253 \sim 507$ $P_{H,0} = 253 \sim 507$	.....do.....	1	1 (220 °C)			6 ($P_E = P_H = 380$)	[100]
		Supported on SiO_2	"Sorpsil" silica gel impregnated with $Cu(NO_3)_2$				Circul., mixture, initial	0.06 ± 0.12	0.69 ± 0.09 (80 °C)			8.4 ± 0.4	[81]
		Supported 9.8% on Al_2O_3	275 °C in H_2		51 ~ 69	$P_{E,0} = 76 \sim 532$ $P_{H,0} = 152 \sim 532$	Circul., mixture, course			$v_h \propto \frac{P_E P_H}{(1 + kP_E)^2}$		> 14.1	[101]
		Supported on kieselguhr	$Cu(NO_3)_2$ reduced at 300 °C in H_2		109 ~ 258	$P_{E,0} = 46$ $P_{H,0} = 113$	Circul., mixture, course	1 ($T < T_X$) 1 ($T > T_X$)	0.5 ($T < T_X$) 0 ($T > T_X$)		~ 200		[102]
$C_2{}^1H_4 + {}^1H_2$ $C_2D_4 + {}^1H_2$	Cu	Powder mixed with MgO	4 : 1 mixture of $Mg(OH)_2$, $Cu(OH)_2$ reduced		−20 ~ 40	$P_{E,0} = 50 \sim 100$ $P_{H,0} = 50 \sim 100$	Static, mixture, course					11.8 ($C_2{}^1H_4$) 11.3 (C_2D_4) ($P_E = P_H = 50$)	[103]
$C_2{}^1H_4 + D_2$	Fe	Evaporated film		None	−120 ~ −100	$P_{E,0} = 2.1$ $P_{H,0} = 8.1$	Static, initial					7	[76]
$C_2{}^1H_4 + {}^1H_2$	Fe	Evaporated film	32.3 °C in $C_2{}^1H_4$ 0.5 hr	32.3 °C in H_2 15 min	30 ~ 80	$P_{E,0} = 10 \sim 300$ $P_{H,0} = 10 \sim 300$	Static, ethylene, initial	−0.6	0.87 (32.3 °C)			7.3 ($P_E = 55$, $P_H = 52$)	[77]
							Static, ethylene, course	Decrease from 0.85 to 0.19 as P_E increases	0.84 (32.3 °C)				
							Static, hydrogen, course	0.94 (32.3 °C)					
		Powder	Fe(II) oxalate reduced, sintered in vac.	Evac. at 360 °C 2 hr	0 ~ 175		Static					8.4 (30 ~ 75 °C)	[104]
$C_2{}^1H_4 + D_2$	Fe	Powder	.....do.....	.....do.....	.....do.....		.....do.....					8.3 (30 ~ 50 °C) 12.5 (55 ~ 75 °C)	
$C_2{}^1H_4 + {}^1H_2$	Fe	Powder, 0.15% Al_2O_3 as impurity	425 ~ 450 °C in H_2 60 hr and 525 °C 8 hr	450 °C in H_2 1 hr, evac. 2 hr	−89 ~ −40	$P_{E,0} = 80 \sim 585$ $P_{H,0} = 110 \sim 335$	Static, mixture, course	0	1 ~ 0.5 (−79 °C)			5.1 (−89 ~ −79 °C, $P_E = P_H = 240$)	[105]

TABLE 7. *Reaction kinetics of catalyzed hydrogenation of ethylene.* – Continued

I	II	III	IV	V	VI	VII	VIII	IX			X	XI	XII
								Rate law					
Reaction	Metal	Form	Preparation	Pretreatment	Reaction temp. °C	Initial pressures of ethylene ($P_{E,0}$) and hydrogen ($P_{H,0}$) mm Hg	Modes of measurement	$\frac{\partial \ln v_h}{\partial \ln P_E} \equiv m$	$\frac{\partial \ln v_h}{\partial \ln P_H} \equiv n$	Given by the authors	Optimum temp. t_X °C (= T_X °K − 273)	Activation heat kcal · mole^{-1}	Author
$C_2{}^1H_4 + {}^1H_2$	Fe	Powder, 1.59% K_2O 1.3% Al_2O_3	450 ~ 500 °C in H_2 80 hr	450 °C in H_2 1 hr evac. 2 hr	−89 ~ −40	$P_{E,0} + P_{H,0} = 450$	Static, mixture, course					5.3(−50 ~ −40 °C)	[105]
		Powder, 0.15% Al_2O_3 as impurity	Fe oxide reduced at 400 ~ 440 °C 59 hr and 515 532 °C 8 hr in H_2	400 °C in H_2 1 hr	−50 ~ −20	$P_{E,0} = 100 \sim 400$ $P_{H,0} = 50 \sim 300$	Circul., mixture, initial	0.6 (−35 °C)				4.2($P_E = P_H = 200$)	[106]
							course	1.0 (−35 °C)					
		Supported on brick	Fe nitrate calcined at 350 400 °C, reduced in H_2 at 450 °C, sintered at 500 °C		0 ~ 20	$P_{E,0} = 253 \sim 507$ $P_{H,0} = 253 \sim 507$	Static, mixture, initial	~0 (0 °C)	·0			6.2($P_E = P_H = 380$)	[107]
		Supported on SiO_2	"Sorpsil" impregnated with $Fe(NO_3)_3$				Circul., mixture, initial	0.04 ± 0.13 (30 °C)	0.91± 0.11			8.4 ± 0.4	[81]
	Co	Supported on SiO_2	"Sorpsil" impregnated with $Co(NO_3)_2$				.....do.....	−0.19 ± 0.10 (−60 °C)	0.55± 0.66			8.4 ± 0.4	[81]
$C_2{}^1H_4 + D_2$	W	Evaporated film		None	−120 ~ −100	$P_{E,0} = 2.7$ $P_{H,0} = 8.1$	Static, initial					5 ~ 6	[76]
$C_2{}^1H_4 + {}^1H_2$	Ag	Foil		700 °C in H_2 24 hr	550 ~ 700	$P_{E,0} + P_{H,0} = 760$ $P_{H,0} = 103 \sim 388$	Flow, differential					27.1	[49]
		Supported on brick	$AgNO_3$ calcined at 350 ~ 400 °C, 150 ~ 250 °C in H_2		50 ~ 100	$P_{E,0} = 253 \sim 507$ $P_{H,0} = 253 \sim 507$	Static, mixture, initial	0 (100 °C)	1			9.8 ($P_E = P_H = 380$)	[107]
	Cu-Ni alloy	Foil		700 °C in H_2 24 hr	400 ~ 600	$P_{E,0} + P_{H,0} = 760$ $P_{E,0} = 114 \sim 395$	Flow, differential					2.5 (max. at ca. 50 atom % Ni)	[47]
			Outgassed in ultra high vacuum at 900 °C	Ar^+ bombardment	35 ~ 85	$P_{H,0} > P_{E,0}$ $P_{E,0} = 0.02 \sim 21.7$	Static, mixture, initial					11	[65]
		Evaporated film	Evaporated from Cu and Ni wires, annealed in H_2 at 300 °C overnight	250 ~ 300 °C in H_2 40 min	−15 ~ 15	$P_{H,0}/P_{E,0} = 1$ $P_{E,0} + P_{H,0} = \sim 1.5$	Static, mixture, course	0 (74.2 % Ni)	0.4			6 ~ 8	[78]
		Evaporated film 54.6 atom % Cu	Evaporated from alloy pellet	350 °C in H_2 1.5 hr	−28.5 ~ 70	$P_{E,0} = 10 \sim 300$ $P_{H,0} = 10 \sim 300$	Static, mixture, initial	−0.3 (0 °C)	0.9			8.9 ($P_E = P_H = 45$)	[79]

TABLE 7. *Reaction kinetics of catalyzed hydrogenation of ethylene.*—Continued

I	II	III	IV	V	VI	VII	VIII	IX			X	XI	XII
								Rate law					
Reaction	Metal	Form	Preparation	Pretreatment	Reaction temp. °C	Initial pressures of ethylene ($P_{E,0}$) and hydrogen ($P_{H,0}$) mm Hg	Modes of measurement	$\frac{\partial \ln v_h}{\partial \ln P_E} \equiv m$	$\frac{\partial \ln v_h}{\partial \ln P_H} \equiv n$	Given by the authors	Optimum temp. t_X °C ($=T_X$ °K -273)	Activation heat kcal · mole^{-1}	Authors
$^1H_4+{}^1H_2$	Cu-Ni alloy	Powder	Carbonates decomposed, red. in H_2 at 350 °C	250 °C in H_2 overnight	$-73 \sim 125$	$P_{H,0}/P_{E,0}=1.5$ $P_{E,0}+P_{H,0}=760$	Flow, differential					4	[78]
			Nitrates decomposed at 400 °C, in H_2 500 °C 10 hr, in H_2 350 ~ 500 °C 15 hr	100 °C in H_2 1 hr	$-75 \sim 41$	$P_{H,0}/P_{E,0}=1.2$ $P_{E,0}+P_{H,0}=760$	Flow, differential					9.3 ($-70 \sim -41$ °C, 90 % Cu) 9.7 ($-75 \sim -63$ °C, 63 % Cu)	[53]
	Ni-Fe alloy	Evaporated film	Evaporated from alloy pellet of 10.8 atom % Fe	350 °C in H_2 1.5 hr	$-28.5 \sim 70$	$P_{E,0}=10 \sim 300$ $P_{H,0}=10 \sim 300$	Static, mixture, initial	-0.3 (0 °C)	0.8			8.9	[79]
	Ni-Pd alloy	Evaporated film	Evaporated from alloy pellet of 5.5 atom % Pd	……do……	……do……	……do……	……do……	-0.2 (-28.5 °C)	0.6			7	[79]
	Cu-Ag alloy	Wire		700 °C in H_2 24 hr	$550 \sim 700$	$P_{E,0}+P_{H,0}=760$ $P_{E,0}=106 \sim 388$	Flow, differential					$17 \sim 16$ ($3 \sim 92$ % Ag)	[47]
	Cu-Pt alloy	Foil		650 °C in H_2 12 hr	$70 \sim 130$	$P_{H,0}/P_{E,0}=1$ $P_{E,0}+P_{H,0}=760$	Flow, differential					$5.4 \sim 14$	[48]
	Cu-Pd alloy	Foil		……do……	……do……	……do……	……do……					$10 \sim 14$	[48]
	Pd-Ag alloy	Foil	Annealed at 800 °C 2 hr in vac.	400 °C in H_2 1 min	$0 \sim 400$	$P_{E,0}=100$ $P_{H,0}=100$	Static, mixture, course					~ 5.2 (20 ~ 50 % Ag) 8 (60 % Ag)	[52]
	NaH	Lump		Evac. at 200 °C 2 hr	$100 \sim 200$	$P_{E,0}=P_{H,0}=300$	Static, mixture					8	[108]
	LiH	Lump		……do……	……do……	……do……	……do……					17	[108]
	Ta hydride	Powder		Evac. at 800 °C	$200 \sim 500$	$P_{E,0}=50 \sim 500$ $P_{H,0}=50 \sim 500$	Static, hydrogen, initial	1 (250 °C and 300 °C)	From positive to negative as P_H increases			<0 ($P_H<80$, 250 ~ 300 °C) >0 ($P_H>80$, 250 ~ 300 °C)	[109]
	CaH_2	Powder		Evac. at 450 °C 1 hr	$-78 \sim 450$	$P_{E,0}=50 \sim 500$ $P_{H,0}=50 \sim 500$	Static, mixture, initial	1 ($P_E<100$, 0 ~ 50 °C) 0 ($P_E>100$, 0 ~ 50 °C)	1		200 ($P_E=41.6$, $P_H=41.7$)	1.4 (0 ~ 150 °C) ($P_E=41.6$, $P_H=41.7$)	[110]

The catalyzed hydrogenation is throughout approximately first order with respect to hydrogen partial pressure, as seen from table 7, irrespective of the catalyst metal, preparation and pretreatment, whereas the dependence of its rate upon ethylene partial pressure varies considerably with catalyst metal, etc. The linear relation between ln v_h and ln P_E is rather poor in many cases, hence the values of $m \equiv \partial \ln v_h / \partial \ln P_E$ in the table are just as much inaccurate.

4.3. Detailed comments will be made below upon the representative case of nickel.

4.3.1. Zur Strassen [64] has introduced hydrogen over nickel wire environed preliminarily by ethylene under its own vapor pressure (0.03 mm Hg) at liquid air temperature, and observed the decrease of total pressure, which was identified with rate v_h of reaction (4.1). He thus found that the reaction was first order with respect to hydrogen throughout. The quotient v_h/P_H was found to vary with partial pressure P_E of ethylene as [64]

$$v_h/P_H \propto P_E/(1+k'P_E), \qquad (4.2)$$

where k' is a constant at constant temperature, decreasing rapidly with increase of temperature, $k'P_E$ passing unity around the optimum temperature, so that $m \equiv \partial \ln v_h / \partial \ln P_E$ is zero or unity sufficiently below or above the optimum temperature, respectively.

4.3.2. In the above experiment of zur Strassen [64], the catalyst was initially contacted with ethylene as denoted by "ethylene" in column VIII of table 7. Masuda [70] recently observed the hydrogenation rate in the presence of nickel wire over approximately the same ranges of partial pressures, introducing a homogeneous mixture of reactant gases over the catalyst. The reproducibility of catalytic activity was secured within 15 percent by a pretreatment at 300 °C in hydrogen of 15 to 20 mm Hg pressure for 1 hr followed by evacuation to 10^{-6} mm Hg. The initial rate was thus found proportional to $P_E^0 P_H^{0.7}$ from −45 to 0 °C. Figure 11(a) shows the dependence of the initial rate on P_H. It follows that $P_H^{0.3}$ decreases linearly with time, provided the above rate law holds throughout the course of catalyzed hydrogenation, which is verified as shown in figure 11(b), fulfilling the necessary condition, referred to in 4.2., of the real rate law.

4.3.3. We see from table 7 that $m \fallingdotseq 0$ and $n \fallingdotseq 1$ at temperatures below the optimum, while $m \fallingdotseq n \fallingdotseq 1$ above the optimum in most cases, in accordance with eq (4.2). However, v_h depends perceptibly upon P_E even at temperatures appreciably below the optimum in those cases where the total pressure of the catalyzed hydrogenation is higher than 1 atm [82], where the catalyst is preliminarily treated with ethylene of much higher pressure [82, 101] than in the case of the experiment of zur Strassen [64], and where the reaction vessel is preliminarily only incompletely evacuated. Even a negative value of m is reported [71, 74] with nickel powder, as shown in table 7. According to Schwab [113], however, this negative value of m disappears when the catalyst and the reactant gases are purified.

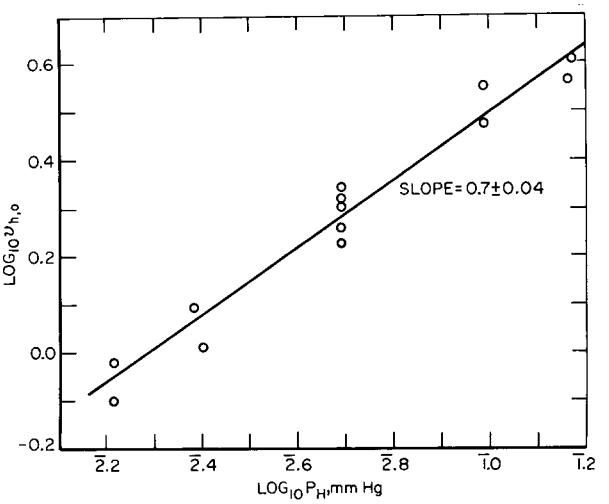

FIGURE 11a. *Dependence of the initial rate,* $v_{h,0}$, *of hydrogenation over* Ni *wire upon* $P_{H,0}$ [70].
$v_{h,0}$ is the initial value of v_h given in hydrogenated percent C_2H_4 min^{-1} at $P_E = 0.049$ mm Hg.

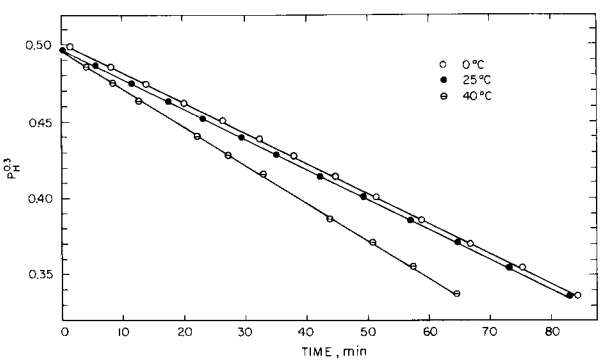

FIGURE 11b. *Partial pressure of hydrogen,* P_H *(in mm Hg), in course of a run of catalyzed hydrogenation in the presence of* Ni *wire* [70].
○: 0 °C. ⊙: 25 °C. ⊖: 40 °C.

4.3.4. Tucholski and Rideal [67] as well as Farkas, Farkas and Rideal [2] reported that the catalyzed hydrogenation in the presence of nickel was zeroth order with respect to total pressure, whereas their experimental results could be fitted adequately to the rate law with $m=0$ and $n=1$, the first order rate $(1/t) \ln (P_{H,0}/P_H)$ remaining fairly constant as shown in table 8, where $P_{H,0}$ is the initial value of P_H.

TABLE 8. *Hydrogenation of light ethylene over* Ni *wire* [2]

React. temp. °C	Time t min	Partial pressures, mm Hg		$k_h=(1/t)\ln(P_{H,0}/P_H)$, min^{-1}	Atom % of deuterium in hydrogen
		P_E	P_H		
20	0	21.5	32.5		30.6
	10	13.5	24.5	0.0123	30.0
	25	5.5	16.5	.0118	33.2
	37	1.0	12.0	.0127	33.8
155	0	20	24		62
	?	13	17		22
155	0	13	16		0
	?	10	13		13

4.3.5. The observations on activation heats are no less divergent than the rate laws. Tuul and Farnsworth [65] have observed the catalyzed hydrogenation of ethylene in the presence of a 2.5 cm^2 nickel plate subjected preliminarily to different pretreatments. The results are, as shown in figure 12, that the activation heat varies between 3.6 kcal and 12 kcal, revealing the so-called compensation effect. The activation heat was derived from rate constants k_h at 35, 55, and 85 °C as deduced from experimental results assuming the rate law, $m=0$, $n=1$. The linearity of ln k_h to $1/T$ is, however, rather poor, hence the activation heat is just as much inaccurate. The cleanest surface is, according to them [65], that bombarded by Ar^+ ion, which reveals the highest activation heat, 12 kcal.

This high value activation heat coincides, however, with that on the carbided nickel surface [13, 82, 114]. Moreover, Tull and Farnsworth's observation of the optimum temperature, T_X, in conjunction with partial pressure of ethylene, P_E, falls into the characteristic correlation between T_X and P_E, referred to below, of the carbided surface. It is possible that adsorbed complex on the nickel plate, which was used for every experiment as mentioned above, is decomposed by the bombardment to form the carbided surface. On the basis of the arguments in section 2, the most adequate value of the activation heat below the optimum is 5 to 6 kcal as obtained by Miyahara and others [22, 26, 61, 64, 70, 80] with equimolar mixtures of the reactant gases over evaporated nickel film.

4.4. An optimum temperature is observed, as seen from table 7, not only for nickel catalyst but also for platinum, palladium, iron, and copper catalysts. Tuul and Farnsworth [65] advanced and empirical relation, in case of nickel, between the optimum temperature t_X(°C) and P_E (in mm Hg) as $t_X=30\log_{10}P_E+105$. Sato and Miyahara [80] found linear relations between $\log_{10}P_E$ and the reciprocal of the absolute temperature of the optimum, T_X, to hold for reduced nickel wire, freshly evaporated surfaces or carbided surfaces of nickel film, respectively as

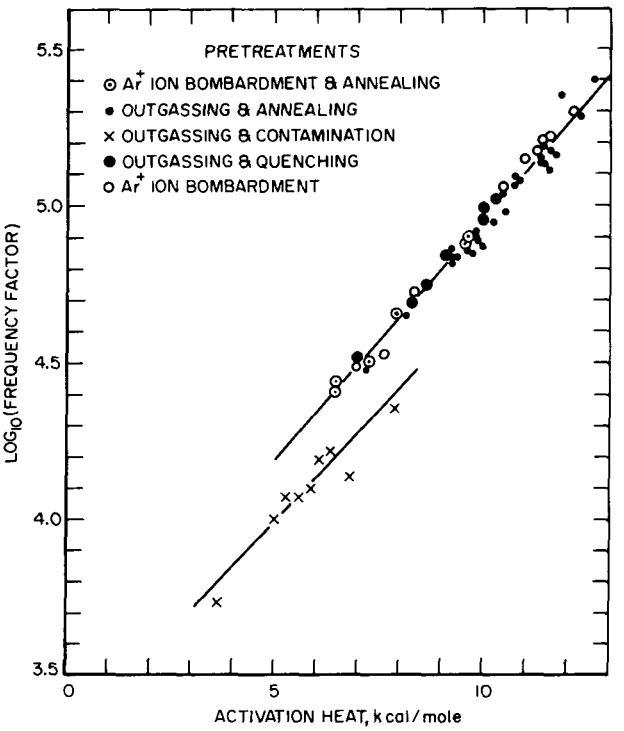

FIGURE 12. *Compensation effect in the catalyzed hydrogenation of ethylene over a nickel plate subjected to different pretreatments* [65].

shown in figure 13; the latter two surfaces have been denoted by F and C, respectively, in 2.8.3. The linear relation over surface F is analytically [80] (P_E in mm Hg)

$$1/T_X=(1/5300)(14.5-\log_{10}P_E). \qquad (4.3)$$

The optima observed by Tuul and Farnsworth [65] fall on the linear relation over surface C observed by Sato and Miyahara [80] as mentioned above.

4.5. Reference is made to the interesting work of Apel'baum and Temkin [91] on the catalyzed hydrogenation on palladium membrane. The apparatus used was separated into a hydrogen chamber, A, and a reaction chamber, B, by a 0.3 mm thick palladium membrane, as shown in figure 14. The membrane had an area of 15.7 cm^2 on the side of the reaction chamber. A mixture of hydrogen and ethylene was circulated through the reaction chamber by means of a circulation pump, C, at a rate of 2 liter/min through a circuit which was steadily fed with reactant gas mixture at a rate of 25 cm^3/min, while a corresponding amount of circulating gas was led out simultaneously. The reaction was followed by measuring the amount of ethane in the gas led out. Apel'baum and Temkin have thus investigated the kinetics of the catalyzed hydrogenation, simultaneously following the fugacity of adsorbed hydrogen on the side of reaction chamber, which was identified with the hydrogen pressure P_A in the hydrogen chamber adjusted

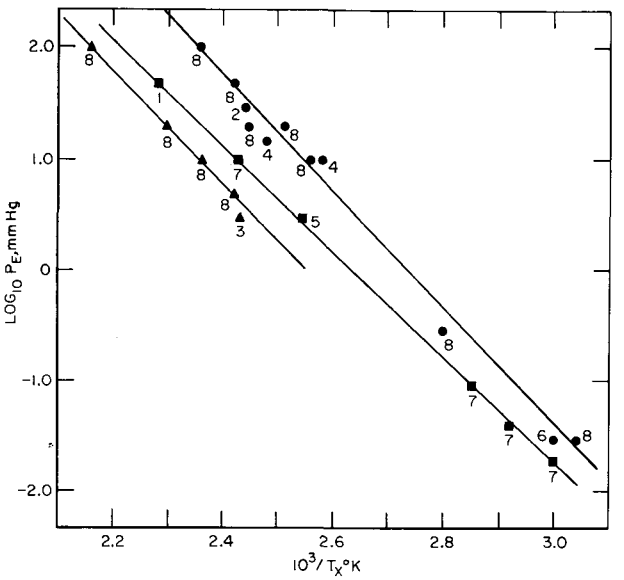

FIGURE 13. *Dependence of optimum temperature,* T_X, *on ethylene partial pressure,* P_E, *in catalyzed hydrogenation of ethylene in the presence of nickel [80].*

○: Freshly evaporated surface, F, of evaporated film or pretreated foil.
□: Carbided surface, C, of evaporated film.
△: Pretreated wire.

Annexed figures refer to respective authors as
1: Jenkins and Rideal [13], 2: Rideal [63], 3: Tucholski and Rideal [67], 4: Miyahara and Narumi [114], 5: Tuul and Farnsworth [65], 6: zur Strassen [64], 7: Miyahara [80], 8: Sato and Miyahara [80].

TABLE 9. *Catalyzed hydrogenation of ethylene over palladium, with fugacity of adsorbed hydrogen followed simultaneously [91]*
$v_{h,x=0}$: Hydrogenation rate, v_h, at $x=0$.
x: Diffusion rate of hydrogen through the Pd-membrane.

Tem. °C	No. of experiment	Partial pressure, mm Hg in reaction chamber			Fugacity of adsorbed hydrogen, P_A mm Hg	$v_{h,x=0}$ C_2H_6 cm³ NTP/hr
		C_2H_4	C_2H_6	H_2		
22	15	231	84.5	424	165	156
	16	239.5	77.5	439	205	141
	18	254.5	59.0	456	235	107
	20	263.5	35.5	453	64	70
176	1	15	242	496	492	186
	2	184	345	227	224	456
	4	26	231	504	500	350
	7	85	332	336	327	470
	8	111	290.5	357.5	353	419

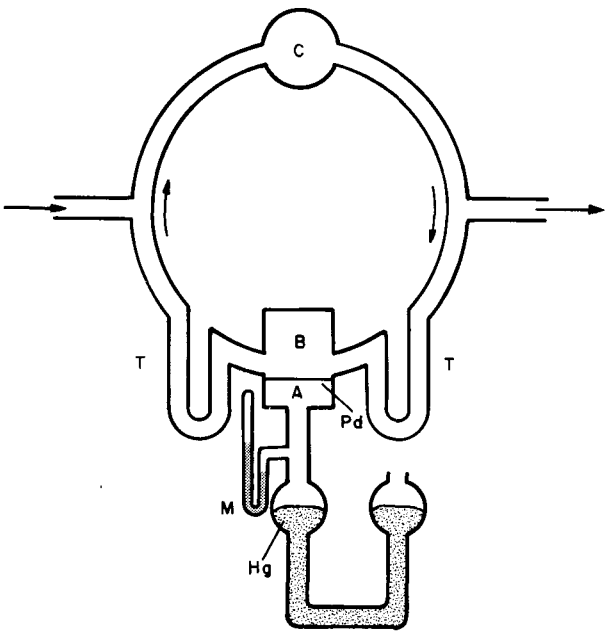

FIGURE 14. *Apparatus for simultaneous observation of the catalyzed hydrogenation of ethylene over* Pd *and of the fugacity of adsorbed hydrogen [91].*
A: H_2-chamber, B: reaction chamber, C: circulation pump, T: cold trap at −78 °C, M: Hg-manometer.

to zero diffusion rate of hydrogen through the membrane. The conditions of experiments and observed kinetics are shown in table 7 and the associated observations of P_A-values in table 9.

We see from table 9 that $P_H \doteqdot P_A$ at 176 °C but $P_H \gg P_A$ at 22 °C, which shows that adsorbed hydrogen is in equilibrium with hydrogen in gas or adsorption and desorption are so much rapid at 176 °C but not at 22 °C.

Apel'baum and Temkin observed further the rate v_h of hydrogenation in conjunction with the rate x of diffusion of hydrogen through the membrane to find the increment in number of ethane molecules per diffused hydrogen atom, i.e.,

$$n = \frac{v_h - v_{h,x=0}}{x}.$$

The result, $n \doteqdot 0.01$ at 176 °C and $n \doteqdot 0.5$ at 22 °C. indicates that the hydrogen used in the catalyzed hydrogenation originates almost all from gaseous hydrogen in the reaction chamber at 176 °C but from diffused hydrogen at 22 °C in conformity with the above conclusion on the adsorption.

5. Reactions Associated With the Catalyzed Hydrogenation

Farkas, Farkas, and Rideal [2] discovered that the catalyzed hydrogenation of ethylene is accompanied by parahydrogen conversion and exchange of hydrogen atoms when they followed the parahydrogen content and deuterium content in hydrogen by means of the thermal conductivity method. Since 1950, relative amounts of different deuteroethylenes and deuteroethanes in the deuteration product of ethylene have become traceable by means of mass spectrometry. Infrared spectrometry has

also become popular in the analysis of deuterocompounds. The profiles thus disclosed of the catalyzed hydrogenation impressed an unexpected complexity of the problem on the one hand but promised to be powerful tools of solving it on the other hand.

5.1. Experimental Methods

Such profiles of the reaction which are traceable by means of the thermal conductivity gage alone are dealt with in 5.1, and those extended by means of mass and infrared spectrometry in 5.2.

5.1.1. Farkas, Farkas, and Rideal [2] followed the parahydrogen conversion or the deuterium atom fraction in hydrogen in course of the hydrogenation of ethylene at 20 °C in the presence of nickel wire

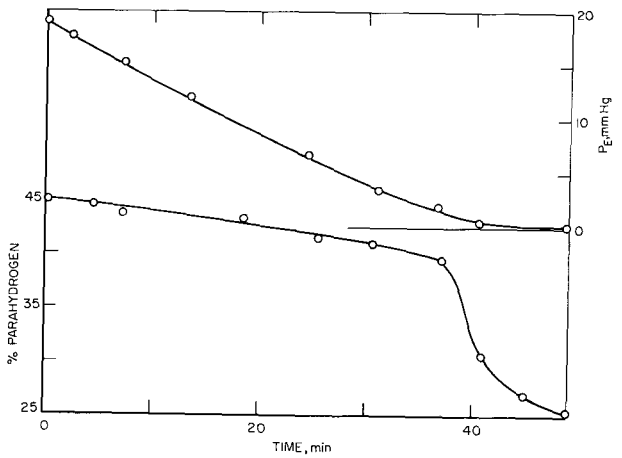

FIGURE 15. *Parahydrogen conversion associated with catalyzed hydrogenation of ethylene [2].*

$P_{E,0}=19$ mm Hg, $P_{H,0}=23$ mm Hg, 20 °C.

preliminarily oxidized at 600 °C and reduced by hydrogen at 300 °C, grew distinctly rapid as soon as ethylene was exhausted by hydrogenation, as seen in figure 15, (1) its rate being approximately equal to that in the absence of ethylene [2]; (2) that the rate of parahydrogen conversion at 20 °C of 25 mm Hg parahydrogen was unchanged by admixture of 17 mm Hg ethane, (3) that the partial pressure of ethylene due to catalyzed hydrogenation decreased linearly with time at 20 °C for the first 30 min as seen in figure 15, and (4) that such a linear decrease was no longer observed above 60 °C. By means of deuterohydrogen they [2] observed (5) that the deuterium content of hydrogen at 20 °C remained nearly constant during the whole course of hydrogenation, or it even increased slightly, as seen in table 8 until ethylene was almost exhausted, and (6) that at 155 °C the deuterium content in hydrogen decreased rapidly, in contrast with (5), (see table 8) from 66 to 22 atom percent while light hydrogen, by which the residual hydrogen was replaced, regained 13 percent deuterium from the ethylene during just a slight progress of hydrogenation as seen in table 8.

The exchange reaction is practically arrested at 22 °C but released at 155 °C as seen in results (5) and (6). The slight increase in deuterium content at 22 °C can be attributed to the isotopic effect on the reaction rate, which enriches deuterium in hydrogen.

5.1.2. Twigg and Rideal [68] observed the catalyzed deuteration of light ethylene with equimolar pure deuterium in the presence of the same nickel catalyst as used by Farkas, Farkas, and Rideal [2] with special reference to the deuterium content of hydrogen. Successive measurements of hydrogenation and exchange rate conducted without pretreatments were corrected for an appreciable decay of catalytic activity by measuring the hydrogenation rate at a fixed temperature and the partial pressures of reactants just before every run; then, the hydrogenation rates and exchange rates measured were multiplied by the correction factor r_1/r_n, where r_1 and r_n are the hydrogenation rates observed at the fixed conditions just before the first and the nth run, respectively. Twigg and Rideal [68] observed, on the one hand, the initial rate of hydrogenation and the initial rate of hydrogen exchange $v_{ex,H} \equiv -dx_H/dt$, at 156 °C at different partial pressures of reactants, finding that both reactions were first and zeroth order with respect to hydrogen and ethylene pressure, respectively. They followed, on the other hand, the course of deuteration by determining the deuterium atom fraction, x_H, in hydrogen and the nonequilibrium fraction, $1-u$, of hydrogen, where $u \equiv [^1HD]/[^1HD]_{eq}$ is the ratio between the actual concentration, $[^1HD]$, of ^1HD and the concentration $[^1HD]_{eq}$ which would result, were the existent hydrogen equilibrated, i.e., brought to equilibrium with respect to the reaction, $^1H_2 + D_2 = 2^1HD$. The nonequilibrium fraction $1-u$ is plotted against x_H in figure 16.

The activation heat of hydrogen exchange $RT^2\partial \ln v_{ex,H}/\partial T$ was found to be 18.6 kcal over the range of temperatures from 84 to 100 °C, and to decrease gradually with increase of temperature down to 4 kcal at 207 °C. It was in excess of the activation heat of hydrogenation, $RT^2\partial \ln v_h/\partial T$, by $4 \sim 5$ kcal throughout. Twigg and Rideal [68] remarked that the equilibration was much faster in the absence of ethylene than in its presence and, with reference to the result of figure 16, that the plots of $1-u$ against x_H at 156 °C and below accumulated around one straight line (indicated by a broken line in fig. 16) which passed a point $x_H = 0.33$ on the axis of abscissa; other straight lines were obtained at higher temperatures, and these intersect the first line on the axis of abscissa. Horiuti [8, 9] has accounted for these experimental results by theoretical calculations on the basis of the associative mechanism and predicted, as

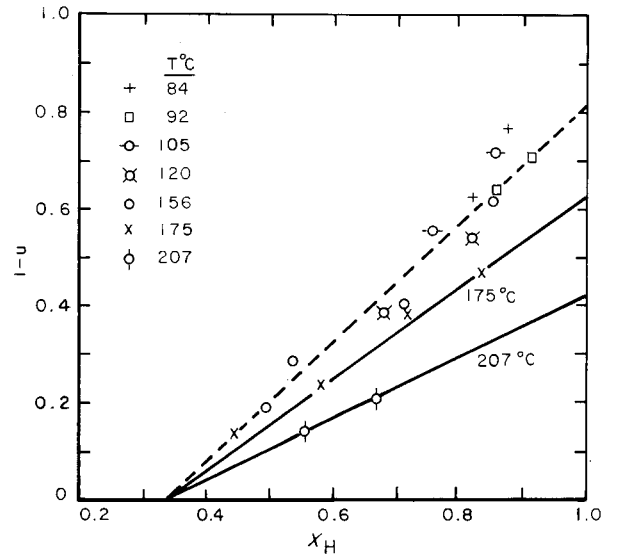

FIGURE 16. *Nonequilibrium fraction* 1 − u *versus deuterium fraction* x_H *of hydrogen in course of catalyzed deuteration of light ethylene over* Ni-*wire* [68].

$u = [^1HD]/[^1HD]_{eq}$. $[^1HD]$: concentration of HD. $[^1HD]_{eq}$: concentration of ^1HD which would result if existent hydrogen were brought to equilibrium with respect to the reaction $^1H_2 + D_2 = 2HD$.

elucidated in 14.4, that the slope of curves such as those indicated by broken lines in figure 16 against x_H-axis increase considerably when the temperature is lowered below those in the experiments of Twigg and Rideal [68], so that curves run down almost vertically along a perpendicular at $x_H = 1$. Matsuzaki [115] confirmed the results of Twigg and Rideal's experiments by tracing them, on the one hand, and observed relations between $1 - u$ and x_H at temperatures as low as 0 or −25 °C as shown in figure 17,

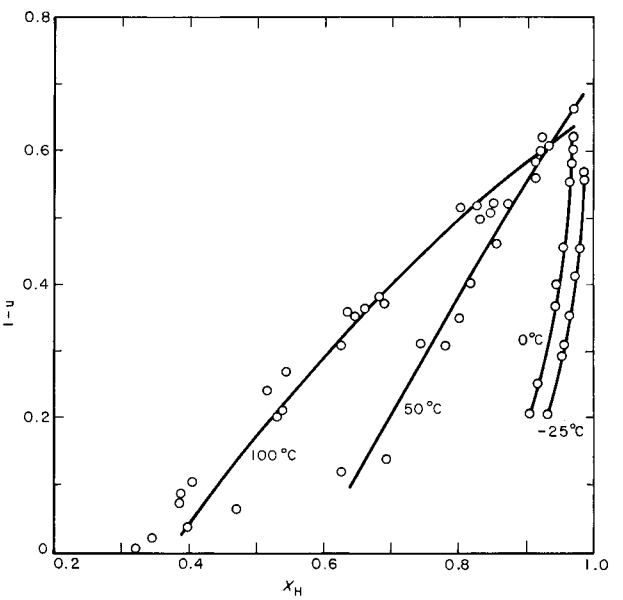

FIGURE 17. *Experimental results on the relation between* 1 − u *and* x_H *in course of deuteration of light ethylene over nickel* [115].

$P_{E,0} = P_{H,0} = 10$ mm Hg.

on the other hand, in semiquantitative agreement with the theoretical prediction of Horiuti [8, 9] as described in 14.4.

5.1.3. Farkas and Farkas [85] experimented with platinized platinum foil on the parahydrogen conversion associated with the catalyzed hydrogenation. Table 10 shows the half-life values τ_c and τ_h, respectively, of parahydrogen conversion and catalyzed hydrogenation from 0 to 27 °C. We see from the table that the presence of ethylene retards the parahydrogen conversion as in the case of nickel and that τ_c and τ_h are the same in the presence of excess ethylene, whereas τ_c is much greater in the presence of excess hydrogen, or the relative rate of parahydrogen conversion is much smaller than that of hydrogenation.

TABLE 10. *Parahydrogen conversion associated with hydrogenation of ethylene over platinized platinum foil* [85]

Reaction temp. °C	Initial partial pressures, mm Hg		Half-life time, min.	
	$P_{E,0}$	$P_{H,0}$	Parahydrogen conversion, τ_c	Hydrogenation, τ_h
25	40	21	80	80
25	0	21	14	.....
0	0	21	72	.....
0	0	40	6	.....
0	19	40	50	13
23	0	15	8	.....
24	42.5	17.5	45	45
27	0	12.5	16	.....
27	36.5	12.5	45	45

The optimum temperature was found at 160 °C for 20 mm Hg ethylene and 40 mm Hg hydrogen, and the activation heat of the catalyzed hydrogenation below the optimum 10 ~ 11 kcal [85], which equaled the activation heat of parahydrogen conversion in the absence of ethylene [85]. The activation heat of the exchange was given as 22 kcal by them.

TABLE 11. *Exchange equilibrium between ethylene and hydrogen in course of catalyzed deuteration over platinized platinum foil* [85]

$P_{E,0} = 20$ mm Hg, $P_{H,0} = 40$ mm Hg

$x_{H,obs}$: Deuterium atom fraction in residual hydrogen at the exhaustion of ethylene.
$x_{H,calc}$: Deuterium atom fraction in equilibrium distribution between hydrogen and ethylene.

Temp. °C	% Deuterium in residual hydrogen		% exchange $= \frac{1 - x_{H,obs}}{1 - x_{H,calc}} \times 100$
	$100x_{H,obs}$	$100x_{H,calc}$	
25	99	37	1.5
54	95	40	8
79	80	41	34
100	75	40	42
120	63	41	63
146	59	42	70
187	51	43	86
235	48	44	93

5.1.4. Farkas and Farkas [85] observed the hydrogen exchange associated with deuteration of light ethylene in the presence of platinized platinum foil. Since, however, the deuteration was quite rapid under the conditions where the hydrogen exchange proceeded with measurable rate, the deuterium content in residual hydrogen was measured on exhaustion of ethylene. Starting from a mixture of 20 mm Hg ethylene and 40 mm Hg deuterium, they obtained the results shown in table 11. The values $x_{H,obs}$ are atom percent of deuterium in the residual hydrogen, $x_{H,calc}$ those in exchange equilibrium calculated allowed for the isotopic effect, and percent exchange is the percent amount of exchange accomplished. Since there occurs no hydrogen exchange between hydrogen and ethane under the experimental conditions [85], one can take from table 11 that the exchange between ethylene and hydrogen is so rapid at around 230 °C that they practically attain the exchange equilibrium.

5.2. Modern Observations

5.2.1. Twigg [116] has catalytically hydrogenated 107 mm Hg light ethylene over nickel-kieselguhr catalyst at −78 °C either with 120 mm Hg equimolar mixture of $^1H_2$ and D_2 or with 120 mm Hg equilibrated mixture of $^1H_2$, ^1HD, and D_2 to the exhaustion of the light ethylene. He thus found that the infrared adsorption spectrum of the product, (A), of hydrogenation of the light ethylene with equimolar mixture of $^1H_2$ and D_2 was identical with that of the product, (B), of hydrogenation with an equilibrated mixture of $^1H_2$, ^1HD, and D_2, and that the identical spectra of (A) and (B) were different from the infrared absorption spectrum of an equimolar mixture, (C), of $C_2{}^1H_6$ and $C_2{}^1H_4D_2$. He found [116], moreover, that the conversion of 75.8 mm Hg parahydrogen over the same catalyst at the same temperature was almost inhibited by coexistent 48.9 mm Hg ethylene and that deuteroethylene was scarcely produced by catalyzed deuteration of light ethylene at −37 °C over the same catalyst.

The result that (A) and (B) have the same infrared absorption spectra but that of (C) is different excludes the possibility of hydrogenation being effected by a single act of addition of a hydrogen molecule to ethylene but verifies the mechanism of hydrogenation through dissociated hydrogen atoms.

5.2.2. Turkevich, Bonner, Schissler, and Irsa [117] followed the catalyzed deuteration of light ethylene over nickel wire by mass-spectrometric analysis of the product in several stages of the progress of deuteration. The catalyst of nickel wire was mounted in a reaction vessel, oxidized at 600 °C, reduced at 330 °C and, before every run, pretreated in deuterium gas at 300 °C. The reaction vessel was kept at 0 °C, deuterium was first, light ethylene subsequently admitted over the catalyst. The reaction was started by applying an appropriate current to the wire to keep it at 90 °C for a recorded time, and the product thus obtained was analyzed. The results are shown in figure 18, where any curve, A_n or E_n, gives the partial pressure of ethane-d_n or ethylene-d_n against percent of ethylene deuterated. $C_2{}^1H_6$ was the predominant initial product of deuteration, as seen in the figure, contrary to the expectation of the authors [117] of finding $C_2{}^1H_4D_2$ instead.

5.2.3. Kemball [76] followed the deuteration of light ethylene at −100 °C over films of Ni, Fe, Rh, and W, respectively, evaporated on glass wall kept at liquid nitrogen temperature, by analyzing the reacting gas that leaked steadily through a capillary into a mass spectrometer. Table 12 shows the relative

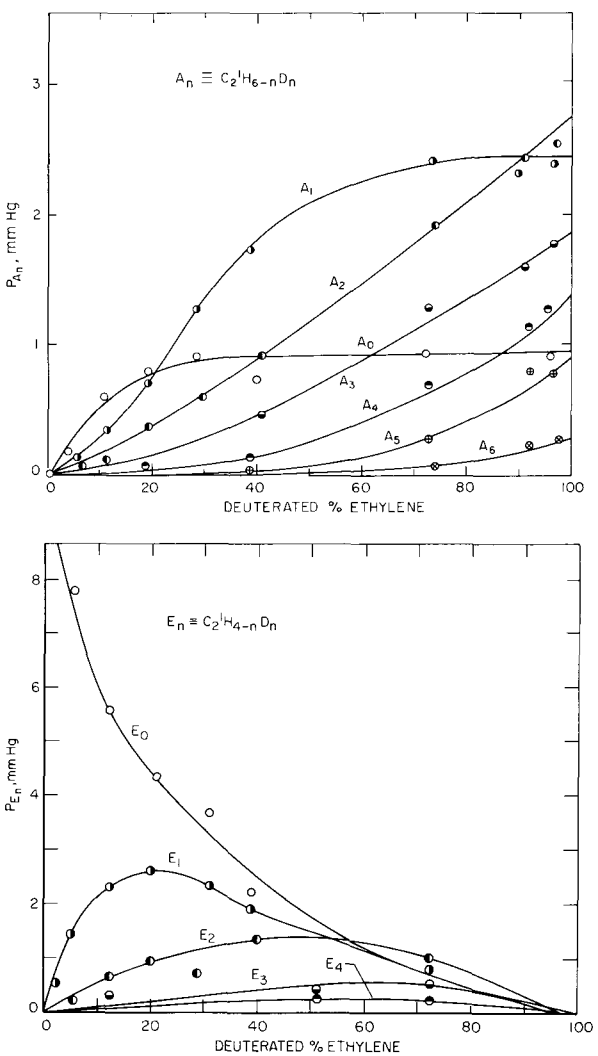

FIGURE 18. *Product of deuteration of 10 mm* Hg *light ethylene with 20 mm* Hg D_2 *over* Ni *wire at 90 °C [117].*
P_{A_n}, P_{E_n}: partial pressures of $A_n \equiv C_2{}^1H_{6-n}D_n$ and $E_n \equiv C_2{}^1H_{4-n}D_n$.

TABLE 12. *Relative amounts of ethylenes-*$d_n \equiv E_n$ *and ethanes-*$d_n \equiv A_n$ *in the initial product of deuteration of 2.7 mm Hg light ethylene with 8.1 mm Hg deuterium over evaporated metal films [76].*

Evaporated film		Ni	Fe	Rh	W
React. temp., °C		−100	−100	−100	−100
E_n	E_1	46.7	55.5	34.4	7
	E_2	13.2	9.4	7.0	0
	E_3	2.7	1.3	1.7	0
	E_4	0.7	0.2	0.9	0
A_n	A_0	7.8	13.7	8.4	3.1
	A_1	12.5	9.2	14.4	14.7
	A_2	9.5	6.6	15.8	69.8
	A_3	4.0	2.4	7.4	4.5
	A_4	2.0	1.0	5.0	0.7
	A_5	0.8	0.5	3.6	0.2
	A_6	.2	.2	1.4	0

amounts of different ethylenes-d_n and ethanes-d_n in the initial stage of the deuteration. In case of tungsten, deuterium is hardly taken up at all by ethylene and the result is marked by the maximum abundance of $C_2{}^1H_4D_2$ among the ethanes-d_n.

It was found [76] that the total number of moles of ethane as well as the number of deuterium atoms taken up by a definite amount of ethylene increases proportional to the time of reaction. Table 13 [76] shows initial values of rate of ethane formation, v_h, and exchange rate of ethylene, $v_{ex,E}$. The kinetics of both reactions was found to correspond to $m=0$ and $n=0.5$. The activation heats derived as usual from both rates are approximately uniformly $5 \sim 6$ kcal for W and 7 kcal for Ni, Fe, and Rh. Table 14 shows the relative amounts of ethanes-d_n on exhaustion of ethylene by deuteration [76].

5.2.4. Miyahara and Narumi [114] conducted a complete analysis of the product of catalyzed deuteration of light ethylene in the initial stage of deuteration over freshly evaporated nickel surface F (cf. 2.8.3) as shown in tables 15 and 16. "Deuterated percent C_2H_4" is the amounts of ethane in percent of the initial amount of ethylene which were identified with the decreases of total pressure in percent of the initial partial pressure of ethylene. Tables 15(b) and 16(b) show the mass spectra of run 2 in table 15(a) and run 12 in table 16(a), respectively, as observed at various stages of deuteration. The first column of these tables shows the mass spectra of gases sampled immediately after the introduction of the reactant mixture into the reaction vessels, which were assured free from ethane. The considerably high values of M_2 and M_3 are interpreted as due to an appreciable dehydrogenated adsorption of light

[7] The previous result 2.9.1 over the F surface contrasts with the present one, which is ascribed to a faster conversion of the F surface into an S surface in the present case, caused by the higher partial pressure of ethylene (10 mm Hg) than in 2.9.1 (0.05 mm Hg partial pressure).

TABLE 13. *Rates of deuteration and hydrogen exchange of ethylene,* v_h *and* $v_{ex,E}$*, on evaporated metal films [76]*

v_h: Percent C_2H_4 deuterated per min per 10 mg film.
$v_{ex,E}$: Number of deuterium atoms transferred per 100 C_2H_4 molecules per min per 10 mg film.

Metal	React. temp. °C	v_h	$v_{ex,E}$
Fe	−100	1.54	3.60
Ni	−100	2.30	5.25
Rh	−104	18.0	18.2
W	−99	3.42	0.26

ethylene on the fresh surface, F, as described in section 2, which is enhanced at the higher temperature in the latter case.

It is concluded from tables 15 and 16 with reference to the optimum temperature, 137 °C, as inferred from the result in figure 19 (cf. 6.2), (1) that the predominant product of deuteration at 0 °C, amply below the optimum, is $C_2{}^1H_6$; as in the case of Turkevich et al. [117], but switches over to $C_2{}^1H_4D_2$ as the partial pressure of deuterium is increased, (2) that $^1H_2$ or ^1HD is hardly evolved at all in course of the catalyzed deuteration of 10 mm Hg light ethylene with equimolar deuterium below the optimum, as seen from table 15(b), or, in other words, that protium atoms from light ethylene hardly enter hydrogen gas,[7] (3) that at 200 °C, in contrast with the latter result, the predominant initial product of deuteration is $C_2{}^1H_4D_2$, while great quantities of $^1H_2$ and ^1HD are evolved from the beginning of catalyzed deuteration as seen from tables 16(a) and 16(b), and (4) that an appreciable amount of deuteroethylene is evolved both at 0 and 200 °C.

5.2.5. Data are compiled in table 17 from table 3 with special reference to the catalyzed deuteration over an S surface of nickel [26], where the dehydrogenated adsorption of ethylene is substantially inhibited. Parenthesized figures show the percentages of the respective compounds-d_n in a random distribution of isotopes as calculated on the basis of the total deuterium atom fraction in ethylene or in hydrogen. It is concluded from table 17, referring to the fact that the observed value 0.992 of y_H is just that of original deuterium gas, (1) that hardly any protium appears in hydrogen gas in course of the catalyzed deuteration at −45 or −23 °C, tem-

TABLE 14. *Relative amounts of ethane-*$d_n \equiv A_n$ *produced on exhaustion of light ethylene by deuteration over evaporated metal films [76]*

Metal	Initial partial pressures		React. temp. °C	Ethanes-d_n, %						
	$P_{E,0}$ mm Hg	$P_{H,0}$ mm Hg		A_0	A_1	A_2	A_3	A_4	A_5	A_6
Rh	2.7	8.1	−104	11.5	27.2	29.1	13.7	9.1	6.8	2.6
Fe	2.7	8.1	−100	20.1	28.4	22.1	12.7	8.6	5.2	2.9
W	2.7	8.1	−99	4.8	15.5	70.5	6.7	1.6	0.5	0.1
Ni	2.7	8.1	−100	17.9	26.8	23.2	14.0	9.6	5.9	2.6
Ni	2.7	24.3	−92	12.4	29.9	25.4	14.3	9.7	5.9	2.4
Ni	8.1	24.3	−81	17.1	30.5	20.7	13.8	9.4	6.2	2.3

peratures which are amply below the optimum at ca. 30 °C as gathered from the table, whereas above the optimum, $^1H_2$ and ^1HD appear approximately in accordance with a random distribution of isotopes, (2) that ethylenes-d_n appear in accordance with the random distribution of isotopes irrespective of temperature and (3) that the activation heat of catalyzed deuteration varies only slightly with the total pressure as indicated by its value

TABLE 15(a). *Relative amounts of ethylenes-*$d_n \equiv E_n$ *and ethanes-*$d_n \equiv A_n$ *in the deuteration product of 10 mm* Hg *light ethylene at 0 °C over a freshly evaporated surface* F *of nickel film [114]*

No. of run	Initial partial pressure of D_2 mm Hg	Deuterated % C_2H_4	Relative amounts of hydrocarbons-d_n, %										
			E_1	E_2	E_3	E_4	A_0	A_1	A_2	A_3	A_4	A_5	A_6
2	10	33	13	1	0	0	45	23	18	0	0	0	0
3	10	45	12	1	0	0	35	28	19	4	1	0	0
4	43	12	27	3	0	0	40	24	3	2	0	0	0
5	107	29	29	5	2	0	23	19	13	4	2	1	0
7	138	36	14	1	0	0	27	10	36	7	2	1	1

TABLE 15(b). *Mass spectrum of reacted hydrogen gas of run 2 in table* 15(*a*)

Deuterated % C_2H_4		0	15	20	27	33
Relative heights of peaks	M_2	4	5	5	7	5
	M_3	2	2	2	2	2
	M_4	94	93	93	91	93

TABLE 16(a). *Relative amounts of ethylenes-*$d_n \equiv E_n$ *and ethanes-*$d_n \equiv A_n$ *in the deuteration product of 10 mm* Hg *light ethylene with equimolar deuterium at 200 °C over a freshly evaporated surface* F *of nickel film [114]*

No. of run	Deuterated % C_2H_4	Relative amounts of hydrocarbons-d_n, %										
		E_1	E_2	E_3	E_4	A_0	A_1	A_2	A_3	A_4	A_5	A_6
11	20	38	27	13	0	4	6	7	4	2	0	0
12	31	25	25	11	3	3	8	12	7	4	1	0

TABLE 16(b). *Mass spectrum of reacted hydrogen of run 12 in table 16(a)*

Deuterated % C_2H_4		0	13	31
Relative heights of peaks	M_2	11	35	47
	M_3	5	31	27
	M_4	84	34	26

7.2 kcal at 0.1 mm Hg total pressure, derived from its rate given in table 17, and 8.4 kcal at 20 mm Hg total pressure, as indicated in figure 19.

5.2.6. Kazanskii and Voevodskii [119] analyzed mass-spectrometrically the products of catalyzed deuteration of ethylene at 90, 135, and 185 °C in the presence of palladium plate. Deuteroethylenes were hardly found at all at 90 °C but at higher temperature they were present in large amounts, as shown in figures 20(a), 20(b), and 20(c). The amounts of deuteroethylenes produced at 135 °C, if repre-

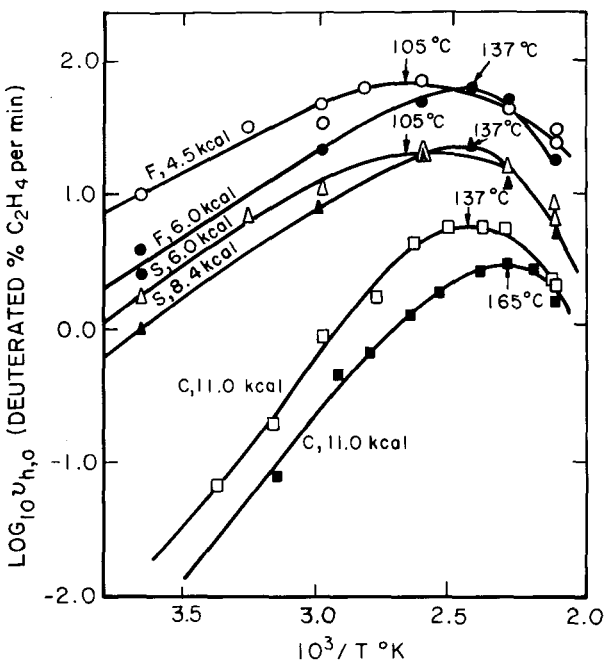

FIGURE 19. *Initial rate,* $v_{h,0}$, *of hydrogenation of light ethylene with protium* (○, △, □) *or deuterium* (●, ▲, ■) *over fresh* (F), *once used* (S) *or carbided* (C) *surface of evaporated nickel film [114].*

$P_{E,0} = P_{H,0} = 10$ mm Hg.

$v_{h,0}$ is the initial value of v_h, i.e., deuterated percent of ethylene per min. Each curve is specified by the surface state, F, S, or C, and the activation heat derived from the curve at lower temperatures. The optimum points for the F, S, and C surfaces are indicated by vertical arrows.

sented by the respective molecular formulas, are in the order of $C_2{}^1H_3D > C_2{}^1H_2D_2 > C_2{}^1HD_3 > C_2D_4$ throughout the reaction and attain their respective maxima approximately at the same percentage of deuteration of ethylene, whereas at 185 °C the maximum shifts towards the greater percentage of deuteration of ethylene the higher the number n of $C_2{}^1H_{4-n}D_n$ as seen in figures 20(a) and 20(b). The distribution of ethanes-d_n over n does not vary with temperature or the progress of deuteration and reaches a peak at $C_2{}^1H_4D_2$ as seen in table 18.

5.2.7. Matsuzaki and Nakajima [120] showed by adding the product of catalyzed deuteration of light ethylene to a mixture of light ethylene and hydrogen, that the mass spectrum of deuteroethanes, i.e., the relative heights of peaks of mass numbers greater than 30 remained unchanged, even if the light ethylene and hydrogen are allowed to be catalytically combined in ethane, which verified that

TABLE 17. *Relative amounts of ethylenes-*$d_n \equiv E_n$ *and hydrogens-*$d_n \equiv H_n$ *in the reaction product of equimolar mixture of* $C_2{}^1H_4$ *and* D_2 *of 0.1 mm Hg initial total pressure over S surface of nickel [26, 118] (compiled from table 3 [26])*

React. temp. °C	Deuterated % C_2H_4	Rate of hydrogenation deuterated % C_2H_4 min^{-1}	E_n, %					H_n, %			Deuterium atom fraction in	
			E_0	E_1	E_2	E_3	E_4	$^1H_2$	^1HD	D_2	C_2H_4	H_2
−45	2	3.5	93	7	0	0	0	0	1.6	98.4	0.017	0.992
			(93	7	0	0	0)	(0	1.6	98.4)		
−23	10	18.2	90	10	0	0	0	0	1.6	98.4	0.025	0.992
			(90	10	0	0	0)	(0	1.6	98.4)		
0	20	56.9	64	30	6	0	0	0	6	94	0.105	0.970
			(64	29	5	2	0)	(0	6	94)		
28	43	98.0	66	28	5	1	0	2	10	88	0.103	0.930
			(65	30	5	0	0)	(0	13	87)		
32	41	107.1	40	36	20	4	0	10	19	71	0.220	0.805
			(37	42	18	3	0)	(4	31	65)		
75	38	97.0	29	38	24	7	2	30	29	41	0.263	0.555
			(30	42	20	5	3)	(20	49	31)		
110	21	50.2	21	29	37	10	2	14	39	47	0.340	0.665
			(19	30	38	10	2)	(11	45	44)		

Parenthesized figures show the relative amounts of E_n and H_n calculated assuming random distribution of deuterium. Those of E_n were calculated according to eq (12.32) with $x_{E(a)}$ derived from observed values of $X_{E_n(a)}$'s by eq (12.21.x). Those of H_n were similarly calculated.

TABLE 18. *Relative amounts of ethanes-*$d_n \equiv A_n$ *in the product of catalyzed deuteration of 50 mm* Hg $C_2{}^1H_4$ *with 200 mm* Hg D_2 *over* Pd *plate at 135 °C* [119]

Deuterated % C_2H_4	Relative amounts of ethanes-d_n, %						
	A_0	A_1	A_2	A_3	A_4	A_5	A_6
10	0	25	50	12	8.5	3	1.5
25	0	25	50	12.5	8	3	1.5
37	0	20	49.5	13	10.5	5	2
50	0	24.5	46	14	10.5	3.5	1.5
70	0	26	41.5	13.5	12	5	2

ethane was not involved in the catalyzed hydrogenation.

5.2.8. Kowaka [121] has investigated the effect of protium and deuterium diffused through palladium, in advance of Apel'baum and Temkin [91], upon $C_2{}^1H_4$, or a mixture of $C_2{}^1H_4$, and $^1H_2$, or a mixture of $C_2{}^1H_4$ and D_2, respectively, contained inside a palladium thimble, by analyzing mass-spectrometrically the product. The palladium thimble was evacuated, before use, at 800 °C for 2 hr, corroded with *aqua regia* on both sides and again evacuated at 800 °C with the aim of removing occluded hydrogen. Protium or deuterium were now let diffuse toward the inside by electrolyzing protium or deuterium oxide, using the external surface of the thimble as a cathode.

TABLE 19. *Effect of deuterium diffused through palladium upon* $C_2{}^1H_4$ *or* $C_2{}^1H_4 + {}^1H_2$ *[121]*

Substance upon which deuterium is diffused	React. temp. °C	React. time min	Composition of product, mole %				
			ethylene	$^1H_2$	^1HD	D_2	ethane
100 mm Hg $C_2{}^1H_4$	40	30	52.5	6.7	0.9	16.2	23.7
	65	30	44.0	8.2	7.0	14.3	26.5
	90	17	47.5	18.9	5.2	0	28.4
	90	30	0	21.3	24.2	15.0	39.5
100 mm Hg $C_2{}^1H_4$ + 50 mm Hg $^1H_2$	40	30	55.8	6.7	0.8	11.0	25.7
	65	30	29.0	18.0	7.0	5.5	40.5
	90	10	65.4	21.1	2.5	0	11.0

Table 19, figure 21(a) and figure 21(b) show the effects of diffused deuterium upon 100 mm Hg $C_2{}^1H_4$ and upon a mixture of 100 mm Hg $C_2{}^1H_4$ and 50 mm Hg $^1H_2$ inside the thimble, and figure 21(c) that of diffused protium upon a mixture of 100 mm Hg $C_2{}^1H_4$ and 50 mm Hg D_2. An appreciable amount of protium, to be traced back to light ethylene, is evolved as $^1H_2$ or ^1HD, as seen in table 19, although the ^1HD-evolution is suppressed at lower temperature. As shown by figures 21(b) and 21(c), diffused hydrogen is considerably active, and it is remarkable that in the former case the maximum abundance switches over from $C_2{}^1H_6$ to $C_2{}^1H_4D_2$ through the decrease of temperature just by 25 °C.

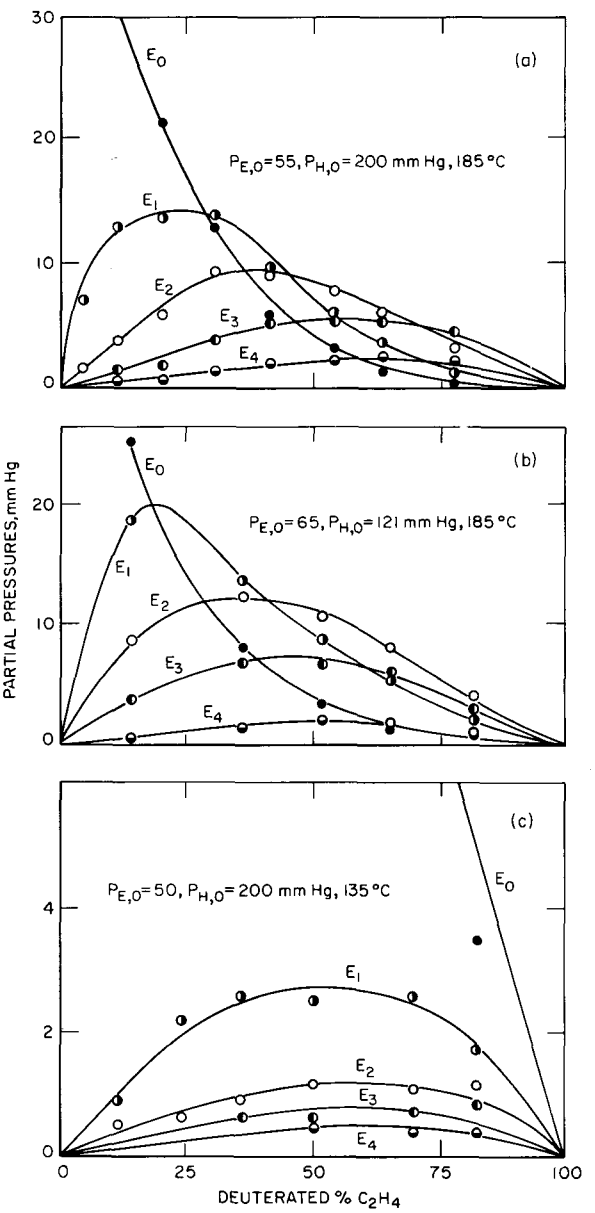

FIGURE 20. *Ethylenes-*$d_n \equiv E_n$ *in the product of catalyzed deuteration of light ethylene [119].*

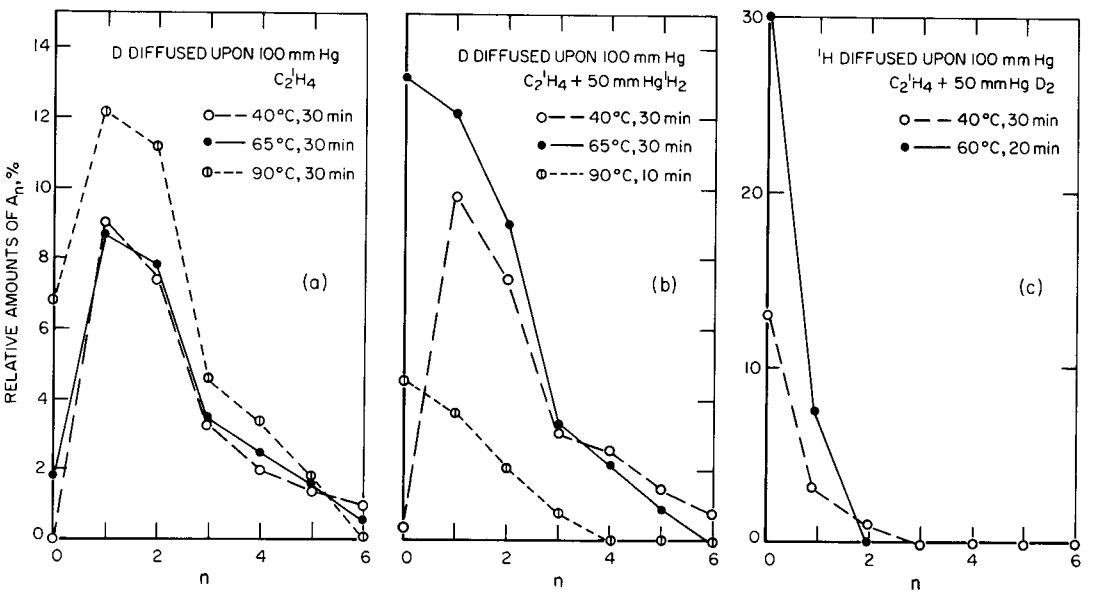

FIGURE 21. *Relative amounts of ethane-*$d_n = A_n$ *in the product of hydrogen atom diffused through* Pd *upon* $C_2{}^1H_4$ *or* $C_2{}^1H_4 + H_2$ *[121].*

6. Isotopic Effect on Hydrogenation Rate

The isotopic effect on hydrogenation is defined as

$$\alpha = v_h(^1H_2)/v_h(D_2)$$

where $v_h(^1H_2)$ and $v_h(D_2)$ are the rates of hydrogenation of $C_2{}^1H_4$ with pure protium and deuterium, respectively, of the same partial pressure under otherwise identical conditions.

6.1. Tucholski and Rideal [67] observed the rates, $v_h(^1H_2)$ and $v_h(D_2)$, of catalyzed hydrogenation with $^1H_2$ and D_2, respectively, in the presence of nickel wire oxidized at 600 °C and reduced at 330 °C. Activity lost by prolonged use was restored by keeping it at 200 °C in ca. 0.1 mm Hg protium or deuterium. The results are shown in table 20. The optimum temperature is around 139 °C both in the cases of $v_h(^1H_2)$ and $v_h(D_2)$, as seen from the table, whereas the optimum of $v_h(D_2)$ was reproducibly located at 160 °C in another series [67] of experiments by the same authors [67]. Table 20 shows that α decreases gradually with rise of temperature down to unity or below around the optimum and increases with temperature above it.

TABLE 20. *Isotropic effect* $\alpha \equiv v_h(^1H_2)/v_h(D_2)$ *on hydrogenation rate of light ethylene on* Ni *wire [67]*

$v_h(^1H_2)$, $v_h(D_2)$: rate of hydrogenation with $^1H_2$ or D_2. $P_{E,0} = 3$ mm Hg, $P_{H,0} = 5$ mm Hg.

React. temp., °C	0	17	120	139	165	180	198
$v_h(^1H_2)$ mm Hg min^{-1}	0.40	0.58	3.1	3.36	1.90	1.01	0.81
$v_h(D_2)$ mm Hg min^{-1}	0.24	0.38	2.25	2.54	1.84	1.34	0.54
α	1.66	1.52	1.38	1.32	1.03	0.75	1.5

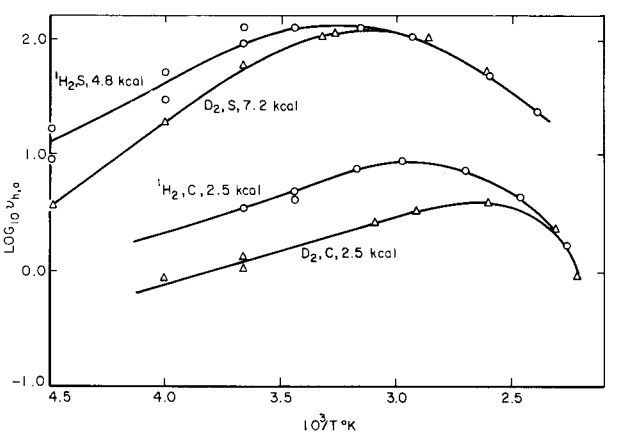

FIGURE 22. *Initial hydrogenation rate,* v_h, *of light ethylene with equimolar protium or deuterium versus* $10^3/T$ °K *[118].*

$P_{E,0} + P_{H,0} = 0.1$ mm Hg.

$v_{h,0}$ is the initial value of v_h given in hydrogenated percent C_2H_4 min^{-1}. $^1H_2$, S, 4.8 kcal, etc., on the curves signify the hydrogenation with protium over S surface and the activation heat determined at lower temperatures 4.8 kcal/mole, etc., respectively.

6.2. Miyahara and Narumi [114] and Miyahara [118] observed the initial rates, $v_{h,0}(^1H_2)$ and $v_{h,0}(D_2)$, of hydrogenation of light ethylene with equimolar protium or deuterium over a surface of evaporated nickel film at surface state, F, S, or C (cf. 2.8.3), at different temperatures and at different initial total

pressures. Figures 19 and 22 show the results obtained at 20 mm Hg [114] and 0.1 mm Hg [118] initial total pressure, respectively. The values of α derived in both cases of total pressure are shown in figure 23, with curves marked with S, 0.1 mm Hg, etc., which indicate the surface states of the evaporated nickel film and the initial total pressures. The optimum temperatures of hydrogenation with $^1H_2$ respectively appropriate to the surface states and the total pressures are shown by vertical chain lines traced, respectively, up to the

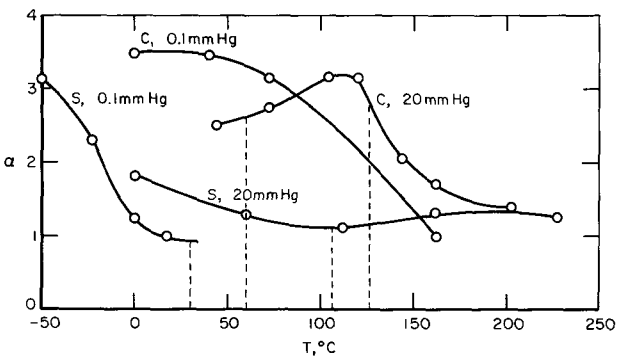

FIGURE 23. *Isotopic effect α versus temperature [118].*
S and C signify the surface states of evacuated nickel film over which the initial value of hydrogenation rates with protium and deuterium, $v_h(^1H_2)$ and $v_h(D_2)$, were determined, and the associated figures the initial total pressure of the equimolar reactant gas mixutre. The optimum temperature is shown by a vertical chain line traced up to the corresponding α-curve, which is relevant to the same surface state and initial total pressure as is the optimum temperature, in accordance with the results of figures 19 and 22.

relevant α-curves. The values of α over the S surface decrease with temperature down to a minumum at the optimum and then increase qualitatively in accordance with the result 6.1. The α-values of carbided film are much higher than those over S surfaces as seen in figure 23.

TABLE 21. *Activation heat and optimum temperature of catalyzed hydrogenation of light ethylene with equimolar protium or deuterium over evaporated nickel films [26, 114, 118]*

Surface state of evaporated Ni film	Initial total pressure mm Hg	Hydrogen	Activation heat kcal/mole	Optimum temp. °C
S	0.1	$^1H_2$	4.8	30
		D_2	7.2	50
S	20	$^1H_2$	6.0	105
		D_2	8.4	137
C	0.1	$^1H_2$	2.5	66
		D_2	2.5	110
C	20	$^1H_2$	11.0	137
		D_2	11.0	165

Table 21 summarizes the results shown in figure 23. The optimum temperature of deuteration is 20 ~ 40 °C higher than that of hydrogenation with protium over either surface.

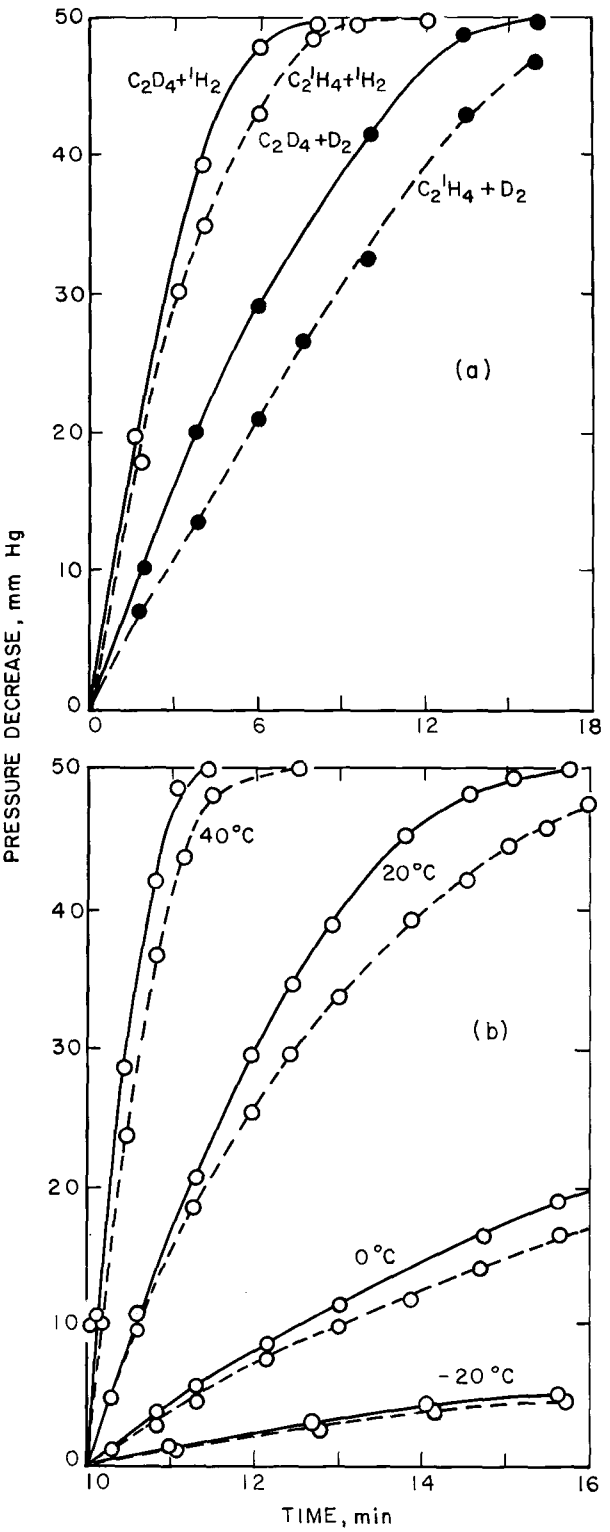

FIGURE 24a. *Catalyzed hydrogenation of ethylene over* Cu(+MgO) *in four isotopically different cases [103].*
$P_{E,0}=P_{H,0}=50$ mm Hg, 40 °C.

FIGURE 24b. *Catalyzed hydrogenation of ethylene over* Cu(+MgO) *in cases of* $C_2{}^1H_4+{}^1H_2$ *(broken line) and* $C_2D_4+{}^1H_2$ *(full line) at different temperatures [103].*
$P_{E,0}=P_{H,0}=50$ mm Hg.

6.3. Table 22 shows the results obtained by Klar [104] with an iron catalyst prepared by thermal decomposition of iron oxalate followed by reduction of the resulting oxide. The observations were conducted with equimolar mixtures of ethylene and hydrogen of ca. 2 mm Hg total pressure. It is remarkable that α is smaller than unity, indicating that deuterium reacts faster than protium, above 100 °C. It is inferred from the table that the optimum temperatures of hydrogenation are 125 and 150 °C with protium and deuterium, respectively, and the activation heats of hydrogenation with protium and deuterium are 7.5 and 9.5 kcal/mole, respectively, below the optimum. No description is given in the original paper [104] of the unit of rate.

TABLE 22. *Ratio, $\alpha \equiv v_h(^1H_2)/v_h(D_2)$, between the hydrogenation rates of light ethylene with protium $v_h(^1H_2)$, and that with deuterium $v_h(D_2)$ over iron catalyst [104]*

React. temp., °C	0	25	40	55	75	100	125	150	175
$v_h(^1H_2)$	0.005	0.0127	0.0253	0.0517	0.110	0.207	0.271	0.217	0.18
α	2.5	1.69	1.58	1.67	1.22	0.98	0.79	0.56	0.51

6.4. Table 23 shows the isotopic effect on the hydrogenation rate of light ethylene over copper catalyst [122]. The isotopic effect on the homogeneous hydrogenation rate is appended for reference. The catalyst Cu(+MgO) was the reduction product of a mixture of oxides of Cu and Mg. In the presence of the latter catalyst, Joris, Taylor, and Jungers [103] observed the course of hydrogenation of ethylene in four isotopically different cases at 40 °C, as shown in figure 24(a), and also the course of hydrogenation of $C_2{}^1H_4 + {}^1H_2$ and of $C_2D_4 + {}^1H_2$ comparatively at different temperatures, as shown in figure 24(b). The ratio of the initial rate of $C_2{}^1H_4 + {}^1H_2$ to that of $C_2{}^1H_4 + D_2$ was found unity at 20 °C with a fresh catalyst but 0.75 over a catalyst whose activity had declined with 20 repeated uses. The activation heats of the reactions of $C_2{}^1H_4 + {}^1H_2$ and $C_2{}^1H_4 + D_2$ were found to be 11.5 and 12 kcal/mole, respectively, over a fresh catalyst.

TABLE 23. *Ratio, $\alpha \equiv v_h(^1H_2)/v_h(D_2)$, between the hydrogenation rates of light ethylene with protium, $v_h(^1H_2)$, and that with deuterium, $v_h(D_2)$ over copper catalyst [122]*

Catalyst	React. temp. °C	Initial partial pressure mm Hg		α
		$C_2{}^1H_4$	H_2	
Cu [123]	0	375	375	2
Cu (+MgO) [103]	20	50	50	2
	40	50	50	2.5
Homogeneous reaction [123]	534 ~ 567	190	580	2.5

7. Supported Catalysts

7.1. Nickel-kieselguhr catalyst is of frequent practical use for hydrogenation but its behavior is remarkably different from that of unsupported nickel catalysts in the following points.

(1) Ethylene or propylene does not polymerize over unsupported reduced nickel powder at 100 °C for several tens of hours but does perceptibly so over 15 percent nickel kieselguhr at 0 °C within 1 hr [124].

(2) The exchange of hydrogen atoms between $C_2{}^1H_4$ and C_2D_4 at room temperature [24] is barely perceptible over nickel wire of 730 cm^2 area, and even at 300 °C it takes more than 3 hr to attain an exchange equilibrium over nickel wire of 990 cm^2 area [125], whereas the exchange is completed at room temperature within several minutes over 17 ~ 19 wt percent nickel-kieselguhr catalyst [125].

(3) No deuteroethylene was produced in course

of catalyzed deuteration of light ethylene over 60 wt percent nickel-kieselguhr catalyst both at −50 and +50 °C [126] as shown in table 24, in contrast with the result 5.2.4 (4), which showed that an appreciable amount of deuteroethylene was evolved over unsupported nickel. A mere 0.45 or 5.2 atom percent protium were found [126] in hydrogen gas at −50 or 50 °C, respectively, at the end of the experiments. The absence of deuteroethylene in the deuteration product of light ethylene was also observed by Twigg [116] in the presence of nickel-kieselguhr catalyst as mentioned in 5.2.1.

(4) Table 24 shows no preferential evolution of $C_2{}^1H_6$ in the initial stage of deuteration as found by Turkevich et al. [117] in the presence of unsupported catalyst but constant relative amounts of ethanes-d_n in the deuteration product, with a maximum at $n=2$ ($C_2{}^1H_4D_2$) irrespective of temperature and extent of deuteration.

7.2. No such distinct differences are found between supported and unsupported catalysts of metals of the platinum group, which cause less dehydrogenated adsorption of ethylene as seen in section 2. Bond [88] investigated the kinetics and the distribution of compounds-d_n in the deuteration product of $C_2{}^1H_4$ in the presence of platinized Pt, 5 weight percent Pt-pumice, 1 weight percent Pt-alumina, 1 weight percent Pt-silica and 1 weight percent Pt-silica-alumina. One gram of each catalyst was dried in air, evacuated at 200 °C in a reaction vessel of 45 cm^3 capacity, pretreated in hydrogen at 200 °C for 12 hr and evacuated. Admitting $C_2{}^1H_4$ first and D_2 subsequently over the catalyst, the deuteration was followed by total pressure decrease and by mass-spectrometric analysis of the product at different temperatures and partial pressures of reactants. The results indicated, as shown in table 25, that no significant difference exists between the five different platinum catalysts, except that $C_2{}^1H_4D_2$ is distinctly predominant only in the cases of 1 weight percent Pt-silica-alumina and 1 weight percent Pt-silica. Neither is there any distinct difference between the distributions of ethanes-d_n at 50 and 100 deuterated percents of ethylene under similar conditions of partial pressures as seen in table 24 of nickel-kieselguhr catalyst. Bond et al. [88, 89, 94], also dealt with rates of hydrogen exchange, which is not reviewed here, however, as this was quite unintelligible to the present writers.

TABLE 24. *Relative amounts of ethylene-*$d_n \equiv E_n$ *and ethanes-*$d_n \equiv A_n$ *in the product of catalyzed reaction of 1:10 molar mixture of light ethylene and deuterium over 60 percent* Ni-*kieselguhr [126]*

$P_{E,0}$ = 44.7 mm Hg (−50°C), 64.8 mm Hg (50 °C) (partial pressures computed from reported experimental conditions).

React. temp. °C	React. time min	deuterated % C_2H_4	Relative amounts of hydrocarbons-d_n, %								
			E_0	E_1	A_0	A_1	A_2	A_3	A_4	A_5	A_6
−50	5	22	78	0	4.7	6.6	6.5	3.3	0.9	0	0
	15	59	41	0	12.5	14.0	16.5	8.7	4.7	2.6	0
	35	87	13	0	15.6	22.2	24.0	13.6	7.0	3.5	1.3
	80	99	1	0	15.8	24.0	28.4	16.8	9.3	3.9	1.8
	185	100	0	0	17.8	25.6	27.4	16.1	7.8	3.6	1.5
50	5	39	61	0	1.8	5.8	11.9	7.3	6.1	3.8	2.3
	15	83	17	0	5.0	14.7	24.2	15.8	11.7	7.6	4.0
	60	94	6	0	7.2	16.5	26.4	17.0	10.0	9.1	7.9

TABLE 25. *Relative amounts of ethanes-$d_n \equiv A_n$ in the deuteration product of light ethylene in the presence of platinum catalysts* [88]

Catalyst		Platinized-Pt						5 Wt % Pt-pumice						
temp. °C		0	0	24.5	51.8	0	0	−18	0	0	24.3	50.2	0	0
$P_{E,0}$ mm Hg		46.9	48.4	50.7	50.0	12.7	101.0	47.6	51.0	51.0	50.8	51.2	10.8	98.0
$P_{H,0}$ mm Hg		61.5	60.5	54.8	57.0	123.0	14.3	62.8	47.0	47.0	61.4	62.2	108.7	12.8
deuterated % C_2H_4		51	100	44	50	100	50	54	52	100	51	55	60	47
Relative amounts of A_n, %	A_0	20.1	12.7	24.3	25.5	12.8	32.4	11.2	11.1	13.2	16.1	17.1	10.4	18.3
	A_1	31.7	31.9	30.1	29.1	16.9	28.1	30.9	33.4	31.7	28.8	27.4	25.3	32.4
	A_2	27.3	30.1	21.5	22.0	55.3	14.7	34.9	31.8	29.0	23.0	24.2	37.8	20.9
	A_3	9.1	10.4	11.7	12.2	8.3	10.3	11.0	10.3	10.8	14.1	13.5	12.8	11.7
	A_4	6.1	6.9	7.7	7.3	3.2	6.6	6.0	6.3	7.5	9.8	9.9	7.0	7.5
	A_5	3.7	5.6	3.9	3.0	2.4	5.3	4.2	4.7	5.7	2.7	5.5	4.3	5.3
	A_6	2.0	2.4	0.9	0.9	1.1	2.6	1.8	2.3	2.3	2.5	2.4	2.4	3.9

TABLE 25. *Relative amounts of ethanes-$d_n \equiv A_n$ in the deuteration product of light ethylene in the presence of platinum catalysts* [88]—Continued

Catalyst		1 Wt % Pt-alumina								1 Wt % Pt-silica-alumina							1 Wt % Pt-silica					
temp. °C		−18	0	0	25	52	0	0	0	0	0	19.3	53.5	78	0	0	0	0	25.5	52	0	0
$P_{E,0}$ mm Hg		48.8	52.3	52.3	51.3	48.0	108.8	13.2	2.0	48.5	46.7	46.8	48.6	51.8	11.4	95.2	56.6	61.8	51.2	52.8	12.4	104.3
$P_{H,0}$ mm Hg		70.0	56.0	56.0	60.2	63.0	13.0	119.8	253.0	68.8	65.3	63.8	64.2	64.8	114.0	13.5	65.0	67.0	66.5	65.7	103.0	12.0
deuterated % C_2H_4		39	43	100	47	54	51	100	100	44	100	49	50	52	100	100	45	100	48	50	100	97
Relative amounts of A_n, %	A_0	21.5	22.2	16.3	20.4	15.8	32.5	11.9	4.7	18.6	14.2	14.5	13.8	10.5	7.3	14.1	7.9	9.9	10.4	11.2	5.8	21.1
	A_1	27.1	28.4	30.1	30.6	29.6	31.0	20.9	13.7	30.0	28.2	26.3	26.0	26.0	15.1	29.0	25.5	26.1	27.8	30.1	19.5	31.0
	A_2	33.2	30.8	29.2	26.1	27.8	23.1	42.6	67.1	33.8	33.0	36.3	36.7	37.5	51.2	39.6	46.6	43.5	40.8	36.9	56.1	34.5
	A_3	10.4	10.0	12.6	11.8	14.2	7.1	12.7	11.4	10.4	12.3	11.6	11.8	13.7	14.3	10.1	10.8	11.3	12.0	12.4	11.2	7.1
	A_4	4.4	4.5	6.3	7.2	8.3	3.4	6.5	2.5	4.5	6.8	6.1	6.4	6.7	6.2	4.3	5.3	5.1	5.1	5.3	4.0	3.4
	A_5	2.5	2.6	3.6	3.4	3.8	1.9	3.6	0.6	1.9	3.9	3.5	3.4	3.6	3.7	2.2	2.7	2.8	2.5	2.9	2.2	1.9
	A_6	0.9	1.4	1.8	0.6	0.5	1.0	1.8	0.0	0.8	1.6	1.7	1.9	2.0	2.2	0.7	1.2	1.3	1.4	1.2	1.2	1.0

TABLE 26. *Relative amounts of ethanes-*$d_n \equiv A_n$ *and ethylene-*$d_n \equiv E_n$ *in*

Metal		Pt							Ir						
temp. °C		0	25	54	102	150	150	150	−16	−16	−16	9	86	124	152
$P_{E,0}$ mm Hg		99	51	99	99	99	96	52	100	99	50	100	100	100	100
$P_{H,0}$ mm Hg		98	60	98	98	98	29	188	100	26	237	100	100	100	100
Deuterated % C_2H_4		Less than 10 for all cases							Less than 15 for all cases						
Relative amounts %	A_0	10.0	19.2	19.3	9.5	4.9	8.2	5.7	4.4	0	0	3.5	4.6	1.7	0
	A_1	32.6	27.2	28.2	24.3	11.2	13.0	11.1	30.1	32.0	32.8	32.0	25.7	21.3	18.5
	A_2	37.8	23.2	25.6	26.8	23.9	14.6	28.2	36.9	37.5	40.0	39.6	30.0	28.9	27.0
	A_3	6.8	10.5	8.7	7.5	4.3	2.2	5.2	14.7	13.8	14.4	12.0	12.5	11.0	9.8
	A_4	3.3	6.4	4.9	4.2	2.9	0.5	2.4	7.2	9.1	8.2	7.5	9.4	9.3	8.1
	A_5	1.9	3.0	2.3	1.5	1.7	0.3	1.3	2.2	3.3	2.7	1.7	4.8	5.8	3.9
	A_6	0.8	0.5	0.4	0.5	0.2	0.1	0.9	0.4	0.4	0.4	0.2	1.2	1.4	0.8
	E_1	6.0	7.4	9.2	19.6	36.5	44.0	32.8	2.9	3.1	1.1	2.9	8.1	14.5	19.6
	E_2	0.8	2.7	1.2	4.5	8.6	11.4	6.6	0.6	0.4	0.2	0.4	2.8	4.3	7.9
	E_3	0	0.8	0.2	1.3	3.9	4.7	3.4	0.4	0.4	0.1	0.2	0.7	1.4	3.4
	E_4	0	0	0	0.3	2.1	1.0	2.4	0.2	0	0.1	0	0.2	0.4	1.1

Bond et al. [89, 95], conducted similar experiments with 5 mole percent metal-alumina catalysts of Pt, Ir, Os, and Ru comparatively; the results are shown in table 26. The distributions of ethanes-d_n and ethylenes-d_n are similar for the supported catalysts of Ir and Pt but those observed on the supported catalysts of Os and Ru differ from the former and between each other.

8. Carbided Catalysts

The activity of metallic catalysts, especially nickel, declines in general irreversibly, as mentioned in 2, on account of adsorbed complex produced by dehydrogenated adsorption of ethylene. Jenkins and Rideal [13] prepared a carbided surface by keeping an evaporated film in ethylene at 190 °C for 30 min. They found that the rate of hydrogenation over the carbided surface was quite reporducible, although smaller than that over the freshly evaporated surface by a factor of several tens. Taking advantage of this reporducibility they investigated the rate law on the carbided surface and discussed the mechanism of hydrogenation. This procedure has been extended to supported Ni [82, 83], Pd foil [87] and Pt wire [87], but it is questionable whether the carbided surface preserves any intrinsic property of the basic metal surface.

8.1. *Miyahara [26, 118]* observed the adsorption of ethylene and hydrogen by the catalyst in the course of the hydrogenation of light ethylene, the kinetics of the hydrogenation, the hydrogen exchange between ethylene molecules and the distribution of deuterium in the product of catalyzed deuteration over F (fresh), S (once used for a run of hydrogenation) and C (carbided) surfaces of evaporated nickel film; the conclusion was that F and S behaved similarly to each other, except that the dehydrogenated adsorption of ethylene was inhibited over S, while C behaved quite differently from both F and S. The activity of C is smaller than that of S by a factor of several tens; apart from that, C differs from S in the following points:

(a) Ethylene is adsorbed by S and C approximately to the same extent in course of the catalyzed

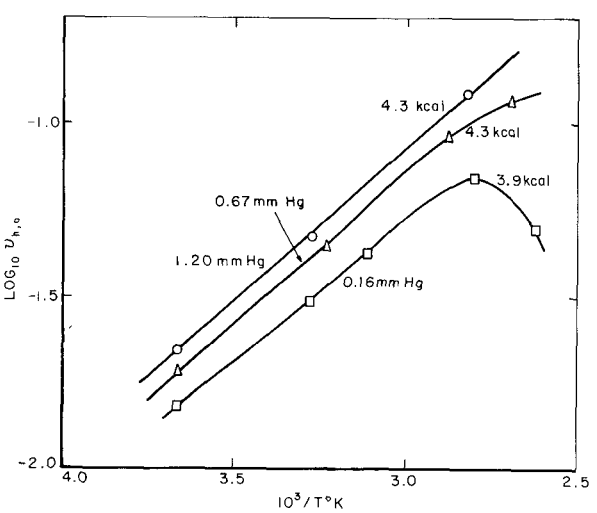

FIGURE 25. *Initial hydrogenation rate,* $v_{h,0}$, *of light ethylene with equimolar protium over carbided surface versus* $10^3/T$ *°K [118].*

$v_{h,0}$ is the initial value of v_h given in hydrogenated percent C_2H_4 min^{-1}. Figures attached to a curve indicate the initial total pressure and the activation heat determined from the part of the curve over the range of lower temperature.

the deuteration product of light ethylene over 5 mole % metal-γ alumina [89, 95]

Ru							Os						
54	54	54	54	32	64	80	24	24	24	24	17	36	47
100 54	100 165	27.5 50	100 50	75 76	75 76	75 76	50 27	50 50	50 152	50 203	50 50	50 50	50 50
5.5	5.5	10.9	11.2	7.3	7.3	7.3	16	16	16	16	15	15	15
2.6	0.7	2.1	2.6	2.2	2.9	4.1	3.1	0	0	0	1.0	3.2	0
9.9	11.3	10.0	11.0	10.4	9.7	10.7	14.2	14.3	11.3	10.6	9.8	15.1	12.3
29.0	35.7	29.5	29.3	41.6	26.8	25.9	46.8	52.0	55.4	62.8	59.0	41.3	44.4
2.5	3.1	2.4	2.5	2.1	2.6	3.5	6.1	8.1	7.7	6.0	6.4	6.2	7.0
0	0	0	0	0	0	0	2.5	3.5	3.3	1.8	3.0	3.2	3.0
0	0	0	0	0	0	0	0.6	0.7	1.0	0.9	0.7	1.0	0.6
0	0	0	0	0	0	0	0.6	0.7	0.9	0.9	0.7	0.8	0.6
52.1	45.1	52.3	51.7	42.8	54.0	49.8	24.8	18.2	18.9	15.9	18.9	27.5	30.7
3.9	4.1	3.7	2.9	0.9	4.0	6.2	1.6	2.4	1.6	1.1	0.4	1.7	1.5
0	0	0	0	0	0	0	0	0	0	0	0.1	0	0
0	0	0	0	0	0	0	0	0	0	0	0	0	0

hydrogenation, whereas hydrogen is appreciably adsorbed only by S but not by C (cf. table 2) [26].

(b) The optimum temperature of hydrogenation over C is ca. 30 °C higher than that over S (cf. figs. 13, 19, and 22 and table 21) [118].

(c) The activation heat over S at temperatures below the optimum is 5 ~ 6 kcal/mole and practically independent of the total pressure of the reactant gas mixture, whereas that on C below the optimum increases from 2.5 to 11 kcal/mole with increase of the total pressure from 0.1 to 20 mm Hg [118] (cf. table 21 and figs. 19, 22, and 25).

(d) The distribution of deuterium in hydrogen in course of the catalyzed deuteration of light ethylene is equilibrated over C, whereas it is not over S, although the deuterium in ethylene is of random distribution in both the cases [118] (cf. tables 17 and 27).

TABLE 27. *Relative amounts of ethylenes-*$d_n \equiv E_n$ *and hydrogens-*$d_n \equiv H_n$ *formed by deuteration of light ethylene by equimolar deuterium on carbided nickel film at ca. 0.1 mm* Hg *initial total pressure* [118]

React. temp. °C	Deuterated % C_2H_4	Rate of deuteration deuterated % $C_2H_4 \cdot min^{-1}$	E_n, %					H_n, %			Deuterium atom fraction in	
			E_0	E_1	E_2	E_3	E_4	$^1H_2$	^1HD	D_2	C_2H_4	H_2
−23	1.2	0.86	88 (87.8	12 11.6	1 0.6	0 0	0 0)	2 (0.1	4 5.8	94 94.1)	0.032	0.970
0	1.0	1.26	80 (79.7	18 18.6	2 1.6	0 0.1	0 0)	3 (0.2	6 8.4	91 91.4)	0.055	0.956
70	6.4	3.16	16 (16.0	32 37.1	32 32.4	15 12.6	4 1.9)	53 (53.0	40 39.6	7 7.4)	0.368	0.272
110	3.1	3.75	19 (19.0	32 39.1	32 30.2	14 10.4	3 1.3)	53 (53.0	40 39.6	7 7.4)	0.340	0.272
160	3.1	2.12	21 (21.0	32 40.1	31 28.7	13 9.1	3 1.1)	50 (50.0	42 41.4	8 8.6)	0.323	0.293

9. Reaction Mechanisms

Representative mechanisms are here reviewed which have been selected from those put forward up to now for the catalyzed hydrogenation in the presence of metals, especially nickel. It is the concept of the rate-determining step, that is indispensable in dealing with mechanisms. Confusions arise often, however, by giving it an ambiguous definition and unconvincing applications. Therefore, a definition of the rate-determining step is advanced and its application illustrated by mechanisms here.

9.1. Dissociative Mechanism

Farkas and Farkas put forward a mechanism on the basis of experimental results of the catalyzed hydrogenation as well as of the associated reactions, i.e., parahydrogen conversion and $^1H_2$–D_2 equilibration, over nickel [2] and platinum catalysts [85]. They [2, 85] assumed that the rate-determining step of the catalyzed hydrogenation as well as of parahydrogen conversion [8] was the dissociative adsorption of hydrogen molecules, i.e.,

$$H_2 \rightarrow 2H(a), \tag{9.1}$$

on the grounds that hydrogenation and parahydrogen conversion had activation heats of the same magnitude, i.e., 10 ~ 11 kcal/mole, and a constant ratio of rates throughout in spite of a widely varying activity of platinum catalysts [85].[9] Ethylene was assumed, on the other hand, to be adsorbed as

$$C_2H_4 \rightarrow C_2H_4(a) \tag{9.2}$$

and combine with 2H(a) so as to complete the hydrogenation thus

$$C_2H_4(a) + 2H(a) \longrightarrow C_2H_6. \tag{9.3}$$

The exchange reaction of ethylene was assumed by them to occur separately, through a step of dissociation of ethylene, i.e.,

$$C_2H_4(a) \longrightarrow C_2H_3(a) + H(a), \tag{9.4}$$

(hence the name "dissociative mechanism"), on the grounds that the activation heat of exchange was greater than that of catalyzed hydrogenation both over nickel [2] and platinum [85] as reviewed in 5.1.2 and 5.1.3, respectively.

They attributed [85] parahydrogen conversion and $^1H_2$–D_2 equilibration to step (9.1) and its reverse, on the one hand, and their inhibition to the preoccupation of sites of these reactions by ethylene, on the other hand. However, the inhibition follows necessarily from the proposed rate-determining step (9.1) irrespective of the preoccupation, since ethylene consumes the "moving spirits," H(a)'s, of the reverse of step (9.1) through step (9.3) at a rate greater than that of the proposed rate-determining step (9.1).

9.2. Associative Mechanism

9.2.1. Horiuti and Polanyi [7] found that the rate of exchange between ethylene and water was smaller than that between ethylene and hydrogen by a factor of ca. 10^5 and that the exchange rate between ethylene and benzene under the same conditions was still smaller [7] by orders of magnitude. On this experimental basis, they discussed step (9.4) as proposed to be responsible for the exchange. Let step (9.4) be in partial equilibrium; $C_2H_4(a)$ is admitting H(a)'s through its reverse including such ones originating from other molecules. The rate of the picking up is that of the reverse of step (9.4), which equals the rate of step (9.4), i.e., a "unimolecular" dissociation; the rate of the latter is constant irrespective of the activity of H(a), apart from the effect of adsorption, hence the rate of picking up H(a) is constant as well. Step (9.4) can hence not be responsible for the exchange, insofar as the absorption does not make a difference of orders of magnitude such as observed.

Horiuti and Polanyi [7], thus put forward with reference to the experimental results [7], of the wandering of the double bond, the scheme

$$\begin{array}{l} C_2H_4 \xrightarrow{I_a} C_2H_4(a) \\ H_2 \xrightarrow{I_b} \begin{cases} H(a) \\ H(a) \cdots\cdots\cdots \end{cases} \end{array} \Bigg\} \xrightarrow{II} C_2H_5(a) \Bigg\} \xrightarrow{III} C_2H_6, \tag{9.5}$$

where $C_2H_4(a)$ represents so-called associatively adsorbed ethylene, in which the π-bond of ethylene is broken and two carbon-metal bonds are formed, and $C_2H_5(a)$, termed *half-hydrogenated state* by them [7], is an ethyl radical linked with the metal by its methylene radical. The two hydrogen atoms

[8] Cf. 9.2.2 and 9.2.2.1.
[9] Cf. 5.1.3.

from a methylene radical of C_2H_4(a) and one from H(a) assume equivalent positions in the methyl radical of C_2H_5(a), so that the exchange results on reversal of steps II.

Step II in partial equilibrium is accelerated by increase of the activity of H(a), hence its backward act must be likewise accelerated. The rate of C_2H_4(a) embodying hydrogen atoms from H(a) depends in consequence on the activity of H(a), in distinction from the case where dissociation (9.4) is responsible for exchange. The exchange rate of hydrogen atoms between ethylene and water or benzene is hence by far smaller than that between ethylene and hydrogen, as observed, owing to their widely divergent capacities of sustaining the activity of H(a).

9.2.2. Scheme (9.5) is now discussed with special reference to the rate-determining step of the relevant overall reaction. The rate-determining step is defined only for such an overall reaction where each of the constituent steps has unique, definite stoichiometric number [127].[10] The constituent step r of a stoichiometric number different from zero, is defined as rate-determining if the steady rate of the overall reaction is given practically as that in the equilibria of all constituent steps but r. These partial equilibria determine the activity products, a_I and a_F, of the initial and the final system of r, irrespective of the kinetic particulars of any step. The net rate of r is $k_I a_I - k_F a_F$ or $k_I(a_I - a_F/K)$, where $K = k_I/k_F$ is the equilibrium constant of r, which is thermodynamically definite irrespective of the kinetic particulars of r.[11] The steady rate of the overall reaction is thus proportional to k_I, which alone involves the kinetic particulars of r, while the other factor, $a_I - a_F/K$, of the net rate is thermodynamically defined by the system [12] of step r and the conditions of the assembly in which the reaction in question is going on. Step r thus literally determines the steady rate of the overall reaction through its kinetic particulars which are exclusively incorporated in k_I.

9.2.2.1. A rate-determining step cannot be defined in this way, e.g., for parahydrogen conversion in gear with the overall reaction. Neither is it necessary to assign a similar concept to this conversion, as seen later. We should admit a wording like "the rate-determining step of parahydrogen conversion," if this occurs in gear with the hydrogenation, as designating a step assumed (by the broacher of the wording) to have the same rate as the parahydrogen conversion in question.

The rate-determining step of scheme (9.5) is now discussed on this basis. It is noted that step III may be rate-determining, but it can never be in partial equilibrium since it practically lacks backward acts, as verified by result 5.2.7 that ethane is never involved in any constituent step of the catalyzed hydrogenation of ethylene. Nevertheless, any step other than III, e.g., I_b may be qualified as rate-determining, if $k_F a_F$ is diminished by an amount which is ignorable as compared with $k_I a_I - k_F a_F$, by reducing all steps but I_b (inclusive of III) from the actual steady state to equilibria.

9.2.2.2. Let III be rate-determining, leaving the other three steps in their respective partial equilibria. A step is kept in partial equilibrium notwithstanding the progress of the overall reaction, which of course imposes a finite amount of net rate upon the step, insofar as its forward and backward rates are large enough as compared with their difference, i.e., the net rate. There hence occurs a lively exchange of hydrogen atoms between gaseous ethylene and hydrogen, as seen readily by tracing scheme (9.5) with step III supposed to be arrested. Parahydrogen conversion and $^1H_2$–D_2 equilibration proceed just as in the absence of ethylene, apart from the effect, if any, of preoccupation of sites by adsorption. Deuterium atoms are randomly distributed over C_2H_4, H_2 and C_2H_6 composed of the former two throughout.

9.2.2.3. If step II is to determine the rate, leaving steps I_a and I_b in their partial equilibria, transfer of hydrogen atoms between gaseous ethylene and gaseous hydrogen is retarded in either direction. Parahydrogen conversion and $^1H_2$–D_2 equilibration proceed as lively as in 9.2.2.2.

9.2.2.4. In case of I_b determining the rate, leaving I_a and II in their partial equilibria, admission of hydrogen atoms originating from gaseous ethylene into gaseous hydrogen, is retarded whereas the reverse transfer occurs. Parahydrogen conversion and $^1H_2$–D_2 equilibration are practically inhibited.

9.2.2.5. If I_a determines the rate, leaving I_b and II in their partial equilibria, parahydrogen conversion and $^1H_2$–D_2 equilibration will occur as in the absence of ethylene and hydrogen atoms from ethylene penetrate hydrogen while the reverse transfer is retarded on the contrary to the case of 9.2.2.4. Hydrogen atoms are randomly distributed over gaseous hydrogen and C_2H_4(a), but not over gaseous ethylene and C_2H_4(a) throughout; in the particular case of hydrogenation of light ethylene with pure deuterium C_2H_4(a) is exclusively C_2D_4(a) so that gaseous ethylene should consist in the beginning of the hydrogenation only of $C_2{}^1H_4$ and C_2D_4 but not of ethylene-d_n of intermediate composition.

9.2.3. Tables 3 and 17 show that deuterium in gas keeps its atom fraction of 0.992 at −23 and −45 °C, amply below the optimum at 28 °C, during the catalyzed deuteration of light ethylene. Protium of ethylene got thus hardly into gaseous hydrogen, whereas an appreciable amount of deuterium atoms entered gaseous ethylene and became distributed randomly there as seen by comparison of the observed percentage of ethylenes-d_n with calculated value shown in parentheses. The tables show, on

[10] The number of times a step occurs for every completion of the relevant overall reaction in the steady state. The set of steps, $H^+ + e^- \longrightarrow H(a)$, $2H(a) \longrightarrow H_2$ and $H(a) + H^+ + e^- \longrightarrow H_2$ has the stoichiometric numbers, (2, 1, 0) or (1, 0, 1) as given in the order of the steps for *the overall reaction*, $2H^+ + 2e^- = H_2$, where H^+ is hydrogen ion in solution and e^- metal electron. The stoichiometric number of each step of the above set is not unique. The stoichiometric number of every constituent step of scheme (9.5) is unity uniquely for the overall reaction of eq (4.1).

[11] All steps, heterogeneous or homogeneous, which have common I and F, have the same K quite independently from their rates, i.e., kinetic particulars, provided that all activities involved are referred to common standard states.

[12] A set of particles involved in a step.

the other hand, that above the optimum there occur a rapid exchange between gaseous ethylene and deuterium and a lively $^1H_2$–D_2 equilibration, the results below the optimum fit in exclusively with the conclusions of 9.2.2.4, while those above the optimum fit in exclusively with those of 9.2.2.2. We are thus inevitably led to the conclusion that the rate-determining step switches over from I_b below the optimum to III above.

The same conclusion has previously been arrived at by Horiuti [9] from the analysis of experimental results of zur Strassen [64]. It may be noted that the switchover in the rate-determining step is necessarily connected with the appearance of an optimum, the excess of activation heat of exchange over that of hydrogenation and other profiles of the reaction, as shown by a statistical mechanical theory developed in section 12.

The term "associative mechanism" will be used in what follows just to signify the kinetic theory of scheme (9.5) without specializing in any particular rate-determining step.

9.2.4. The chemisorbed states, H(a) etc., included in scheme (9.5), are experimentally verified as follows. Parahydrogen conversion and $^1H_2$–D_2 equilibration proceed over evaporated nickel films perceptibility around −100°C with a rate increasing with temperature [128],[13] whereas the transition from "normal" to "activated" adsorption with low or high adsorption heat respectively occurs around −150 °C as traced on an isobar [129] of hydrogen adsorption over the same catalyst. These experimental results afford the basis for accepting the existence of H(a) under the conditions in question.

Pliskin and Eischens [130] demonstrated infrared-spectrometrically the existence of associatively adsorbed ethylene, $C_2H_4(a)$, and the formation of ethyl radical, $C_2H_5(a)$, from $C_2H_4(a)$ on admission of hydrogen gas over adsorbed ethylene. Ethylene and hydrogen are adsorbed simultaneously on S-film without dehydrogenated adsorption of ethylene as referred to in 2.E.1, which further confirms the existence of three intermediates H(a), $C_2H_4(a)$, and $C_2H_5(a)$ there.

9.2.5. The experiment of Apel'baum and Temkin [91] on palladium indicates unambiguously a definite fall of fugacity from gaseous hydrogen to adsorbed hydrogen on the catalyst at 22 °C but none at 176 °C. Step I_b is thus rate-determining at lower temperatures and in partial equilibrium at higher temperatures, in accord with a similar conclusion in 9.2.3 in the case of nickel.

9.3. Twigg and Rideal's Mechanism

9.3.1. Twigg and Rideal [68] contradicted the dissociative adsorption (9.4) of ethylene as responsible for the exhange reaction on the ground of Conn and Twigg's experiment [23] referred to in 2.7, which showed that $C_2{}^1H_4$ and C_2D_4 did not exchange hydrogen atoms at 76 °C. Twigg and Rideal [68] found, as reviewed in 5.1.2, that $^1H_2 - D_2$ equilibration was inhibited by the presence of ethylene, and that the plot of the nonequilibrium fractions $1-u$ of hydrogen gas against its deuterium atom fraction, x_H, converged into a single straight line for temperatures below and including 156 °C, as seen in figure 16. From these experimental results they gathered [68] that $^1H_2$–D_2 equilibration was not effected by step (9.1) but, as suggested by the latter close connection between equilibration and exchange, was alternatively in gear with steps resulting in the exchange between ethylene and hydrogen, as

$$C_2H_4 \rightleftharpoons C_2H_4(a),$$

$$C_2H_4(a) + H_2(a) \rightleftharpoons C_2H_5(a) + H(a), \qquad (9.6)$$

and

$$C_2H_5(a) \rightleftharpoons C_2H_4(a) + H(a), \qquad (9.7)$$

where $H_2(a)$ is the physically adsorbed hydrogen molecule.

They attributed the hydrogenation, on the other hand, to a single step

$$C_2H_4(a) + H_2(a) \rightarrow C_2H_6 \qquad (9.8)$$

on the ground that the activation heat of exchange exceeded appreciably that of hydrogenation [68, 69]. This mechanism of hydrogenation should lead, however, to different products when light ethylene is hydrogenated, in one case with an equimolar mixture of $^1H_2$ and D_2, and in the other case with an equilibrated mixture of $^1H_2$, ^1HD, and D_2. This is contrary to the observation of Twigg [116] in 5.2.1, provided that the peculiarities of nickel-kieselguhr used in the latter observation are ignored.

9.3.2. Twigg has thus revised the mechanism as [116]

$$\left.\begin{array}{c} C_2H_4 \underset{2}{\overset{1}{\rightleftharpoons}} C_2H_4(a) \\ C_2H_4(a) + H_2(a) \underset{4}{\overset{3}{\rightleftharpoons}} C_2H_5(a) + H(a) \xrightarrow{7} C_2H_6 \\ C_2H_5(a) \underset{6}{\overset{5}{\rightleftharpoons}} C_2H_4(a) + H(a) \end{array}\right\} \qquad (9.9)$$

with the aim to account for the observed difference between the activation heats of hydrogenation and of exchange, by ascribing, respectively, different rate-determining steps[14] to them similarly to the proposal of Twigg and Rideal [68] reviewed in 9.3.1. The rate-determining steps of hydrogenation and

[13] Cf. Chapter 8 of ref. 18.

[14] Cf. 9.2.1 and 9.2.2.2.

exchange were thus indicated to be steps 7 and 4, respectively, which have the same initial system,[15] $C_2H_5(a)+H(a)$, hence give rise to the same rate law for both the reactions, as observed.

Twigg [116] assumed next that below the optimum, step 7 was overwhelmingly faster than step 4. If, then, the system $C_2H_5(a)+H(a)$ is once created by step 3, it should be converted with predominant probability into C_2H_6 rather than reconverted into $C_2H_4(a)+H_2(a)$ through step 4. Step 3 thus determines the rate of hydrogenation,[16] rather than step 7, in conflict with Twigg's statement. This is, however, just a contradiction in terms and, remaining true to the postulated predominance of step 7, his arguments apply just by terminological revision. The rate of rate-determining step 3 is $k_3\theta_{C_2H_4}\theta_{H_2}$, denoting the rate constant of step n by k_n and the respective coverages by adsorbates $C_2H_4(a)$ etc. by $\theta_{C_2H_4}$ etc. The latter rate is written, admitting the proportionality of θ_{H_2} to P_H, as $k_3\theta_{C_2H_4}P_H$, which just reproduces the rate expression of the catalyzed hydrogenation given by Twigg himself. The steady state condition of hydrogenation is now

$$k_3\theta_{C_2H_4}P_H - k_4\theta_{C_2H_5}\theta_H = k_7\theta_{C_2H_5}\theta_H. \qquad (9.10)$$

Hence, we have below the optimum

$$k_3\theta_{C_2H_4}P_H = k_7\theta_{C_2H_5}\theta_H, \qquad (9.11)$$

ignoring the rate of step 4 as compared with that of 7 according to the postulate. The rate of exchange is similarly $k_4\theta_{C_2H_5}\theta_H$ or, according to eq (9.11), $k_3(k_4/k_7)\theta_{C_2H_4}P_H$, which assures the rate law of exchange to be the same as that of hydrogenation.

Above the optimum, it follows from postulate $k_4 \gg k_7$ and eq (9.10) that the forward and backward rates of step 3 are balanced with each other, hence that step 7 functions as the rate-determining step, provided that step 1 is also in partial equilibrium. We are thus led to concluding from the kinetic postulates of Twigg that the part of determining the rate of hydrogenation is switched over from step 3 below the optimum to step 7 above.

As shown by Twigg [116], the activation heat of exchange exceeds that of hydrogenation above and below the optimum by E_4-E_7 throughout, where $E_4=RT^2\partial \ln k_4/\partial T$ and $E_7=RT^2\partial \ln k_7/\partial T$. The difference E_4-E_7 below the optimum is the difference of the activation heat of the reverse of step 3 from that of rate-determining step 3 as seen from the above expression for the exchange rate, $k_3(k_4/k_7)\theta_{C_2H_4}P_H$; the forward flow of the exchange rate, $k_3\theta_{C_2H_4}P_H$, is sparingly reversed, to a ratio of k_4 to k_7, to form the backward flow giving rise to the exchange. The ratio k_4/k_7 in the expression for the backward flow is connected with the difference between heights of the two energy humps which enclose $C_2H_5(a)+H(a)$ as $RT^2\partial \ln(k_4/k_7)/\partial T = E_4-E_7$. Above the optimum, k_4/k_7 equals directly the ratio of exchange rate to hydrogenation rate, the latter now being governed by step 7, hence the difference is once again E_4-E_7.

The above inference would illustrate that the difference of activation heats provides no ground to exclude the reverse of step (9.1), assigned to be the rate-determining step of hydrogenation, as done by Farkas et al. [2], from being the "rate-determining step of exchange." It may be noted, however, that the switchover of the rate-determining step that follows from the postulate of Twigg, can only occur, according to the statistical mechanical theory of the reaction developed in 11 and 12, between steps having systems of different materials,[17] such as steps I_b and III of scheme (9.5), but it can scarcely occur otherwise, cf. steps 3 and 7 in scheme (9.9).

9.4. Jenkins and Rideal's Mechanism

Jenkins and Rideal [13] revised the above mechanism supposing that the catalyst's surface was complex covered or carbided and capable of adsorbing further hydrogen but no more ethylene.[18] The exchange was postulated to occur under these conditions through a step

$$C_2H_4 + 2H(a) \rightleftharpoons C_2H_5(a) + H(a),$$

in which one of the two adjacent adatoms is picked up, whereas both of them are captured to complete the hydrogenation as

$$C_2H_4 + 2H(a) \rightarrow C_2H_6. \qquad (9.12)$$

They postulated further that the reverse of step (9.1) occurs slower than step (9.12) at temperatures below and faster above the optimum, respectively. Below the optimum, 2H(a) once formed by step (9.1) should be converted almost certainly into C_2H_6 by step (9.12) rather than reconverted into H_2, so that step (9.1) is essentially rate-determining for hydrogenation, while above the optimum step (9.12) determines the rate, as shown by arguments

[15] The initial and final systems of a step are its system, respectively, in the state before and after the occurrence of the step.

[16] Equation (9.10) is expressed for $k_4 \ll k_7$ as

$$k_3\theta_{C_2H_4}P_H = k_7\theta_{C_2H_5}\theta_H \gg k_4\theta_{C_2H_5}\theta_H$$

(the θ's are adsorbate coverages defined in the text); the first and the third member are the rates of step 3 and 4, respectively, which are by no means balanced, hence step 3 is by far not in partial equilibrium. We can bring the latter step up to equilibrium by increasing $\theta_{C_2H_5}\theta_H$ by a factor k_7/k_4. The rate of step 7 thus increases k_7/k_4 fold. Since the latter increased rate does not approximate by any means the steady rate, step 7 is excluded from being rate-determining according to 9.2.2.

Step 3 is now similarly examined. By reducing step 7 to its partial equilibrium, $\theta_{C_2H_5}\theta_H$ vanishes when the rate of hydrogenation is $k_3\theta_{C_2H_4}P_H$ rather than $k_3\theta_{C_2H_4}\theta_{H_2} - k_4\theta_{C_2H_5}\theta_H$ as in the steady state. Since $k_4\theta_{C_2H_5}\theta_H$ is negligibly small by premise, the steady rate is closely approximated by that in equilibrium of step 7, i.e., $k_3\theta_{C_2H_4}P_H$. Step 3 is thus duly rate-determining according to 9.2.2, provided that step 1 is also practically in equilibrium.

An actual example of the similar rate-determining step is given in 13.4.2.

[17] Materials of systems of step I_b and III of scheme (9.5) are H_2 and $C_2H_4+H_2$, respectively, whereas those of steps 3 and 7 are commonly $C_2H_4+H_2$.

[18] Just contrary to result 8.1(a).

similar to those on steps 3 and 7 in 9.3.2. The rate-determining step of hydrogenation thus switches over from step (9.1) below the optimum to step (9.12) above, which is something in common with the associative mechanism outlined in 9.2.1.

Beeck [6] proposed, in advance of the above revisal [13], that the hydrogenation proceeded through step (9.12) and its rate-determining step was the evacuation by hydrogenated desorption of sites for adsorption of 2H(a) preoccupied by acetylenic complex, although this is inapplicable as remarked in 3.1.3.

9.5. Redistribution Mechanism

We have seen in 7.1.3 that hardly any deuterium enters the ethylene in gas in course of its catalyzed deuteration over Ni-kieselguhr catalyst, while deuterium is abundantly contained and randomly distributed in the ethane molecules thus evolved. This result admitted, according to Wilson, Otvos, Stevenson, and Wagner [126], of no explanation by mechanisms proposed up to that time. They put forward, for an explanation, the redistribution mechanism in which a rapid exchange of hydrogen atoms among "adsorbed hydrocarbon fragments," e.g., $C_2H_4(a)$ or $C_2H_5(a)$, on the catalyst effected an exchange equilibrium or random distribution of deuterium atoms among them as well as the hydrogenation through steps such as

$$2C_2H_5(a) \rightarrow C_2H_4(a) + C_2H_6.$$

They [126] reproduced the fractions of ethanes-d_n at -50 °C in table 24 approximately by its probability $\{6!/n!(6-n)!\}x_A^n(1-x_A)^{6-n}$ in random distribution, but the peak of distribution at $n=2$ observed in 50 °C was not thus reproduced. They similarly calculated the fraction of butane-d_n in the deuteration product of light butylene, but the calculated abundance of butane-d_2 fell appreciably short of observation.

9.6. Adsorbed State of Intermediates

With special reference to the adsorbed state of the intermediates implied, Semenov [131] proposed the constituent steps of catalyzed hydrogenation in terms of free valencies, V, furnished by metal atoms of the catalyst. Ethylene is thus combined with V to form a free radical as

$$C_2H_4 + V \rightarrow V\text{CH}_2\text{—CH}_2\text{—}. \qquad (9.13)$$

The free radical reacts upon H_2 to form $C_2H_5(a)$ or upon another V to form a stable $C_2H_4(a)$ as

$$V\text{CH}_2\text{—CH}_2\text{—} + H_2 \rightarrow V\text{CH}_2\text{—CH}_3 + H \qquad (9.14)$$

or

$$V\text{CH}_2\text{—CH}_2\text{—} + V \rightarrow V\text{CH}_2\text{—CH}_2V.$$

The H formed by step (9.14) is so unstable that it attacks $C_2H_5(a)$ to form ethane as

$$H + V\text{CH}_2\text{CH}_3 \rightarrow C_2H_6 + V.$$

In the case where sufficient $C_2H_4(a)$ and $C_2H_5(a)$ are present, there occur frequently forward and backward acts of the steps

$$H + V\text{CH}_2\text{—CH}_2V \rightarrow V\text{CH}_2\text{CH}_3 + V$$

and

$$V\text{H} + V\text{CH}_2\text{—CH}_2\text{—} \rightarrow V\text{CH}_2\text{CH}_3 + V.$$

and the $V\text{CH}_2 - \text{CH}_2$—'s react upon each other to form polymer, which poisons the catalyst. Semenov [131] did not refer to step (9.1) of hydrogen chemisorption in this connection.

Bond et al. [132], has recently advanced the view that the bonds which link ethylene to metal are not σ-bonds as admitted so in 3.1.2, but π-bonds between surface metal atoms and ethylene, with the double bond of C_2H_4 left intact, as in the case of complex compounds between olefine and metal salts, which is, however, not verified thus far and, if it should be at all, makes no difference in the kinetic treatments.

10. Current Theoretical Treatments

10.1. Outline

The rate v of combination, e.g., of species A and B distributed homogeneously in a macroscopic phase is expressed according to the mass action law in terms of the concentrations, [A] and [B], of the respective species as

$$v \propto [A][B]. \qquad (10.1)$$

If either or both of species A and B are adsorbed, as denoted by appendix (a), i.e., as A(a) or B(a), the rate of combination is usually expressed by

$$v \propto \theta_A[B] \qquad (10.2.A)$$

or

$$v \propto \theta_A\theta_B, \qquad (10.2.B)$$

where θ_A and θ_B are the fractions of the catalyst surface covered by A and B, respectively.

Schwab [133] expressed the rate of the step

$$H_2(a) + C_2H_4(a) \rightarrow C_2H_6,$$

assumed by him to be rate-determining in the catalyzed hydrogenation of rate v_h according to eq (10.2.B) as

$$v_h = k_h b_E b_H P_E P_H (1 + b_E P_E)^{-1}, \qquad (10.3)$$

substituting $\theta_{C_2H_4}$ in eq (10.2.B) from Langmuir's adsorption isotherm:

$$\theta_{C_2H_4} = b_E P_E (1 + b_E P_E)^{-1}, \qquad (10.4)$$

and similarly for θ_{H_2}:

$$\theta_{H_2} = b_H P_H (1 + b_H P_H)^{-1},$$

but ignoring $b_H P_H$ as compared with unity, where k_h is the so-called "true" rate constant. Schwab [133] assumed that $b_E P_E \gg 1$ below the optimum and $b_E P_E \ll 1$ above the optimum, hence according to eq (10.4) that $\theta_{C_2H_4} \doteqdot 1$ or $\theta_{C_2H_4} \doteqdot 0$, respectively, or in words that ethylene saturates the catalyst's surface below the optimum but is desorbed as the temperature is raised past the optimum, T_X. The rate laws below and above the optimum are, in consequence,

$$v_h = k_h b_H P_H \qquad (T < T_X)$$

and

$$v_h = k_h b_E b_H P_E P_H \qquad (T > T_X),$$

and the activation heats below the optimum, $E_{T<T_X}$, and above the optimum, $E_{T>T_X}$, are

$$E_{T<T_X} = E_0 + \Delta H_H \qquad (10.5.a),$$

and

$$E_{T>T_X} = E_0 + \Delta H_H + \Delta H_E = E_{T<T_X} + \Delta H_E, \qquad (10.5.b)$$

respectively, where

$$E_0 = RT^2\partial \ln k_h/\partial T \qquad (10.6.k)$$

is the so-called "true" activation heat and

$$-\Delta H_E = -RT^2\partial \ln b_E/\partial T \qquad (10.6.E),$$

and

$$-\Delta H_H = -RT^2\partial \ln b_H/\partial T \qquad (10.6.H)$$

are the adsorption heats of ethylene and hydrogen, respectively. Schwab [133] determined, from the plot of v_h/P_H against P_E by zur Strassen [64] as shown in figure 26, $k_h b_H$ and b_E and hence $E_{T<T_X}$ and ΔH_E as

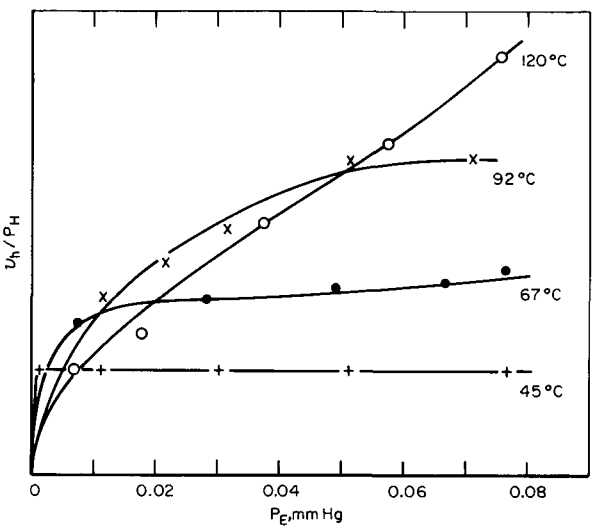

FIGURE 26. *Proportional constant* v_h/P_H *of* v_h *to* P_H *versus* P_E [64].
v_h: hydrogenation rate in arbitrary unit.

$$E_{T<T_X} = 7.3 \text{ kcal/mole}, \qquad (10.7.E),$$

$$-\Delta H_E = 17.3 \text{ kcal/mole}. \qquad (10.7.H)$$

He [133] thus described the optimum as the point of desorption of ethylene. This theory of optimum does not, however, fit in with new results as shown in what follows. The quantity of ethylene adsorbed on an S surface of evaporated nickel film in course of the progress of hydrogenation (cf. table 2) was found approximately constant and corresponded to the coverage of $\theta_{C_2H_4} = 0.33$ over the temperature range from -50 to 110 °C [61], which comprises the optimum temperature, 35 °C; the above value of $\theta_{C_2H_4}$ was calculated from the observed quantity of adsorption by geometric considerations on the basis of 10^{15} surface metal atoms per unit BET area, any two neighboring atoms among them being taken as available for occupation by one adsorbed ethylene molecule. This disproves the hypothesized desorption of ethylene, provided that the observed amount of adsorption directly represents those and only those molecules occupying the sites of critical complex.[19]

The above provision might be questioned with regard to the active center theory, in the sense that just a minute fraction of the observed amount of ethylene adsorbed may block the active centers and evaporate at the optimum to release them, while the observation of the total adsorbed quantity

[19] Cf. footnote 5 to 3.1.6.

would be quite insensitive to this fraction. It is, however, established [38] that the number of sites of critical complex involved amounts to around 10^{15} cm^{-2}, as referred to in 3.1.6. Therefore, if ethylene is desorbed at the optimum to set these sites free, according to Schwab's hypothesis, then the desorbed amount must be of about this magnitude, which is by no means negligible as compared with the amount of adsorbed ethylene observed, and would never escape detection; the approximately constant $\theta_{C_2H_4}$ over the above temperature range thus excludes the possibility of the desorption as responsible for the optimum.

The above hypothesis is further contradicted by the observed dependence of the optimum temperature upon the partial pressure of ethylene. Assigning the optimum to the point where $\{\partial \ln v_h/\partial(1/T)\}_{P_E, P_H}=0$, we have, on substitution of v_h from eq (10.3),

$$RT^2\partial \ln k_h/\partial T+\{RT^2/(1+b_EP_E)\}\partial \ln b_E/\partial T + RT^2\partial \ln b_H/\partial T=0.$$

The value of $\log_{10} b_E$ at $T=T_X$ is obtained by integrating eq (10.6.E) for constant ΔH_E, as

$$\log_{10}b_E=\log_{10}b_{E,0}-\Delta H_E/2.303RT_X,$$

where $\log_{10} b_{E,0}$ is the integration constant. Eliminating $RT^2\partial \ln k_h/\partial T$, $RT^2\partial \ln b_E/\partial T$, $RT^2\partial \ln b_H/\partial T$ and b_E from the above two equations and eqs (10.6.k), (10.6.E), and (10.6.H), we have

$$\frac{1}{T_X(°K)}=\frac{2.303R}{-\Delta H_E}\left\{\log_{10}\frac{-\Delta H_E-\Delta H_H-E_0}{b_{E,0}(E_0+\Delta H_H)}-\log_{10}P_E\right\} \quad (10.8)$$

The constant $\log_{10}b_{E,0}$ is evaluated from the above linear relation as

$$\log_{10}b_{E,0}=-9.1. \quad (10.9)$$

The value of $(E_0+\Delta H_H)$ is given by eqs (10.5.a) and (10.7.E), while that of $-\Delta H_E$ is given by eq (10.7.H). Substituting these values of $(E_0+\Delta H_H)$, ΔH_E, and that of $\log_{10}b_{E,0}$ from eq (10.9) into eq (10.8), we have

$$1/T_X=(1/3760)(9.3-\log_{10}P_E), \quad (10.10)$$

(T_X in °K, P_E in mm Hg) which deviates considerably from eq (4.3) as observed by Sato and Miyahara [80].

Jenkins and Rideal [13] expressed the rate of catalyzed hydrogenation as $v_h=k_3P_E\theta_{H_2}$ according to their mechanism (which was reviewed in 9.4), where k_3 is the rate constant of step (9.12). Denoting the rate constants of step (9.1) and of its reversal with k_1 and k_2, respectively, one can write the steady condition of the reaction, as regards the intermediates 2H(a), as

$$k_1P_H(1-\theta_{H_2})=k_2\theta_{H_2}+k_3P_E\theta_{H_2}$$

or neglecting the rate of repulse of hydrogen adsorption, $k_1P_H\theta_{H_2}$, as compared with the sum of the rate of adsorbed hydrogen leaving the adsorbed state both by desorption ($k_2\theta_{H_2}$) and by hydrogenation ($k_3P_E\theta_{H_2}$), as

$$k_1P_H=k_2\theta_{H_2}+k_3P_E\theta_{H_2}.$$

Eliminating θ_{H_2} from this equation and the above expression for the hydrogenation rate, $v_h=k_3P_E\theta_{H_2}$, we have

$$v_h=k_1k_3P_EP_H/(k_2+k_3P_E), \quad (10.11)$$

which is of the same form as eq (10.3) due to Schwab and agrees with the rate law observed by Jenkins and Rideal [13] at the optimum temperature, 165 °C, as given in table 7. They assumed, as reviewed in 9.4, that $k_2 \ll k_3P_E$ at temperatures below and $k_2 \gg k_3P_E$ above the optimum, hence $v_+ \propto P_H$ or $v_+ \propto P_HP_E$, respectively, from eq (10.11), in accordance with experiments. The rate-determining step is in consequence (9.1) at temperatures below but (9.12) above the optimum, as discussed in 9.4. The change of activation heat may occur, hence, by switchover in the rate-determining step at the optimum because of the difference in materials of the systems [20] of step (9.1) (H_2) and that of step (9.12) ($H_2+C_2H_4$) as mentioned in 9.8.2, whereas there exists then little difference from the associative mechanism, insofar as the hydrogenation is concerned.

10.2. Critical Review of Current Treatments

The formulation of rate of steps by the mass action law referred to in 10.1. is applicable only in cases where the system (see footnote 20) of the step is statistically independent, i.e., the system assumes any state under given macroscopic constraints, e.g., confinement to a definite volume, as if it were alone under the same constraints. The statistical independence is secured in cases where the species of variable concentrations concerned are sparse enough, whether the step be homogeneous or heterogeneous.[21] The covered fraction of one-tenth might be thought of as moderate, but the corresponding three-dimensional concentration is, for 10^{15} cm^{-2} sites and the appropriate thickness of 10^{-8} cm, $10^{15}\times10^{-1}\times(10^{-8})^{-1}$ cm$^{-3}=10^{22}$ cm^{-3}, which matches the molecular concentration of liquids. The applicability of the mass action law is

[20] Set of particles involved in the step.

[21] A step is called homogeneous or heterogeneous according as its critical complex [cf. footnote 5 to 3.1.6] is situated in a macroscopic phase or in a surface phase. A macroscopic phase will be called simply phase in what follows.

thus a problem which is rather more serious in case of heterogeneous steps than in case of homogeneous steps, just because of the different concentrations of species in the state of interest.

The applicability must of course be decided on the basis of a general theory of reaction rates which does not rest upon the statistical independence of the system of the given step. Readers are referred, in this regard, to an article "On the Theory of Heterogeneous Catalysis" by Horiuti and Nakamura [134].

There exist two kinds of deviations from the statistical independence of a system of a step in case of heterogeneous steps [134]. First, a species is not admissible to a site of adsorption if the site is preoccupied by another species. Secondly, there exist in general repulsive or attractive interactions between species which occupy their respective sites exclusively. In the semiquantitative treatments presented in this monograph, we will be content to take account of the former kind of deviation only, ignoring the latter throughout. Under this limitation, the current treatments referred to in 10.1 are critically reviewed on the basis of the general theory [134]; conclusions only are cited, leaving out any detailed arguments.

(A) Equation (10.2.B) is exact, if the critical complex[22] of the step occupies the combined sites of A and B.

(B) If the critical complex occupies a single site, either of A or B, the exact equations is

$$v_+ \propto \theta_A[B] \qquad (10.12.A),$$

or

$$v_+ \propto [A]\theta_B, \qquad (10.12.B)$$

respectively. Equations (10.12) are applicable when A and B are alternative occupants of one kind of sites, or when A and B occupy different kinds of sites exclusively, or when either one of them is the exclusive occupant of any sites. The necessary and sufficient condition for eqs (10.12.A) and (10.12.B) to be valid is that the critical complex occupies a single site, either of A or of B, respectively [134]; it is not necessary that either of A and B is adsorbed and collided with by the other from the gas phase. On the other hand, eqs (10.12.A) and (10.12.B) do not apply even if the one from the gas phase collides with the other one which is adsorbed, provided that the critical complex thus formed occupies combined sites of A and B; in the latter case eq (10.2.B) holds instead.

It may be noted that eq (10.12.A) is identical with eq (10.2.A).

11. Statistical Mechanical Formulation of Rates

Rates are statistical mechanically formulated under the premise mentioned in 10.2 with the aim of formulating the catalyzed hydrogenation of ethylene statistical mechanically on the basis of the associative mechanism.

11.1. Outline

The general theory assures, under the premise in 10.2, that an exact result is obtained by the procedure of Glasstone, Laidler, and Eyring, which treats sites of adsorption as if they were constituent species of a statistically independent system of the step. We start from eq (72) on p. 378 of "The theory of Rate Processes" by Glasstone, Laidler, and Eyring, McGraw-Hill Book Company, 1941, for the rate v of a bimolecular step in case of sparse coverage, i.e.,

$$v = \frac{1}{2} s C_g C_{g'} C_s \frac{kT}{h} \frac{f_\ddagger}{F_g F_{g'} f_s}$$

by which two molecules of different kinds in gas, of concentrations C_g and $C_{g'}$, respectively, are combined on the catalyst; the catalyst provides sites of adsorption for the molecules, each of them being occupied by any of them at a given time, and the activated complex[23] of the step occupies adjacent two sites. C_s is the number of available single sites per unit area, and s is the number of sites adjacent to each site. F_g and $F_{g'}$ are the complete partition functions of molecules of the respective kinds per unit volume, which are substituted for the partition functions in the original equation in Glasstone, Laidler and Eyring's book, so that the Boltzmann factor of the total elevation, ϵ_0, of the ground state in the original equation is absorbed into the partition functions. The factor $(1/2)sC_s$ represents the total number, $N_\ddagger$, of sites of the activated complex per unit area under the above premise of a sparse coverage. The quantities $f_\ddagger$ and f_s are termed, by the book's authors, the partition functions of the activated complex and of the reaction sites, respectively, whereas partition functions are defined in this book only for a statistically independent assembly and not for an adsorbed species or a site which are not statistically independent. This amounts to a leap of argument but can be reconciled by an alternative interpretation of $f_\ddagger$ and f_s as follows.

[22] Cf. footnote 5 to 3.1.6.

[23] Under the present approximation, activated complex may be taken synonymous with the critical complex referred to in 3.1.6.

The factor $f_\ddagger$ in the above equation is read for the partition function (complete) of the catalyst with a single activated complex attached to a definite site, and f_s for the partition function (complete) of the bare catalyst. These definitions are acceptable since both subjects may be taken to be statistically independent. Since F_g and $F_{g'}$ are partition functions of molecules A and B, both detached from the catalyst, the product $F_g F_{g'} f_s$ is the partition function of an assembly consisting of the bare catalyst, A and B, all separated from each other. The factor $f_\ddagger/F_g F_{g'} f_s$ is hence the ratio of the probabilities of the state where the activated complex is attached to a definite site and that where the assembly is in the separated state; this ratio, when multiplied by the universal frequency, kT/h, gives the specific rate of the step in question, which pertains to a single pair of A and B on the definite site; the transmission coefficient is assumed unity throughout the present treatment. Assuming the physical identity of all sites of the activated complex on the catalyst, the last-mentioned specific rate times the number, $N_\ddagger$, of sites of the activated complex gives the specific rate of the step which occurs to this single pair of A and B per unit area. The overall rate of the step per unit area is now the last mentioned specific rate times the number of pairs of A and B, i.e., the product of the numbers of both kinds of molecules. This product is reduced to the product, $C_g C_{g'}$, of the concentrations, with regard to the above equation of v, by referring F_g and $F_{g'}$ respectively to unit volume. This equation is readily generalized for any type of step under the condition that its initial system is a set of gas molecules and the catalyst surface is just sparsely covered, as

$$v = (kT/h) N\, q^\ddagger a_\mathrm{I}, \qquad (11.1.v)$$

where

$$q^\ddagger = f_\ddagger/f_s, \quad a_\mathrm{I} = \prod_i a_i^{\nu_i}, \quad a_i = C_i/F_i \qquad (11.1.q), (11.1.\mathrm{I}), (11.1.i)$$

and ν_i is the number of ith constituents of the initial system, I, in gas. The quantity $q^\ddagger$ is by definition the Boltzmann factor of the work required to add a system of the step in question to a definite site on the catalyst as an activated complex, keeping the whole assembly involved in statistical mechanical equilibrium throughout the process [134, 135].

11.2. Function a_I

Function a_I in eq (11.1.v) is now developed for the sake of an expedient application. Equation (121) in the same monograph of Glasstone et al., states that

$$K_c = \frac{F_\mathrm{L}^l F_\mathrm{M}^m F_\mathrm{N}^n \ldots}{F_\mathrm{A}^a F_\mathrm{B}^b F_\mathrm{C}^c \ldots}$$

for the concentration equilibrium constant K_c of the reaction in gas,

$$a\mathrm{A} + b\mathrm{B} + c\mathrm{C} + \ldots = l\mathrm{L} + m\mathrm{M} + n\mathrm{N} + \ldots,$$

defined as

$$K_c = \frac{C_\mathrm{L}^l C_\mathrm{M}^m C_\mathrm{N}^n \ldots}{C_\mathrm{A}^a C_\mathrm{B}^b C_\mathrm{C}^c \ldots}$$

in terms of equilibrium concentrations, C_L etc., of molecules L etc., in gas. We have, equating the above alternative expressions of K_c to each other

$$\left(\frac{C_\mathrm{A}}{F_\mathrm{A}}\right)^a \left(\frac{C_\mathrm{B}}{F_\mathrm{B}}\right)^b \left(\frac{C_\mathrm{C}}{F_\mathrm{C}}\right)^c \ldots = \left(\frac{C_\mathrm{L}}{F_\mathrm{L}}\right)^l \left(\frac{C_\mathrm{M}}{F_\mathrm{M}}\right)^m \left(\frac{C_\mathrm{N}}{F_\mathrm{N}}\right)^n \ldots,$$

or with reference to eq (11.1.i)

$$a_\mathrm{A}^a a_\mathrm{B}^b a_\mathrm{C}^c \ldots = a_\mathrm{L}^l a_\mathrm{M}^m a_\mathrm{N}^n \ldots$$

It follows, if a set of molecules in gas, $\mathrm{I} = \sum_i \nu_i \mathrm{I}_i$, is in equilibrium with another set of molecules in gas, $\mathrm{I}' = \sum_{i'} \nu_{i'}' \mathrm{I}_{i'}'$, that

$$a_\mathrm{I} = a_{\mathrm{I}'}, \qquad (11.2.\mathrm{eq})$$

where

$$a_\mathrm{I} = \prod_i a_{\mathrm{I}_i}^{\nu_i}, \qquad a_{\mathrm{I}'} = \prod_{i'} a_{\mathrm{I}_{i'}'}^{\nu_{i'}'}. \qquad (11.2.\mathrm{I}), (11.2.\mathrm{I}')$$

a_{I_i} and $a_{\mathrm{I}'_{i'}}$ are called by Fowler and Guggenheim [136] the *absolute activities* of species I_i and $\mathrm{I}_{i'}'$ respectively; the a_I and $a_{\mathrm{I}'}$ are those of the sets I and I'.

12. Statistical Mechanical Formulation of the Associative Mechanism

The statistical mechanical theory of rates in section 11 is applied to the associative mechanism in order to derive the steady rate of catalyzed hydrogenation on the basis of associated reactions. Functions $k(s)$ appropriate respectively to steps s of scheme (9.5) are first derived; $k(s)$ is the forward, unidirectional rate of step s, under the supposition that all other constituent steps are in equilibria.

12.1. Formulation of $k(s)$'s

The formulation of $k(s)$ is exemplified with step II. The relevant activated complex is in equilibrium [24] with the initial system, $C_2H_4(a) + H(a)$, which determines the concentration of the activated complex, hence the rate. Suppose now the presence of hypothetical molecules $C_2H_4(g)$ and H(g) in gas which are, respectively, in equilibrium with $C_2H_4(a)$ and H(a). The activated complex is then in equilibrium with $C_2H_4(g) + H(g)$. The forward rate of step II, $v_+(II)$, is thus expressed according to eqs (11.1) as

$$v_+(II) = (kT/h) N_{\ddagger(II)} q^{\ddagger(II)} a_{C_2H_4(g)} a_{H(g)}. \qquad (12.1)$$

The rate $k(II)$ is now by definition the particular value of $v_+(II)$ in the case where all other constituent steps of scheme (9.5) are in equilibria. C_2H_4 in gas is thus in equilibrium with $C_2H_4(a)$, hence with $C_2H_4(g)$ and H_2 in gas with H(a), hence with H(g). We have in consequence according to eq (11.2)

$$a_{C_2H_4(g)} = a_E \text{ and } a^2_{H(g)} = a_H,$$

where a_E and a_H are the absolute activities of C_2H_4 and H_2 in gas, respectively. Substituting $a_{C_2H_4(g)}$ and $a_{H(g)}$ from the above equations into eq (12.1), $v_+(II)$ assumes its particular value, $k(II)$, i.e.,

$$k(II) = (kT/h) N_{\ddagger(II)} q^{\ddagger(II)} a_E a_H^{1/2}. \qquad (12.2.II)$$

The $k(s)$'s of other constituent steps of scheme (9.5) are formulated similarly as

$$k(I_a) = (kT/h) N_{\ddagger(I_a)} q^{\ddagger(I_a)} a_E, \qquad (12.2.I_a)$$

$$k(I_b) = (kT/h) N_{\ddagger(I_b)} q^{\ddagger(I_b)} a_H \qquad (12.2.I_b)$$

and

$$k(III) = (kT/h) N_{\ddagger(III)} q^{\ddagger(III)} a_E a_H. \qquad (12.2.III)$$

12.2 Expressions for a_E and a_H

The functions a_E and a_H can be written according to eq (11.1.i), developing F and F_H statistical mechanically and substituting $1333 P_i/kT$ (P_i in mm Hg) for C_i, as

$$a_E^{-1} = \frac{kT}{1333 P_E} \frac{(2\pi m_E kT)^{3/2}}{h^3} \frac{2\pi^2 (2\pi I_E kT)^{3/2}}{h^3} \prod_{j=1}^{12} \left\{1 - \exp\left(-\frac{h\nu_j}{kT}\right)\right\}^{-1} \exp\left(-\frac{\epsilon_E}{RT}\right)$$

and

$$a_H^{-1} = \frac{kT}{1333 P_H} \frac{(2\pi m_H kT)^{3/2}}{h^3} \frac{4\pi^2 I_H kT}{h^2} \exp\left(-\frac{\epsilon_H}{RT}\right),$$

where m_E and m_H are the masses of ethylene and hydrogen, I_E is the geometric mean of the three principal moments of inertia of ethylene, I_H the moment of inertia of hydrogen,

$$\prod_{j=1}^{12} \{1 - \exp(-h\nu_j/kT)\}^{-1}$$

the vibrational partition function of ethylene, ν_j the frequency of jth normal vibration and ϵ_E and ϵ_H the ground state molar energies of ethylene and hydrogen, respectively. The vibrational partition function of hydrogen is taken as unity. As to the derivation of partition functions, readers are referred to chapter IV of the book by Glasstone et al., mentioned in 11.1.

The functions a_E and a_H are now recast in the form of $\frac{P_i}{Q_{i,0}} \exp\left(-\frac{\bar{H}_i}{RT}\right)$, where $Q_{i,0}$ and $\bar{H}_i$ are constant, by replacing T in the preexponentional factors with $T_N \exp(1 - T_N/T)$ (a function which for small differences between T and T_N varies closely to T) and assigning to T_N a medium value of the temperature range in question. T in the vibrational partition function

$$\prod_{j=1}^{12} \{1 - \exp(-h\nu_j/kT)\}^{-1}$$

[24] This postulate of the theory of absolute rate is often criticized (General Discussion "Reaction Kinetics," Trans. Faraday Soc. **34**, 57, 71, 75 (1938)). Of course the equilibrium of such sort, could not always be established in the thermodynamic sense. It has been shown [135], however, that, in case where the transmission coefficient is unity, the unidirectional rate may be exactly deduced according to the postulate even in the absence of such thermodynamic equilibrium.

can simply be replaced with T_N, since it varies little with temperature. T_N is taken to be 373.15 °K in the present treatment. We have thus

$$a_E = P_E/Q_E, \qquad a_H = P_H/Q_H, \tag{12.3.E), (12.3.H}$$

where

$$Q_E = Q_{E,0} \exp\left(-\frac{\epsilon_E + 4RT_N}{RT}\right), \tag{12.4.E}$$

$$Q_H = Q_{H,0} \exp\left(-\frac{\epsilon_H + \frac{7}{2}RT_N}{RT}\right), \tag{12.4.H}$$

$$Q_{E,0} = \frac{kT_N}{1333} \frac{(2\pi m_E kT_N)^{3/2}}{h^3} \frac{2\pi^2 (2\pi I_E kT_N)^{3/2}}{h^3}$$

$$\cdot \prod_{j=1}^{12} \left\{1 - \exp\left(-\frac{h\nu_j}{kT_N}\right)\right\}^{-1} e^4 = 3.939 \times 10^{14} \text{ mm Hg}. \tag{12.5.E}$$

and

$$Q_{H,0} = \frac{kT_N}{1333} \frac{(2\pi m_H kT_N)^{3/2}}{h^3} \frac{4\pi^2 I_H kT_N}{h^2} e^{7/2}$$

$$= 1.057 \times 10^{10} \text{ mm Hg}. \tag{12.5.H}$$

It may be noted that the chemical potential μ_i of species i is given as $\mu_i = RT \ln a_i$, from which the partial molar enthalpy of species i, $\bar{H}_i = \mu_i - T(\partial\mu_i/\partial T)_p$, is derived particularly for ethylene and hydrogen as

$$\bar{H}_E = \epsilon_E + 4RT_N, \qquad \bar{H}_H = \epsilon_H + \frac{7}{2}RT_N, \tag{12.6.E), (12.6.H}$$

and the partial molar entropy, $\bar{S}_i = -(\partial\mu_i/\partial T)_p$, follows as

$$\bar{S}_E = R \ln Q_{E,0}/P_E, \qquad \bar{S}_H = R \ln Q_{H,0}/P_H. \tag{12.7.E), (12.7.H}$$

The factor $q^{\ddagger(s)}(s = I_a, II, III)$ in eqs (12.2) is approximated as

$$q^{\ddagger(s)} = \exp(-\epsilon^{\ddagger(s)}/RT), \tag{12.8}$$

where $\epsilon^{\ddagger(s)}$ is the ground state energy of the activated complex of step s, ignoring the Boltzmann factors of excited states, which may be fairly high on account of the narrow space of the site to which the system of the step is confined.

12.3. Practical Expressions of $k(s)$'s

Substituting a_E, a_H and $q^{\ddagger(s)}$ from eqs (12.3) and (12.8) into eqs (12.2) and further T in the factor kT/h by $T_N \exp(1 - T_N/T)$, identifying all $N_{\ddagger(s)}$'s with each other and referring to eqs (12.6), we have

$$k(I_a) = \rho(P_E/Q_{E,0}) \exp(-\Delta^{\ddagger}H(I_a)/RT), \tag{12.9.I_a}$$

$$k(I_b) = \rho(P_H/Q_{H,0}) \exp(-\Delta^{\ddagger}H(I_b)/RT), \tag{12.9.I_b}$$

$$k(II) = \rho(P_E/Q_{E,0})(P_H/Q_{H,0})^{1/2} \exp(-\Delta^{\ddagger}H(II)/RT) \tag{12.9.II}$$

and

$$k(III) = \rho(P_E/Q_{E,0})(P_H/Q_{H,0}) \exp(-\Delta^{\ddagger}H(III)/RT), \tag{12.9.III}$$

where

$$\rho = kT_N N_{\ddagger}/h, \tag{12.10.\rho}$$

$$N_{\ddagger} = N_{\ddagger(s)}, \qquad s = I_a, I_b, II, III, \tag{12.10.N}$$

$$\Delta H(s) = H_{\ddagger(s)} - H_{I(s)_r}, \qquad H_{\ddagger(s)} = \epsilon^{\ddagger(s)} + RT_N \tag{12.11.\Delta^{\ddagger}H), (12.11.H_{\ddagger}}$$

$$H_{I(I_a)_r} = \bar{H}_E, \qquad H_{I(I_b)_r} = \bar{H}_H,$$

$$H_{I(II)_r} = \bar{H}_E + \frac{1}{2}\bar{H}_H, \qquad H_{I(III)_r} = \bar{H}_E + \bar{H}_H,$$

$$(12.12.I_a), (12.12.I_b), (12.12.II), (12.12.III)$$

where $I(s)_r$ is the set of molecules of reactants which constitutes $I(s)$ or is converted into $I(s)$ through steps other than s, i.e.,

$$I(III)_r \equiv C_2H_4 + H_2, \tag{12.13.III}$$

$$I(II)_r \equiv C_2H_4 + 1/2H_2, \tag{12.13.II}$$

$$I(I_a)_r \equiv C_2H_4, \qquad I(I_b)_r \equiv H_2. \tag{12.13.I_a), (12.13.I_b}$$

Equations (12.9) may be given in an alternative form as

$$k(s) = \exp(-\Delta^{\ddagger}G(s)/RT), \qquad s = I_a, I_b, II, III \tag{12.14.k}$$

where

$$\Delta^{\ddagger}G(s) = \Delta^{\ddagger}H(s) - T\Delta^{\ddagger}S(s), \tag{12.14.G}$$

$$\Delta^{\ddagger} S(s) = S_{\ddagger} - S_{\mathrm{I}(s)r}, \qquad (12.14.\Delta^{\ddagger} S)$$

$$S_{\ddagger} = R \ln \rho, \qquad (12.14.S_{\ddagger})$$

$$S_{\mathrm{I(I_a)}r} = \bar{S}_{\mathrm{E}}, \quad S_{\mathrm{I(I_b)}r} = \bar{S}_{\mathrm{H}},$$

$$S_{\mathrm{I(II)}_r} = \bar{S}_{\mathrm{E}} + 1/2\bar{S}_{\mathrm{H}}, \quad S_{\mathrm{I(III)}_r} = \bar{S}_{\mathrm{E}} + \bar{S}_{\mathrm{H}}.$$

(12.15.I_a), (12.15.I_b), (12.15.II), (12.15.III)

The function ρ, as defined by eq (12.10.ρ), is the partition function of activated complexes, with energies referred to the appropriate ground states, which transit the activated state unidirectionally once within unit time.[25] $\Delta^{\ddagger} G(s)$ and $\Delta^{\ddagger} S(s)$ thus defined are the increments of Gibbs energy and of entropy, respectively, of the whole assembly, caused by bringing up the set $\mathrm{I}(s)_r$ of reactants to the state where it is transiting the activated state unidirectionally once within unit time through steps other than s, all supposed to be in equilibrium.

12.4. Rate Equations in Terms of $k(s)$'s

The forward and backward rates, $v_+(s)$ and $v_-(s)$, of the constituent steps of scheme (9.5) are given according to eqs (11.1.v) and (11.1.I) as

$$v_+(\mathrm{I_a}) = (kT/h) N_{\ddagger} q^{\ddagger(\mathrm{I_a})} a_{\mathrm{E}}, \qquad v_-(\mathrm{I_a}) = (kT/h) N_{\ddagger} q^{\ddagger(\mathrm{I_a})} a_{\mathrm{C_2H_4(a)}},$$

$$v_+(\mathrm{I_b}) = (kT/h) N_{\ddagger} q^{\ddagger(\mathrm{I_b})} a_{\mathrm{H}}, \qquad v_-(\mathrm{I_b}) = (kT/h) N_{\ddagger} q^{\ddagger(\mathrm{I_b})} a^2_{\mathrm{H(a)}},$$

$$v_+(\mathrm{II}) = (kT/h) N_{\ddagger} q^{\ddagger(\mathrm{II})} a_{\mathrm{C_2H_4(a)}} a_{\mathrm{H(a)}}, \qquad v_-(\mathrm{II}) = (kT/h) N_{\ddagger} q^{\ddagger(\mathrm{II})} a_{\mathrm{C_2H_5(a)}},$$

$$v_+(\mathrm{III}) = (kT/h) N_{\ddagger} q^{\ddagger(\mathrm{III})} a_{\mathrm{C_2H_5(a)}} a_{\mathrm{H(a)}}, \qquad v_-(\mathrm{III}) = (kT/h) N_{\ddagger} q^{\ddagger(\mathrm{III})} a_{\mathrm{C_2H_6}},$$

where $a_{\mathrm{C_2H_4(a)}}$, $a_{\mathrm{H(a)}}$ and $a_{\mathrm{C_2H_5(a)}}$ are the absolute activities of $\mathrm{C_2H_4(a)}$, H(a) and $\mathrm{C_2H_5(a)}$ defined as those of hypothetical gas molecules, $\mathrm{C_2H_4(g)}$, H(g) and $\mathrm{C_2H_5(g)}$ respectively in equilibrium with $\mathrm{C_2H_4(a)}$, H(a), and $\mathrm{C_2H_5(a)}$. Referring to eqs (12.2), the above expressions of $v_+(s)$ and $v_-(s)$ are written in the form

$$v_+(\mathrm{I_a}) = k(\mathrm{I_a}), \qquad v_-(\mathrm{I_a}) = k(\mathrm{I_a})\gamma(\mathrm{C_2H_4}), \qquad (12.16.\mathrm{I_a})$$

$$v_+(\mathrm{I_b}) = k(\mathrm{I_b}), \qquad v_-(\mathrm{I_b}) = k(\mathrm{I_b})\gamma(\mathrm{H})^2, \qquad (12.16.\mathrm{I_b})$$

$$v_+(\mathrm{II}) = k(\mathrm{II})\gamma(\mathrm{C_2H_4})\gamma(\mathrm{H}), \qquad v_-(\mathrm{II}) = k(\mathrm{II})\gamma(\mathrm{C_2H_5}), \qquad (12.16.\mathrm{II})$$

$$v_+(\mathrm{III}) = k(\mathrm{III})\gamma(\mathrm{C_2H_5})\gamma(\mathrm{H}), \qquad v_-(\mathrm{III}) = k(\mathrm{III})\gamma(\mathrm{C_2H_6}), \qquad (12.16.\mathrm{III})$$

where

$$\gamma(\mathrm{C_2H_4}) = a_{\mathrm{C2H4(a)}}/a_{\mathrm{E}}, \qquad \gamma(\mathrm{H}) = a_{\mathrm{H(a)}}/a_{\mathrm{H}}{}^{1/2}, \qquad (12.17.\mathrm{E}), (12.17.\mathrm{H})$$

$$\gamma(\mathrm{C_2H_5}) = a_{\mathrm{C2H5(a)}}/a_{\mathrm{E}}a_{\mathrm{H}}{}^{1/2}, \qquad \gamma(\mathrm{C_2H_6}) = a_{\mathrm{C2H6}}/a_{\mathrm{E}}a_{\mathrm{H}}; \qquad (12.17.\mathrm{C_2H_5}), (12.17.\mathrm{A})$$

$\gamma(\mathrm{C_2H_4})$ etc, may be called the *activity coefficients* of the relevant species.

12.5. Steady State of Catalyzed Hydrogenation

The steady state is formulated by equating the algebraic sum of rates of formation of each intermediate to zero. The stoichiometric number[26] of each step of scheme (9.5) is thus found to be unity commonly with reference to reaction (4.1), without any isotopic discrimination. Formulating the steady state individually with respect to $\mathrm{E}_n(\mathrm{a}) \equiv \mathrm{C_2{}^1H_{4-n}D_n(a)}$ ($n=0, 1, 2, 3, 4$), ^{1}H(a), D(a) and $\mathrm{A}_n(\mathrm{a}) \equiv \mathrm{C_2{}^1H_{5-n}D_n(a)}$ ($n=0, 1, \ldots, 5$), one can determine the relative amounts of E_n(a) etc., and the evolution rates of ethylenes-d_n, hydrogens-d_n and ethanes-d_n as shown in what follows.

[25] Cf.II.A.2.c of ref. [134]. The functions ρ, $\Delta^{\ddagger}G(s)$ and $\Delta^{\ddagger}S(s)$ are defined there with special reference to the critical complex (cf. footnote 5 to 3.1.6). This definition may be shifted to the activated complex without inconsistency.

[26] Cf. footnote 11 to 9.2.2.

12.5.1. The rate V_s of steady hydrogenation [27] in the associative mechanism is given in terms of $v_+(s)$'s and $v_-(s)$'s, on account of unit stoichiometric numbers for every constituent step, as

$$V_s = v_+(s) - v_-(s), \quad s = \mathrm{I_a}, \mathrm{I_b}, \mathrm{II}, \mathrm{III} \qquad (12.18)$$

or, substituting v_+(s)'s and v_-(s)'s from eqs (12.16). as

$$\begin{aligned} V_s &= k(\mathrm{I_a})\{1-\gamma(\mathrm{C_2H_4})\} = k(\mathrm{I_b})\{1-\gamma(\mathrm{H})^2\} \\ &= k(\mathrm{II})\{\gamma(\mathrm{C_2H_4}\gamma(\mathrm{H}) - \gamma(\mathrm{C_2H_5})\} \\ &= k(\mathrm{III})\{\gamma(\mathrm{C_2H_5})\gamma(\mathrm{H}) - \gamma(\mathrm{C_2H_6})\}. \end{aligned} \qquad (12.19)$$

Eliminating $\gamma(C_2H_4)$, $\gamma(H)$ and $\gamma(C_2H_5)$ from eq (12.19), we have

$$\gamma(\mathrm{C_2H_6}) = \left(1-\frac{V_s}{k(\mathrm{I_a})}\right)\left(1-\frac{V_s}{k(\mathrm{I_b})}\right) - \frac{V_s}{k(\mathrm{II})}\left(1-\frac{V_s}{k(\mathrm{I_b})}\right)^{1/2} - \frac{V_s}{k(\mathrm{III})}. \qquad (12.20)$$

Rates of the catalyzed hydrogenation of diverse definitions have been introduced in reviewing the treatments of various authors, symbolling them commonly with v_h. These v_h's are related with V_s as

$$v_h = (kT/1333V)V_s,$$

if v_h is given in the rate of partial pressure decrease of either reactant in mm Hg in a closed space of constant volume, V. We have

$$v_h = (kT/1333P_E V)V_s,$$

if v_h is the increasing rate of hydrogenated fraction of ethylene of partial pressure, P_E, in mm Hg or

$$v_h = (kT/1333P_H V)V_s,$$

if v_h is the first order rate with respect to hydrogen, which is referred to particularly as the rate constant, k_h.

These v_h differ from V_s, by a factor which depends on temperature and hence makes a difference between the activation heat derived at constant partial pressures of reactants from v_h and that from V_s commonly as

$$RT^2\partial \ln v_h/\partial T = RT^2\partial \ln V_s/\partial T + RT.$$

The common difference RT is about within experimental errors of observation. We deal exclusively with the steady hydrogenation for which $V_s > 0$. It is inferred from eqs (12.19), that

(i) $0 < \gamma(\mathrm{C_2H_4}), \gamma(\mathrm{H}), \gamma(\mathrm{C_2H_5}), \gamma(\mathrm{C_2H_6}) < 1$,

(ii) $0 < V_s/(1-\gamma(\mathrm{C_2H_6})) < k(s)$, $(s = \mathrm{I_a}, \mathrm{I_b}, \mathrm{II}, \mathrm{III})$, and also that,

(iii) as one of the functions $k(s)$, say $k(r)$, lies sufficiently below all other $k(s')$, every steps other than r approaches equilibrium so that r tends to be rate-determining according to 9.2.2. Conversely, as step r tends to be rate-determining, all other rates, $k(s')$, get greater than $k(r)$.

Inference (i) is readily seen from eq (12.19), noting that V_s, $k(s)$'s, $\gamma(C_2H_4)$, $\gamma(H)$, $\gamma(C_2H_5)$, and $\gamma(C_2H_6)$ are all positive. It follows from eq (12.19) and (i) that

$$1 > 1 - V_s/k(\mathrm{I_a}) = \gamma(\mathrm{C_2H_4}) > 0, \quad 1 > 1 - V_s/k(\mathrm{I_b}) = \gamma(\mathrm{H})^2 > 0,$$

hence according to eq (12.20)

$$\gamma(\mathrm{C_2H_6}) < 1 - V_s/k(\mathrm{I_a}), \quad \gamma(\mathrm{C_2H_6}) < 1 - V_s/k(\mathrm{I_b})$$

$$\gamma(\mathrm{C_2H_6}) < (1 - V_s/k(\mathrm{I_b})) - (1 - V_s/k(\mathrm{I_b}))^{1/2} V_s/k(\mathrm{II})$$

$$= (1 - V_s/k(\mathrm{I_b}))^{1/2}\{(1 - V_s/k(\mathrm{I_b}))^{1/2} - V_s/k(\mathrm{II})\} < 1 - V_s/k(\mathrm{II})$$

and $\gamma(C_2H_6) < 1 - V_s/k(\mathrm{III})$, which are summarized in (ii).

It follows from (i) and (ii) that $V_s < k(s)$. As $k(r)$ of step $s = r$ gets smaller than $k(s')$ of the other steps, $s' \neq r$, the coefficient of every $k(s')$ in eq (12.19) tends to zero or, according to eqs (12.16), every step s' approaches equilibrium. As to the converse it is seen readily from eq (12.19) that the coefficient of $k(r)$ approaches $1 - \gamma(C_2H_6)$ while those of $k(s')$ tend, respectively, to zero. The $k(s')$ should hence get greater than $k(r)$, by the same equation, as r tends to be rate-determining.

It may be noted that $\gamma(C_2H_6)$ is extremely small under the usual condition of experiments; $\gamma(C_2H_6)$ is 3.6×10^{-27} at 200 °K and 2.7×10^{-6} at 500 °K for $P_E = P_H = P_A = 10$ mm Hg.[28]

12.5.2. The steady state is formulated with respect to $\mathrm{E}_n(\mathrm{a}) \equiv \mathrm{C_2{}^1H_{4-n}D_n(a)}$ in accordance with the mechanism of exchange specified in 9.2.1., ignoring isotopic differences in rates, as

$$\begin{aligned} &X_{\mathrm{E}_n} v_+(\mathrm{I_a}) - X_{\mathrm{E}_n(\mathrm{a})} v_-(\mathrm{I_a}) - X_{\mathrm{E}_n(\mathrm{a})} v_+(\mathrm{II}) \\ &+ \left\{ \frac{5-n}{6} x_{\mathrm{H(a)}} X_{\mathrm{E}_{n-1}(\mathrm{a})} + \frac{6-n}{6}(1 - x_{\mathrm{H(a)}}) X_{\mathrm{E}_n(\mathrm{a})} \right. \\ &\quad + \frac{2+n}{6} x_{\mathrm{H(a)}} X_{\mathrm{E}_n(\mathrm{a})} \\ &\left. + \frac{1+n}{6}(1 - x_{\mathrm{H(a)}}) X_{\mathrm{E}_{n+1}(\mathrm{a})} \right\} v_-(\mathrm{II}) = 0, \\ &n = 0, 1, 2, 3, 4, \end{aligned} \qquad (12.21.\mathrm{E})$$

where X_{E_n} is the mole fraction of $\mathrm{E}_n \equiv \mathrm{C_2{}^1H_{4-n}D_n}$

[27] V_s here represents the number of ethane molecules evolved by the catalyzed hydrogenation per unit time.

[28] The activity coefficient $\gamma(C_2H_6)$ is expressed according to eqs (12.17.A) and (12.3) as

$$\gamma(\mathrm{C_2H_6}) = (P_A/P_E P_H)(Q_E Q_H/Q_A),$$

where P_A is the partial pressure of ethane and Q_A is a function defined for ethane similar to Q_E as defined for ethylene by eq (12.4.E). We have $\gamma(C_2H_6) = 1$ in equilibrium according to eqs (11.2.eq) and (12.17.A), hence, from the above equation,

$$P_{A,eq}/P_{E,eq}P_{H,eq} = Q_A/Q_E Q_H.$$

where suffix equation signifies quantities in the equilibrium. The left-hand side is the equilibrium constant K_p, which is calculated from spectroscopic data [Landolt "Tabellen" Erg. III. c. (1936), p. 2609, 2622]. We have thus $\gamma(C_2H_6) = P_A/P_E P_H K_p$, which gives the values shown in the text.

over C_2H_4 in gas, $X_{E_n(a)}$ the mole fraction of $E_n(a) \equiv C_2{}^1H_{4-n}D_n(a)$ over $C_2H_4(a)$ and $x_{H(a)}$ the atom fraction of D(a) over H(a). The first two terms give the net rate of creation of $E_n(a)$ by step I_a and its reverse, and the third term the rate of consumption of $E_n(a)$ by step II. The last term gives the rate of regeneration of $E_n(a)$ by the reverse of step II, which is elucidated as follows.

The first term in curly brackets provides, when multiplied by $v_-(II)$, the rate of formation of $E_n(a)$ from $E_{n-1}(a)$ and D(a) by step II and its reverse; two out of three hydrogen atoms on the methyl radical of the half-hydrogenated state originate from the methylene radical of $E_{n-1}(a)$, so that these two contain as an average $(n-1)\cdot 2/4$ deuterium atoms; the third hydrogen atom being deuterium, we have $(n-1)/2+1=(n+1)/2$ deuterium atoms in the methyl radical of the half-hydrogenated state, as an average. The number of protium atoms is thus $3-\frac{n+1}{2}$ $=(5-n)/2$, one of which has to be given off by the reverse of step II, which occurs with the probability of $\frac{5-n}{2}\times\frac{1}{3}=\frac{5-n}{6}$, hence the first term. The second term in curly brackets represents the regeneration of $E_n(a)$ from $A_n(a)$, which acquired one protium atom by step II. The methyl radical of the $A_n(a)$ has $n/2$ deuterium atoms and $3-n/2$ protium atoms as an average; one of the latter has to be given off for the regeneration of $E_n(a)$, which occurs with the probability of $(3-n/2)/3=(6-n)/6$, hence the second term. The third term represents the regeneration of $E_n(a)$ which acquired one deuterium atom on reaching the half-hydrogenated state; its methyl radical has thus $n/2+1$ deuterium atoms, and one of them has to be given off in order to regenerate $E_n(a)$, which occurs with the probability of $(n+2)/6$, hence the third term. The fourth term is referred to the half-hydrogenated state formed by combination of $E_{n+1}(a)$ with $^1H(a)$. The methyl radical, hence, keeps $(n+1)/2$ deuterium atoms exclusively originating from the methylene radical of $E_{n+1}(a)$. One of $(n+1)/2$ deuterium atoms on the methyl radical has to be released by the reverse of step II, which occurs with the probability of $(n+1)/6$, hence the fourth term in curly brackets.

12.5.3. The steady state is formulated with respect to $^1H(a)$ and D(a) similarly as

$$2(1-x_H)v_+(I_b)-2(1-x_{H(a)})v_-(I_b)-(1-x_{H(a)})v_+(II) + \frac{2(1-x_{E(a)})+(1-x_{H(a)})}{3}v_-(II)-(1-x_{H(a)})v_+(III)=0 \qquad (12.21.{}^1H)$$

and

$$2x_Hv_+(I_b)-2x_{H(a)}v_-(I_b)-x_{H(a)}v_+(II) + \frac{2x_{E(a)}+x_{H(a)}}{3}v_-(II)-x_{H(a)}v_+(III)=0, \qquad (12.21.D)$$

where $x_{E(a)}$ is the atom fraction of deuterium in $C_2H_4(a)$, and the coefficient of $v_-(II)$ in eqs (12.21.H) and (12.21.D) is the probability of $^1H(a)$ or D(a) being yielded, respectively, by the reverse of step II. Terms comprising $v_-(III)$ have been ignored according to conclusions 13.4.

12.5.4. The steady state is formulated with respect to $A_n(a) \equiv C_2{}^1H_{5-n}D_n(a)$ as

$$\{x_{H(a)}X_{E_{n-1}(a)}+(1-x_{H(a)})X_{E_n(a)}\}v_+(II) - X_{A_n(a)}v_-(II)-X_{A_n(a)}v_+(III)=0, \qquad (12.21.A)$$

where $X_{A_n(a)}$ is the mole fraction of $A_n(a)$ over $C_2H_5(a)$. The first term gives the rate of $A_n(a)$ formation by combination both of $E_{n-1}(a)$ with D(a) and of $E_n(a)$ with $^1H(a)$, as represented by the two terms in curly brackets, while the second and third terms give the rates of consumption by the reverse of step II and step III, respectively. Terms comprising $v_-(III)$ have been ignored similarly, according to 13.4.

12.5.5. The fraction $x_{E(a)}$ in eqs (12.21.H) and (12.21.D) is related with $X_{E_n(a)}$'s as

$$4x_{E(a)}=\sum_{n=1}^{4}nX_{E_n(a)} \qquad (12.21.x)$$

by definition. $X_{E_n(a)}$ and $X_{A_n(a)}$ satisfy, by definition, the equations,

$$\sum_{n=0}^{4}X_{E_n(a)}=1, \qquad \sum_{n=0}^{5}X_{A_n(a)}=1. \qquad (12.21.X_E),\ (12.21.X_A)$$

Equations (12.21) provide 16 equations for 13 unknowns, i.e., $X_{E_n(a)}(n=0, \ldots, 4)$, $x_{H(a)}$, $x_{E(a)}$ and $X_{A_n(a)}(n=0, \ldots, 5)$. The 16 equations are not all independent. Summation of eqs (12.21.E) over n yields, with reference to eq $(12.21.X_E)$,

$$v_+(I_a)-v_-(I_a)-v_+(II)+v_-(II)=0, \qquad (12.22.E)$$

summation of eqs (12.21.^{1}H) and (12.21.D) gives

$$2v_+(I_b)-2v_-(I_b)-v_+(II)+v_-(II)-v_+(III)=0, \qquad (12.22.H)$$

and summation of eqs (12.21.A) over n with reference to eq $(12.21.X_A)$ gives

$$v_+(II)-v_-(II)-v_+(III)=0. \qquad (12.22.A)$$

Equations (12.22) follow, however, directly from eq (12.18) when similarly neglecting $v_-(III)$. It is thus premised that the $v_+(s)$'s and $v_-(s)$'s comprised in the above sixteen equations satisfy eqs (12.22). Three out of the above 16 equations are in consequence dependent. Thirteen unknowns are determined as a solution of 13 independent equations.

12.5.6. The fractions, $x_{E(a)}$ and $x_{H(a)}$, are determined now as functions of $v_+(s)$'s and $v_-(s)$'s. We have, eliminating $v_-(I_b)$ from eqs (12.22.H) and (12.21.D)

$$3(x_H-x_{H(a)})v_+(I_b)+(x_{E(a)}-x_{H(a)})v_-(II)=0, \qquad (12.23.a)$$

and summing up eqs (12.21.E) multiplied by n from $n=1$ to 4, referring to eq $(12.21.x)$,

$$4x_E v_+(I_a) - 4x_{E(a)}v_-(I_a) - 4x_{E(a)}v_+(II)$$

$$+\left(\frac{2}{3}x_{H(a)} + \frac{10}{3}x_{E(a)}\right)v_-(II) = 0, \qquad (12.23.b)$$

where $x_E = \sum_{n=1}^{4} nx_{E_n}/4$ is the atom fraction of deuterium in C_2H_4 in gas. We have, eliminating $v_-(I_a) + v_+(II)$ from eqs (12.23.b) and (12.22.E),

$$6(x_E - x_{E(a)})v_+(I_a) + (x_{H(a)} - x_{E(a)})v_-(II) = 0. \qquad (12.23.c)$$

Equations (12.23.a) and (12.23.c) are solved simultaneously for $x_{E(a)}$ and $x_{H(a)}$ as

$$x_{E(a)} = \frac{6x_E v_+(I_a) + x_{H(a)}v_-(II)}{6v_+(I_a) + v_-(II)} \qquad (12.24.E)$$

and

$$x_{H(a)} = \frac{2x_E v_+(I_a)v_-(II) + x_H v_+(I_b)(6v_+(I_a) + v_-(II))}{2v_+(I_a)v_-(II) + v_+(I_b)(6v_+(I_a) + v_-(II))}. \qquad (12.24.H)$$

The mole fraction of $A_n(a)$ over $C_2H_5(a)$, $X_{A_n(a)}$, is obtained by eliminating $(v_-(II) + v_+(III))/v_+(II)$ from eqs (12.21.A) and (12.22.A) as

$$X_{A_n(a)} = x_{H(a)}X_{E_{n-1}(a)} + (1 - x_{H(a)})X_{E_n(a)}. \qquad (12.24.A)$$

12.6. Rates of Reaction Associated With the Catalyzed Hydrogenation

The rates of the associated reactions are derived as follows, ignoring the isotopic differences in rates.

12.6.1. Exchange rate in course of hydrogenation is defined respectively for ethylene and hydrogen as follows.

12.6.1.1. Let n_E be the total number of hydrogen atoms comprised in gaseous ethylene and x_E their fraction of deuterium. The rate of increase of deuterium atoms in gaseous ethylene, $d(n_E x_E)/dt$ is given in terms of the rate of penetration into gaseous ethylene of hydrogen atoms originating from gaseous hydrogen, $V_{ex,E}$, and the rate of hydrogen atoms given out from gaseous ethylene to gaseous hydrogen and ethane, V_{+E}, as

$$d(n_E x_E)/dt = x_H V_{ex,E} - x_E V_{+E}$$

The first term on the right-hand side is the rate of deuterium atoms transferred from gaseous hydrogen to gaseous ethylene and the second term those transferred counter from gaseous ethylene to gaseous hydrogen and ethane. V_{+E} should exceed $V_{ex,E}$ by the rate with which constituent hydrogen atoms of gaseous ethylene are lost by hydrogenation, $-\dot{n}_E$, i.e.,

$$V_{+E} = V_{ex,E} - \dot{n}_E.$$

We have from the above two equations

$$V_{ex,E} = n_E\dot{x}_E/(x_E - x_H). \qquad (12.25.E)$$

$V_{ex,E}$ thus defined is called the exchange rate of ethylene.

Similarly, the exchange rate of hydrogen is defined as [29]

$$V_{ex,H} = n_H\dot{x}_H/(x_E - x_H), \qquad (12.25.H)$$

where n_H is the number of hydrogen atoms comprised in gaseous hydrogen.

It may be noted that $V_{ex,E}$ and $V_{ex,H}$ are not necessarily equal to each other under the progress of hydrogenation. For instance, if I_b governs the rate, a good amount of hydrogen atoms from gaseous hydrogen is transferred to gaseous ethylene but hardly conversely, so that $V_{ex,E}$ is significant but $V_{ex,H}$ not. In the special case where n_E, n_H and the total amount of deuterium, i.e., $n_E x_E + n_H x_H$ are kept respectively constant, we have $n_E\dot{x}_E + n_H\dot{x}_H = 0$, hence $V_{ex,E} = V_{ex,H}$ according to eqs (12.25).

12.6.1.2. Equations (12.25) are transformed with reference to the associative mechanism as follows. The rate of increase of deuterium atoms in ethylene in gas, $d(n_E x_E)/dt$, is expressed as

$$d(n_E x_E)/dt = 4v_-(I_a)x_{E(a)} - 4v_+(I_a)x_E.$$

We have, on the other hand,

$$\dot{n}_E = 4v_-(I_a) - 4v_+(I_a)$$

hence from the above two equations

$$n_E\dot{x}_E = 4(x_{E(a)} - x_E)v_-(I_a). \qquad (12.25.x_E)$$

[29] Twigg and Rideal [68] defined the initial exchange rate of hydrogen, $v_{ex,H}$, as $v_{ex,H} = -x_H$ at $x_E = 0$ and $x_H = 1$ as mentioned in 5.1.2., which is related with $V_{ex,H}$ according to eq (12.25.H) as

$$v_{ex,H} = (1/n_H)V_{ex,H}.$$

The factor, $1/n_H$, is given as $kT/2 \times 1333\,P_H V$ in terms of the partial pressure of hydrogen, P_H, in mm Hg and the volume, V, in which the gas mixture in question is confined. This factor makes difference between the activation heats derived at constant P_H and $v_{ex,H}$ as

$$RT^2\partial \ln v_{ex,H}/\partial T = RT^2\partial \ln V_{ex,H}/\partial T + RT$$

similar to the case of v_h and V_s referred to in footnote 27 to 12.5.1.

Substituting $n_E\dot{x}_E$ from the above equation into (12.25.E), $V_{ex,E}$ is given as

$$V_{ex,E}=4\frac{x_{E(a)}-x_E}{x_H-x_E}v_-(I_a). \qquad (12.26.E)$$

Equation (12.25.H) is similarly transformed as

$$V_{ex,H}=2\frac{x_{H(a)}-x_H}{x_E-x_H}v_-(I_b). \qquad (12.26.H)$$

12.6.2. Parahydrogen conversion is effected according to scheme (9.5), in course of catalyzed hydrogenation, by step I_b and its reverse. Let X_p be the mole fraction of parahydrogen over hydrogen in gas, i.e.,

$$X_p=N_H^p/N_H,$$

where N_H^p is the number of parahydrogen molecules and N_H the total number of hydrogen molecules. We have by differentiation

$$\dot{X}_p=\dot{N}_H^p/N_H-X_p\dot{N}_H/N_H.$$

$\dot{N}_H^p$ and $\dot{N}_H$ are expressed in terms of $v_+(I_b)$ and $v_-(I_b)$ as

$$\dot{N}_H^p=X_{p,\infty}v_-(I_b)-X_pv_+(I_b), \qquad \dot{N}_H=v_-(I_b)-v_+(I_b),$$

where $X_{p,\infty}$ is the particular value of X_p reached in equilibrium of parahydrogen conversion.[30] Eliminating $\dot{N}_H^p$ and $\dot{N}_H$ from the above three equations, we have

$$V_p\equiv N_H\frac{\dot{X}_p}{X_{p,\infty}-X_p}=v_-(I_b), \qquad (12.27)$$

which states that the rate of parahydrogen conversion, V_p, as defined by the second member of eq (12.27) equals $v_-(I_b)$.

12.6.3. The rate of $^1H_2$–D_2 equilibration, V_q, is defined as

$$V_q=N_H\dot{u}, \qquad (12.28.q)$$

where

$$u=N_{^1HD}/N_{^1HD,eq} \qquad (12.28.u)$$

and $N_{^1HD,eq}$ is the number of ^{1}HD molecules, which would exist if hydrogen concerned were equilibrated. V_q is developed as follows.

For a supposed equilibration of the hydrogen present

$$N_H=N_{^1H_2,eq}+N_{^1HD,eq}+N_{D_2,eq}$$

and

$$x_H=(2N_{D_2,eq}+N_{^1HD,eq})/2N_H,$$

where suffix eq signifies particular values in the equilibration. Besides,

$$N_{^1HD,eq}^2/N_{^1H_2,eq}N_{D_2,eq}=4$$

in the absence of isotopic difference of rates.

On elimination of $N_{^1H_2,eq}$ and $N_{D_2,eq}$ from the above three equations, we have

$$N_{^1HD,eq}=2x_H(1-x_H)N_H. \qquad (12.28.N)$$

The ratio u is expressed by substituting $N_{^1HD,eq}$ from the above equation into eq (12.28.u) as

$$u=N_{^1HD}/2x_H(1-x_H)N_H, \qquad (12.29)$$

hence, by logarithmic differentiation,

$$\dot{u}/u=\dot{N}_{^1HD}/N_{^1HD}-\dot{N}_H/N_H+\left(\frac{1}{1-x_H}-\frac{1}{x_H}\right)\dot{x}_H.$$

$\dot{N}_H$ in the above equation is expressed as

$$\dot{N}_H=v_-(I_b)-v_+(I_b)$$

and $\dot{N}_{^1HD}$ as

$$\dot{N}_{^1HD}=2x_{H(a)}(1-x_{H(a)})v_-(I_b)=\frac{N_{^1HD}}{N_H}v_+(I_b).$$

Hydrogen evolved by the reverse of step I_b must be perfectly equilibrated in the absence of isotopic difference of rates. The rate of ^{1}HD formation by the reverse of I_b is thus its rate, $v_-(I_b)$, times the fraction, $2x_{H(a)}(1-x_{H(a)})$, hence the first term of the above equation. The second term gives the rate of consumption of ^{1}HD-molecules by step I_b, i.e., its rate, $v_+(I_b)$, times the fraction of the number of ^{1}HD over N_H. Eliminating $N_{^1HD}$, $N_{^1HD}$ and N_H from the above four equations, we have, referring to eq (12.28.q).

$$V_q=N_H\dot{u}=\left\{\frac{x_{H(a)}(1-x_{H(a)})}{x_H(1-x_H)}-u\right\}v_-(I_b)-\left(\frac{1}{x_H}-\frac{1}{1-x_H}\right)\dot{x}_HN_Hu. \qquad (12.30)$$

12.6.4. The rates of evolution, V_{E_n}, $V_{^1H_2}$, $V_{^1HD}$, V_{D_2}, and V_{A_n}, of ethylene-$d_n\equiv E_n$, $^1H_2$, ^{1}HD, D_2 and ethane-$d_n\equiv A_n$, are given in terms of $X_{E_n(a)}$, $X_{A_n(a)}$, $x_{H(a)}$, $v_+(s)$'s and $v_-(s)$'s, as

$$V_{En}=X_{E_n(a)}v_-(I_a), \quad n=0,1,2,3,4, \qquad (12.31.E)$$

$$V_{^1H_2}=(1-x_{H(a)})^2v_-(I_b), V_{^1HD}=2x_{H(a)}(1-x_{H(a)})v_-(I_b),$$

$$V_{D_2}=x_{H(a)}^2v_-(I_b) \qquad (12.31.H)$$

and

[30] Hydrogen evolved by the reverse of step I_b must be of equilibrium composition, insofar as para- and orthohydrogen enter step I_b with equal chance since, otherwise, the catalyst should shift the equilibrium.

$$V_{A_n} = \{x_{H(a)} X_{A_{n-1}(a)} + (1 - x_{H(a)}) X_{A_n(a)}\} v_+(III),$$

$$n = 0, 1, \ldots, 6. \qquad (12.31.A)$$

12.6.5. Let us assume that deuterium atoms are randomly distributed over E_n and $E_n(a)$, which is realized, where the associative mechanism is concerned, when $v_+(I_a)$ and $v_-(I_a)$ are large enough to give every ethylene molecule, be it in the gas or in the surface phase (adsorbed), an equal chance of acquiring deuterium. We have then

$$X_{E_n} = X_{E_n(a)} = \binom{4}{n} x^n_{E(a)} (1 - x_{E(a)})^{4-n}. \qquad (12.32)$$

Substituting $X_{A_n(a)}$ and $X_{A_{n-1}}(a)$ from eq (12.24.A) into eq (12.31.A), we have

$$V_{A_n} = \{x^2_{H(a)} X_{E_{n-2}(a)} + 2x_{H(a)}(1 - x_{H(a)}) X_{E_{n-1}(a)} + (1 - x_{H(a)})^2 X_{E_n(a)}\} v_+(III)$$

$$n = 0, \ldots, 6, \qquad (12.33.a)$$

x_E or substituting $X_{E_n(a)}$ etc. from eq (12.32) into eq (12.33.a),

$$V_{A_n} = \left\{ \binom{4}{n-2} x^2_{H(a)} x^{n-2}_{E(a)} (1 - x_{E(a)})^{6-n} + 2\binom{4}{n-1} x_{H(a)}(1 - x_{H(a)}) x^{n-1}_{E(a)} (1 - x_{E(a)})^{5-n} + \binom{4}{n} (1 - x_{H(a)})^2 x^n_{E(a)} (1 - x_{E(a)})^{4-n} \right\} v_+(III),$$

$$n = 0, \ldots, 6, \qquad (12.33.b)$$

Where combination $\binom{4}{\nu}$ vanishes, of course, for $\nu > 4$. In the special case where $x_{H(a)} = x_{E(a)} = x_A$, eq (12.33.b) is reduced identically to the equation

$$V_{A_n} = \binom{6}{n} x^n_A (1 - x_A)^{6-n} v_+(III), \qquad (12.33.c)$$

which indicates the random distribution of deuterium over ethane evolved.

13. Estimate of $k(s)$'s

Rates of steady hydrogenation and various associated reactions were given in section 12. in terms of $v_+(s)$'s and $v_-(s)$'s, which in their turn are determined by $k(s)$'s according to eqs (12.16) and (12.19). The rates, $k(s)$'s, are evaluated in this section by adapting the theoretical relations to experimental results. It may be noted that the steady rate, V_s, of the catalyzed hydrogenation is practically given by $k(r)$ of the rate-determining step itself, according to 9.2.2 and 12.5.1, and that the rates of $k(s)$ are given by eq (12.9) in the form of $k(s)_0 \exp(-\Delta^\ddagger H(s)/RT)$, where $k(s)_0$ and $\Delta^\ddagger H(s)$ are constants appropriate to step s which are independent of temperature at constant partial pressures of reactants; the former was already statistical mechanically evaluated, the latter alone remaining to be determined. The rates $k(s)$'s are thus estimated in what follows.

13.1 Estimates of $k(I_a)$

It is inferred, as shown below, that $k(I_a)$ is practically infinite or inestimably higher than V_s, so that $\gamma(C_2H_4)$ is practically unity according to eq (12.19), i.e.,

$$\gamma(C_2H_4) = 1. \qquad (13.1)$$

13.1.1. Table 17 shows that at 110 °C deuterium atoms in ethylenes-d_n are in perfectly random distribution. Those in hydrogens-d_n are also in random distribution, although not as precisely as in the case of ethylene, possibly just because of less accuracy in the measurements (cf. 5.2.5 and 9.2.3). Step I_a and its reverse must be rapid enough to keep the deuterium in ethylene in gas and in the adsorbed state in random distribution throughout, as mentioned in 12.6.5, so that $x_E = x_{E(a)}$, since, otherwise, the distribution of deuterium atoms should deviate from the random one, as mentioned in 9.2.2.5. The atom fraction x_H must also be near $x_{H(a)}$. Identifying x_E with $x_{E(a)}$ and x_H with $x_{H(a)}$, one finds the coefficient of $v_-(I_a)$ in eq (12.33.c) to be zero, while that of $v_-(II)$ in the same equation is finite, as derived from table 17. The rate $v_+(I_a)$ is thus practically infinite as compared with $v_-(II)$.

Step III is rate-determining in the experiment in question, according to 9.2.3. The rate $k(III)$ should, in consequence, be lower than $k(II)$ according to 12.5.1 (iii). We have, on the other hand, from eqs (12.16)

$$\frac{v_-(II)}{v_+(III)} = \frac{k(II)}{\gamma(H) k(III)}$$

which shows that $v_-(II)$ is greater than $v_+(III)$ according to 12.5.1 (i). Since $v_+(III)$ is practically equal to the steady rate of hydrogenation, $v_+(I_a) \gg V_s$ or by eq (12.16.I_a) $k(I_a) \gg V_s$.

13.1.2. It is read from the results of Turkevich et al. [117], as reviewed in 5.2.2, that

$$V_s:V_{E_1}:V_{E_{n>1}}=1:2.33:0 \qquad (13.2.E)$$

and

$$V_{A_0}:V_{A_1}:V_{A_2}:V_{A_{n>2}}=1:0.69:0.154:0 \qquad (13.2.A)$$

at the very beginning of the catalyzed deuteration of light ethylene over nickel wire at 90 °C. Equation (13.2.E) states that E_1 is the only deuteroethylene evolved at the very beginning, which shows that the reverse of step I_a is rapid enough to carry away $E_1(a)$ once formed by step II and its reverse before $E_1(a)$ enters step II again to acquire another deuterium atom. Equation (13.2.A) states, on the other hand, that the only deuteroethanes evolved are A_1 and A_2. It follows, since ethane is formed by two consecutive additions of H(a)'s to $C_2H_4(a)$ according to scheme (9.5), that practically only light $C_2H_4(a)$ are subject to two consecutive additions, endorsing the statement of eq (13.2.E) and, in conjunction with the latter, confirming the conclusion of 13.1.1.

13.2 Estimate of $k(I_b)$

It has been concluded in 9.2.3. that the rate-determining step below the optimum is I_b. The quantity $\Delta^{\ddagger}H(I_b)$ is thus determinable from observations of V_s below the optimum identifying V_s with $k(I_b)$ of eq (12.9.I_b); the value

$$\Delta^{\ddagger}H(I_b)=4.7 \text{ kcal/mole} \qquad (13.3)$$

is adopted; this is the mean of the two observations, $\Delta^{\ddagger}H(I_b)=4.60$ kcal/mole [64] and $\Delta^{\ddagger}H(I_b)=4.80$ kcal/mole [26].

13.3. Estimate of k(II) and k(III)

There are three methods of determining k(III) through $\Delta^{\ddagger}H$(III). One is quite similar to that of determining $\Delta^{\ddagger}H(I_b)$ in 13.2 on the basis of the conclusion in 9.2.3; this method has not, however, been adopted, since the appropriate observations above the optimum are not sufficiently reliable.

The second method consists in comparing a theoretical relation between T_X and P_E with the observed relation (4.3); its result, described in 13.3.2, is used for checking that of the third method adopted here, which determines k(II) and k(III) coherently from the experimental results of eq (13.2), as described in 13.3.1.

13.3.1. The experimental results of eq (13.2) are stated in conjunction with the appropriate condition as

$$x_E=0, \quad X_{E_0(a)}=1, \quad x_H=1, \qquad (13.4.E), (13.4.E(a)), (13.4.H)$$

from which $X_{A_0(a)}$ and $X_{A_1(a)}$ are deduced according to eq (12.24.A) as

$$X_{A_0(a)}=1-x_{H(a)}, \quad X_{A_1(a)}=x_{H(a)} \text{ and } X_{A_{n>1}}=0,$$

ignoring $(1-x_{H(a)})X_{E_1(a)}$, inasmuch as $X_{E_1(a)}$ must be quite small according to eq (13.4.E(a)). We have, from the above equations and eq (12.31.A)

$$V_{A_0}=(1-x_{H(a)})^2 v_+(III), \quad V_{A_1}=2x_{H(a)}(1-x_{H(a)})v_+(III), \quad V_{A_2}=x_{H(a)}^2 v_+(III) \qquad (13.5.a)$$

and

$$V_{A_{n>2}}=0, \qquad (13.5.b)$$

from which the most probable value of $x_{H(a)}$ is determined by eq (13.2.A) as

$$x_{H(a)}=0.264. \qquad (13.6)$$

The fraction $x_{E(a)}=\sum_{n=1}^{4} nX_{E_n(a)}/4$ may be ignored as compared with the above value of $x_{H(a)}$, since the fractions $X_{E_{n>0}(a)}$ are extremely small according to eq (13.4.E(a)). We have thus from eqs (12.23.a) and (13.4.H)

$$v_-(II)=3\frac{1-x_{H(a)}}{x_{H(a)}}v_+(I_b), \qquad (13.7.a)$$

hence by eq (13.6)

$$v_-(II)=8.36\ v_+(I_b). \qquad (13.7.b)$$

We have, on the other hand, from eq (12.21.E) for $n=1$

$$-X_{E_1(a)}v_-(I_a)+\frac{2}{3}x_{H(a)}v_-(II)=0; \qquad (13.8)$$

the first term of eq (12.21.E) vanishes because of eq (13.4.E), since $x_E=\sum_{n=1}^{4} nX_{E_n}/4$; eq (13.8) is arrived at by ignoring all terms containing the factors $X_{E_1(a)}$ and $X_{E_2(a)}$, which are small according to eqs (13.4.E(a)) and (12.21.x), except for the term $-X_{E_1(a)}v_-(I_a)$, on account of the practically infinite magnitude of $v_-(I_a)$, as concluded in 13.1.

V_{E_1} is given by eqs (13.8) and (12.31.E) as

$$V_{E_1}=(2/3)x_{H(a)}v_-(II),$$

hence by eqs (13.2.E) and (13.6)

$$V_s=\frac{2}{3\times 2.33}x_{H(a)}v_-(II)=0.0755\ v_-(II) \qquad (13.9)$$

or, substituting v_-(II) from eq (13.7.b) into eq (13.9),

$$V_s=0.632\ v_+(I_b).$$

Noting that $v_+(I_b)$ equals $k(I_b)$ by eq (12.16.I_b), we have from the first and third members of eq (12.19) and the above equation

$$\gamma(H)=0.607. \qquad (13.10.H)$$

Writing eq (12.18) with special reference to step II as $V_s=(v_+(\mathrm{II})/v_-(\mathrm{II})-1)v_-(\mathrm{II})$ or, according to eq (12.16.II), as $V_s=(\gamma(C_2H_4)\gamma(H)/\gamma(C_2H_5)-1)v_-(\mathrm{II})$, we evaluate $\gamma(C_2H_5)$ using eqs (13.9), (13.10.H) and (13.1) as

$$\gamma(C_2H_5)=0.564. \qquad (13.10.A)$$

Equations (13.1) and (13.10) give, by eq (12.19), the ratio between $k(s)$'s at 90 °C as

$$k(\mathrm{I_b}):k(\mathrm{II}):k(\mathrm{III})$$
$$=(1-\gamma(H)^2)^{-1}:(\gamma(H)-\gamma(C_2H_5))^{-1}:(\gamma(H)\gamma(C_2H_5))^{-1}$$
$$=1:14.7:1.84. \qquad (13.11)$$

The quantities $\Delta^{\ddagger}H(\mathrm{II})$ and $\Delta^{\ddagger}H(\mathrm{III})$ are now determined according to eqs (13.3), (12.5), (12.9) and (13.11), noting that $P_E=10$ mm Hg and $P_H=20$ mm Hg in the experiment [117] in question, as

$$\Delta^{\ddagger}H(\mathrm{II})=-12.6 \text{ kcal/mole}, \qquad (13.12.\mathrm{II})$$
$$\Delta^{\ddagger}H(\mathrm{III})=-18.3 \text{ kcal/mole}. \qquad (13.12.\mathrm{III})$$

13.3.2. The rate-determining step is switched over from step $\mathrm{I_b}$ to III, when the temperature rises past the optimum, according to 9.2.3. An equation for the optimum temperature, T_X, is thus obtained by equating $k(\mathrm{I_b})$ to $k(\mathrm{III})$ at $T=T_X$ in accordance with eqs (12.9) as

$$\Delta^{\ddagger}H(\mathrm{I_b})-\Delta^{\ddagger}H(\mathrm{III})=2.3\ RT_X\log_{10}Q_{E,0}/P_E,$$

which gives, on comparison with the observation of eq (4.3),

$$\Delta^{\ddagger}H(\mathrm{I_b})-\Delta^{\ddagger}H(\mathrm{III})=24.2 \text{ kcal/mole} \qquad (13.13.H)$$

and

$$\log_{10}Q_{E,0}=14.5. \qquad (13.13.Q)$$

We have, from eqs (13.3) and (13.13.H),

$$\Delta^{\ddagger}H(\mathrm{III})=-19.5 \text{ kcal/mole},$$

which agrees tolerably well with the value of (13.12.III), confirming it thus, while the value of eq (13.13.Q) is in excellent agreement with the theoretical value $\log_{10}Q_{E,0}=14.596$ of eq (12.5.E).

13.4. Rates Based on the Estimated $k(s)$'s

We have from eqs (12.9.$\mathrm{I_b}$), (12.5.H) and (13.3)

$$\log_{10}k(\mathrm{I_b})=\log_{10}\rho\frac{P_H}{1.057\times10^{10}}-\frac{1027}{T} \qquad (13.14.\mathrm{I_b})$$

and similarly from eqs (12.9), (12.5) and (13.12) for steps II and III

$$\log_{10}k(\mathrm{II})$$
$$=\log_{10}\rho\left(\frac{P_H}{1.057\times10^{10}}\right)^{1/2}\frac{P_E}{3.939\times10^{14}}+\frac{2751}{T} \qquad (13.14.\mathrm{II})$$

and

$$\log_{10}k(\mathrm{III})=\log_{10}\rho\frac{P_H}{1.057\times10^{10}}\cdot\frac{P_E}{3.939\times10^{14}}+\frac{4008}{T}. \qquad (13.14.\mathrm{III})$$

The rates $k(s)$ determine V_s, $\gamma(H)$ and $\gamma(C_2H_5)$ by eq (12.19) with reference to the values of $\gamma(C_2H_6)$ given in 12.5 and $\gamma(C_2H_4)$ of eq (13.1). These values of $k(s)$'s and of $\gamma(C_2H_4)$, $\gamma(H)$, $\gamma(C_2H_5)$ and $\gamma(C_2H_6)$ determine $v_+(s)$'s and $v_-(s)$'s by eqs (12.16) as shown in figure 27.

The rates V_s, $V_{ex,E}$, $V_{ex,H}$, V_p and V_q are hence developed in terms of $v_+(s)$'s and $v_-(s)$'s by eqs (12.18), (12.26), (12.27), and (12.30); $x_{H(a)}$, as required for the calculation of V_q, for $x_E=0$, $x_H=1/2$ and $u=0$, is determined by an equation

$$x_{H(a)}=\frac{x_Ev_-(\mathrm{II})+3x_Hv_+(\mathrm{I_b})}{v_-(\mathrm{II})+3v_+(\mathrm{I_b})} \qquad (13.15)$$

obtained from eq (12.24.H) for infinite $v_+(\mathrm{I_a})=k(\mathrm{I_a})$. The results are shown in figure 28, side by side with $k(s)$.

We see from figure 27 that $v_+(\mathrm{II})=v_-(\mathrm{II})$ throughout, i.e., step II is practically in equilibrium. The rates $v_+(\mathrm{I_b})$ and $v_+(\mathrm{III})$ coincide at lower temperatures but diverge above the optimum which is located around the intersection of $k(\mathrm{I_b})$ and $k(\mathrm{III})$ in figure 28; $v_+(\mathrm{I_b})$ coincides above the optimum with $v_-(\mathrm{I_b})$ indicating an equilibrium of $\mathrm{I_b}$, while $v_+(\mathrm{III})$ gives practically the steady rate of hydrogenation governed by step III in accordance with 12.5.1 (iii) and figure 28, $v_-(\mathrm{III})$ being vanishingly small as seen in figure 27.

The following is inferred from the above numerical results.

13.4.1. Figure 27 shows that at or below 200 °C, $v_-(\mathrm{III})$ is smaller than $v_+(\mathrm{III})$ by a factor of at least 10^6. Such a small rate, $v_-(\mathrm{III})$ is hardly traceable, insofar as methods reviewed here are concerned. This accounts for the results obtained by Matsuzaki and Nakajima [120] in 5.2.7 that ethane was not perciptibly involved in the catalyzed hydrogenation.

13.4.2. Figure 27 shows that step III is far from being in equilibrium over the temperature range where $\mathrm{I_b}$ determined the rate, according to 9.2.3.

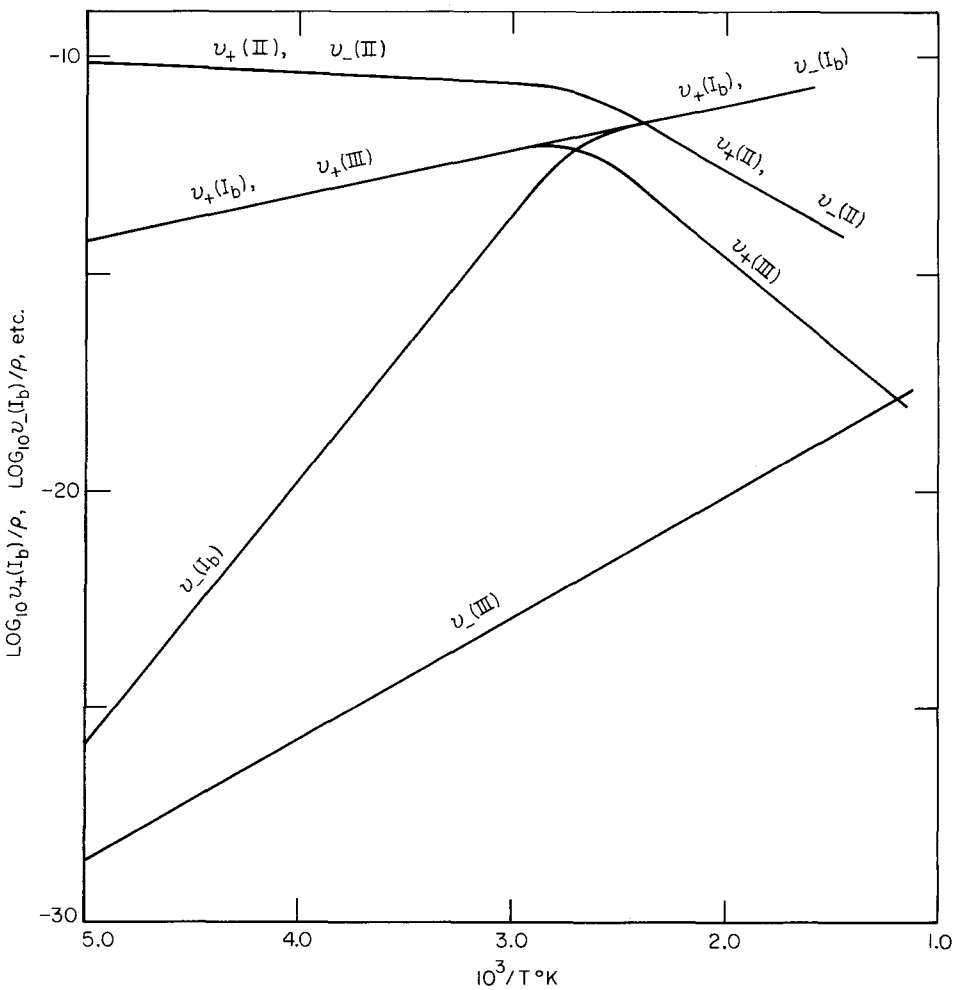

FIGURE 27. *Rates of steps* s, $v_+(s)$, *and of their reverses*, $v_-(s)$, *at the steady state of hydrogenation over nickel;* $s = I_b$, II, III.

$P_E = P_H = P_A = 10$ mm Hg. $\rho = kT_N N_\ddagger / h$.

It is inferred below that I_b actually satisfies the conditions, advanced in 9.2.2, for a step determining the rate, notwithstanding a departure of some other constituent step from equilibrium.

Comparison is made in this regard between the magnitude of $v_-(I_b)$ in the steady state and that in perfect equilibria of all steps other than I_b. The rate $v_-(I_b)$ in the respective case is given according to eq (12.16.I_b) as $v_-(I_b) = \gamma(H)_s^2 k(I_b)$ or $v_-(I_b)_{eq} = \gamma(H)_{eq}^2 k(I_b)$, where suffixes s and eq signify the particular values in the steady state and in the state of perfect equilibria of all steps but I_b, respectively.

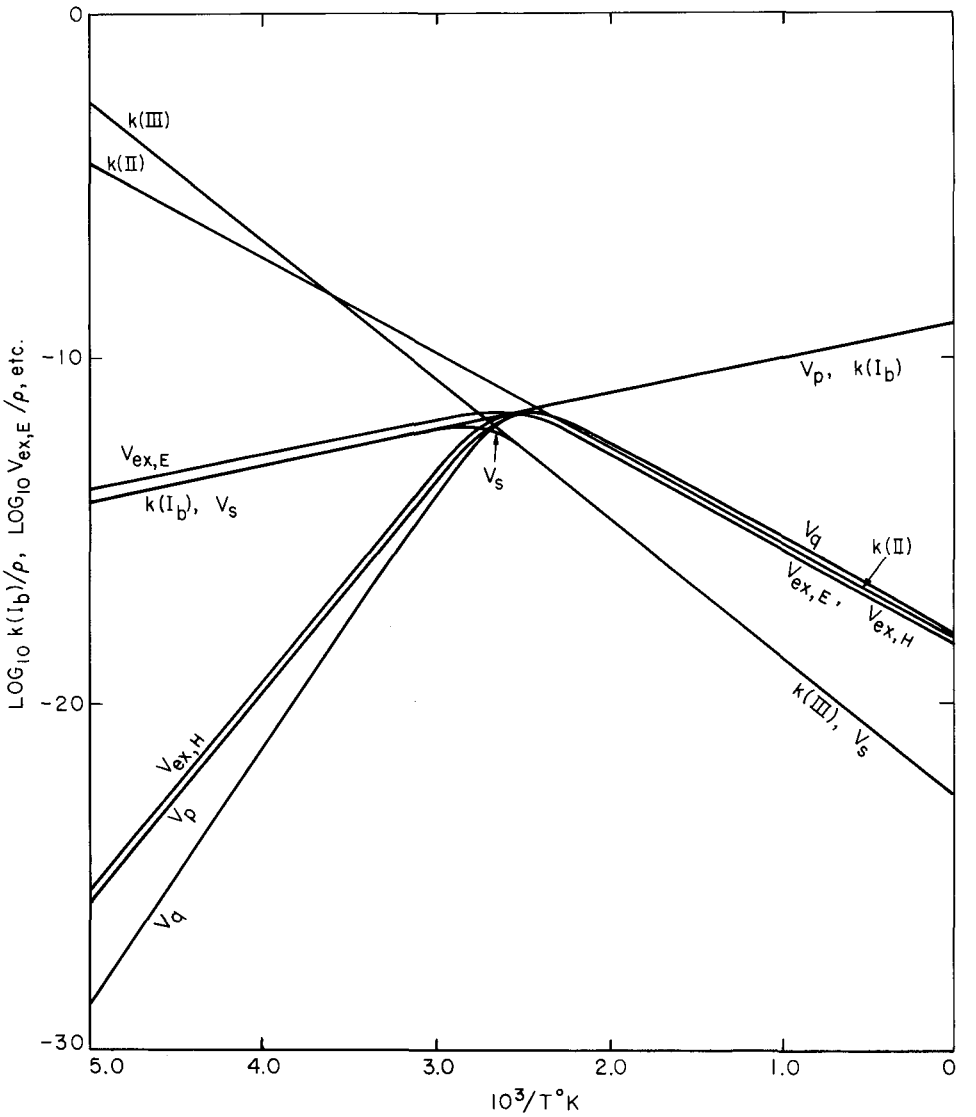

FIGURE 28. *Steady rates,* V_s *etc., of hydrogenation of ethylene over nickel defined by functions* k(s); $s = I_b$, II, III.

V_s: for hydrogenation. $V_{ex,E}$, $V_{ex,H}$: for exchange of ethylene and hydrogen, respectively. V_p: for parahydrogen conversion. V_q: for equilibrium, $x_E = 0$, equimolar $^1H_2 - D_2$ mixture.

The coefficient $\gamma(H)_s$ is determined by eqs (12.19) and (13.14), referring to eq (13.1), whereas $\gamma(H)^2_{eq} = \gamma(C_2H_6)$, as follows readily from eqs (12.16) by equating $v_+(s)$ with $v_-(s)$ for all steps but I_b.

We have thus, e.g., at $T = 250$ °K and $P_E = P_H = 10$ mm Hg, where I_b governs the rate according to 12.5.1(iii), $\gamma(H)^2_s = 10^{-8}$ and $\gamma(H)^2_{eq} = 10^{-18}$, so that $v_-(I_b)_s$ is greater than $v_-(I_b)_{eq}$ by a factor of ca. 10^{10}. This makes, however, practically no difference in the net rate, $V_s \doteq k(I_b)(1 - \gamma(H)^2)$, as given by eq (12.19), illustrating the argument in 9.2.2.1.

14. Application of the Theory of the Associative Mechanism

Various phenomena concerned with the catalyzed hydrogenation of ethylene will be accounted for systematically on the basis of the theory of the associative mechanism developed in the foregoing sections.

14.1. Switchover in the Rate-Determining Step

At the switchover temperature, T_X, of the rate-determining step from I_b to III, we have $k(I_b)=k(III)$, as mentioned in 13.3.2, and hence from eqs (12.14)

$$\Delta^\ddagger G(I_b)=\Delta^\ddagger G(III),$$

i.e.,
$$\Delta^\ddagger H(I_b)-\Delta^\ddagger H(III)=T_X(\Delta^\ddagger S(I_b)-\Delta^\ddagger S(III))$$

and

$$\Delta^\ddagger S(I_b)-\Delta^\ddagger S(III)=S_{I(III)_r}-S_{I(I_b)_r}=\bar{S}_E,$$

hence from eq (12.7.E)

$$\Delta^\ddagger S(I_b)-\Delta^\ddagger S(III)=R\ \ln\ (Q_{E,0}/P_E),$$

which amounts to 62.2 e.u. according to eq (12.5.E) for $P_E=10$ mm Hg. This difference of activation entropy originates from the ethylene molecule that $I(s)_r$ of step III possesses in excess over that of I_b, and compensates for the difference in activation heats which amounts to 24 kcal, leveling $k(I_b)$ and $k(III)$ at T_X.

We see that, while $k(s_1)$ and $k(s_2)$ for steps s_1 and s_2 of different activation entropies equal each other at a certain temperature T_X, one of them is higher than the other below T_X but lower than the other above T_X. No such switchover in the relative magnitudes of $k(s)$'s can take place without a difference in activation entropies. This difference arises now only through difference in the systems $I(s)_r$ of the steps, insofar as the present approximation goes, as seen from eq (12.14.$\Delta^\ddagger S$). Steps 3 and 7 in scheme (9.7) have the same $I(s)_r$, i.e., $C_2H_4+H_2$, hence a switchover in the relative magnitudes of their rates with temperature can hardly occur, as mentioned in 9.3.2.

It is nothing to be wondered at that the activation entropy provides inertia of the reaction intrinsically on equal terms with the activation heats, that the activation entropy must be algebraically smaller in case of an heterogeneous step which amounts to a restriction of a system initially in a three dimensional phase to a surface phase such as to reduce its phase volume by a factor of ca. 10^8 and that heterogeneous steps, which are thus destined to have algebraically smaller activation entropies, have smaller activation heats, or even negative ones, in accordance with the so-called compensation effect, in as far as rates accessible to our measurements are limited to a narrow compass of magnitude.

14.2. Activation Heat of Hydrogen Exchange

The activation heat of exchange of hydrogen has been observed definitely to be greater than that of hydrogenation, which disposed a number of authors [2, 13, 68, 116] to attribute to the exchange of hydrogen some different sequence of steps from that of hydrogenation, as reviewed in section 9. Figure 28 shows that the one and the same sequence of steps of the associative mechanism leads necessarily to an excess of the activation heat of exchange, $RT^2\partial\ \ln\ V_{ex,H}/\partial T$, over that of hydrogenation; the excess amounts to 23 kcal below $T_X=373$ °K and 5.7 kcal at 200 °C, qualitatively in accordance with the experimental results of Twigg and Rideal [68].

The necessity of having this excess is qualitatively demonstrated on the basis of the associative mechanism as follows. The exchange rate, $V_{ex,H}$, is given in general by substitution of $x_{H(a)}$ from eq (13.15) into eq (12.26.H) as

$$V_{ex,H}=2v_-(II)v_-(I_b)/(v_-(II)+3v_+(I_b)), \quad (14.1)$$

which will be discussed now for the respective cases below and above the optimum.

The rate-determining step being either I_b or III in accordance with 9.2.3, we have partial equilibrium of step II throughout, as verified by figure 27, hence according to eqs (12.16.II) and (13.1)

$$\gamma(H)=\gamma(C_2H_5). \quad (14.2)$$

Equations (12.22.H) and (12.22. A) yield, on the other hand, $v_+(I_b)=v_-(I_b)+v_-(III)$ or, substituting $v_+(I_b)$ etc. from eq (12.16) and referring to eq (14.2), $k(I_b)=\gamma(H)^2(k(I_b)+k(III))$.

In the temperature range below the optimum we have ignoring $k(I_b)$ as compared with $k(III)$,

$$\gamma(H)^2=k(I_b)/k(III). \quad (14.3)$$

Figure 27 shows, on the other hand, that $v_+(II)=v_-(II)$ is far greater than $v_+(I_b)$ while $v_+(I_b)$ equals $v_+(III)$, i.e.,

$$v_+(\mathrm{II}) = v_-(\mathrm{II}) \gg v_+(\mathrm{I_b}) = v_+(\mathrm{III}). \qquad (14.4)$$

Ignoring thus $v_+(\mathrm{I_b})$ in comparison with $v_-(\mathrm{II})$, we can reduce eq (14.1) to the form

$$V_{\mathrm{ex,\,H}} = 2v_-(\mathrm{I_b}) \qquad (14.5.a)$$

or, according to eqs (12.16.$\mathrm{I_b}$) and (14.3),

$$V_{\mathrm{ex,\,H}} = 2k(\mathrm{I_b})^2/k(\mathrm{III}). \qquad (14.5.b)$$

Equation (14.5.b) is interpreted as follows. Equation (14.4) shows that an H(a) formed by the forward act of $\mathrm{I_b}$ passes rapidly between the initial and final states of step II until it finally enters step III to finish the hydrogenation or the reverse of $\mathrm{I_b}$ to revert to H_2 in gas. $V_{\mathrm{ex,\,H}}$ counts those H(a) (cf. eq (14.5 a)) which get back into hydrogen molecules in gas per unit time, i.e., the rate of overall supply of H(a), $2v_+(\mathrm{I_b})$, multiplied by $v_-(\mathrm{I_b})/(v_-(\mathrm{I_b}) + v_+(\mathrm{III}))$ which is the fraction of them getting back into H_2, or by $v_-(\mathrm{I_b})/v_+(\mathrm{III})$, according to eqs (12.16.$\mathrm{I_b}$), (14.4), (14.3), which state that $v_-(\mathrm{I_b}) = \gamma(\mathrm{H})^2 v_+(\mathrm{I_b}) = v_+(\mathrm{III})k(\mathrm{I_b})/k(\mathrm{III}) \ll v_+(\mathrm{III})$. This fraction equals $k(\mathrm{I_b})/k(\mathrm{III})$ while $v_+(\mathrm{I_b})$ is given by $k(\mathrm{I_b})$, hence eq (14.5.b).

The activation heat of exchange of hydrogen, $RT^2\partial \ln V_{\mathrm{ex,\,H}}/\partial T$, is hence necessarily greater than that of hydrogenation, $RT^2\partial \ln k(\mathrm{I_b})/\partial T$, by $RT^2\partial \ln k(\mathrm{I_b})/\partial T - RT^2\partial \ln k(\mathrm{III})/\partial T$ (below the optimum), which is inevitably positive as shown in 14.1.

Above the optimum, where step III governs the rate as concluded in 9.2.3, we have from eq (12.19), according to inferences (i) and (ii) in 12.5.1 and to eq (13.1), that

$$\gamma(\mathrm{H}) = \gamma(\mathrm{C_2H_5}) = 1, \qquad (14.6.a)$$

hence

$$v_+(s) = v_-(s) = k(s), \quad s = \mathrm{I_a},\ \mathrm{I_b},\ \mathrm{II} \qquad (14.6.b)$$

and

$$v_+(\mathrm{III}) = k(\mathrm{III}) \qquad (14.6.c)$$

according to eqs (12.16), i.e., all steps but III are in partial equilibrium. We observe the higher extreme of temperature, where $k(\mathrm{I_b}) \gg k(\mathrm{II})$ as seen in figure 28. Equation (14.1) then assumes the form,

$$V_{\mathrm{ex,\,H}} = (2/3)v_-(\mathrm{II}) \qquad (14.7)$$

if we ignore $v_-(\mathrm{II}) = k(\mathrm{II})$ as compared with $3v_+(\mathrm{I_b}) = 3k(\mathrm{I_b})$ and identify $v_-(\mathrm{I_b})$ with $v_+(\mathrm{I_b}) = k(\mathrm{I_b})$.

We have from eq (12.24.E), for the predominance of $v_+(\mathrm{I_a})$ inferred in 13.1,

$$x_{\mathrm{E(a)}} = x_{\mathrm{E}} \qquad (14.8.\mathrm{E})$$

and from eq (13.15), for the predominance of $v_+(\mathrm{I_b})$ over $v_-(\mathrm{II})$,

$$x_{\mathrm{H(a)}} = x_{\mathrm{H}}. \qquad (14.8.\mathrm{H})$$

Equations (14.8) state that the "fall" of deuterium content occurs across step II so that the rate of exchange is proportional to $v_-(\mathrm{II}) = v_+(\mathrm{II}) = k(\mathrm{II})$, as seen from eq (14.7); the proportionality factor 2/3 represents the number of hydrogen atoms transferred from the state where they belong to C_2H_5(a) back to that of H(a) for every reversal of step II; this transfers either of the two hydrogen atoms in the methyl radical originating from C_2H_4(a) with the probability of 1/3; two out of three times does the reversal bring hydrogen atoms from C_2H_4(a) to the state of H(a) as given by the proportionality factor.

The activation heat of exchange of hydrogen is thus $RT^2\partial \ln k(\mathrm{II})/\partial T = \Delta^{\ddagger}H(\mathrm{II}) = -12.6$ kcal which is algebraically greater than that of hydrogenation, -18.3 kcal, but by an excess appreciably smaller than that below the optimum.

14.3. Retardation of Parahydrogen Conversion and $^1H_2$–D_2 Equilibration by the Presence of Ethylene

It may be noted that eq (12.27) for the parahydrogen conversion and eq (12.30) for the equilibration apply irrespective of the presence or absence of ethylene, insofar as these associated reactions are caused by step $\mathrm{I_b}$ and its reverse and the hydrogen desorbed is in equilibrium with respect to parahydrogen conversion or to $^1H_2$–D_2 equilibration.

The rate of parahydrogen conversion in the presence or absence of ethylene is equal according to eq (12.27), to $v_-(\mathrm{I_b})$. This assumes, in the absence of ethylene, its particular value, $k(\mathrm{I_b})$, in equilibrium of $\mathrm{I_b}$ according to eq (12.16.$\mathrm{I_b}$). It follows that the ratio of the rates of parahydrogen conversion in the presence of ethylene, $V_{\mathrm{p}}(\mathrm{P})$, and in its absence, $V_{\mathrm{p}}(\mathrm{A})$, equals $v_-(\mathrm{I_b})/k(\mathrm{I_b})$ or, according to eq (12.16.$\mathrm{I_b}$),

$$V_{\mathrm{p}}(\mathrm{P})/V_{\mathrm{p}}(\mathrm{A}) = \gamma(\mathrm{H})^2, \qquad (14.9)$$

where $\gamma(\mathrm{H})$ is the activity coefficient of hydrogen adatom in the presence of ethylene.

In the temperature range where $\mathrm{I_b}$ governs the hydrogenation rate, $\gamma(\mathrm{H})^2$ is, according to eq (14.3), extremely small as compared with unity, hence the retardation of parahydrogen conversion by ethylene according to eq (14.9). Above the optimum $\gamma(\mathrm{H})^2 = 1$, according to eq (14.6.a), hence no retardation. These

conclusions account for the observation [2] referred to in 5.1.1.

The rate of $^1H_2$–D_2 equilibration, V_q, is given, under the special condition where $u=0$ and $x_E=0$, according to eq (12.30), as

$$V_q=\frac{x_{H(a)}(1-x_{H(a)})}{x_H(1-x_H)}v_-(I_b).$$

The value of $x_{H(a)}$ in the absence of ethylene is nothing but x_H. We have thus, denoting the rates in the presence and absence of ethylene by suffixes (P) and (A), respectively:

$$V_q(P)/V_q(A)=\frac{x_{H(a)}(1-x_{H(a)})}{x_H(1-x_H)}. \qquad (14.10)$$

The value of $x_{H(a)}$ for $x_E=0$ is given by eq (13.15) as

$$x_{H(a)}=\frac{3v_+(I_b)}{v_-(II)+3v_+(I_b)}x_H. \qquad (14.11)$$

Below the optimum, $x_{H(a)}$ is extremely small as compared with unity according to equations (14.11) and (14.4), hence retardation; above the optimum, where $k(I_b)$ predominates over $k(II)$, $x_{H(a)}$ equals x_H according to equations (14.11) and (14.6.b), hence no retardation. The former conclusions explain the experimental result [68] reviewed in 5.1.2.

14.4. The Relation Between Equilibrium Fraction, u, and Deuterium Atom Fraction, x_H, of Hydrogen

The theory of the associative mechanism leads to the expression for u in terms of x_H and $x_{H(a)}$

$$u=\frac{\exp\left(\int_{x_H}^{1}\frac{dx_H}{x_{H(a)}-x_H}\right)}{x_H(1-x_H)}\int_{x_H}^{1}\frac{x_{H(a)}(1-x_{H(a)})}{x_H-x_{H(a)}}\cdot\exp\left(\int_{x_H}^{1}\frac{dx_H}{x_H-x_{H(a)}}\right)dx_H \qquad (14.12)$$

as derived in the following.

On elimination of $V_{ex,H}$ and $v_-(I_b)$ from eqs (12.25.H), (12.26.H) and (12.30), one obtains, noting $n_H=2N_H$ by definition,

$$\frac{du}{dx_H}=\frac{x_{H(a)}(1-x_{H(a)})}{(x_{H(a)}-x_H)x_H(1-x_H)}-\left(\frac{1}{x_{H(a)}-x_H}-\frac{1}{1-x_H}+\frac{1}{x_H}\right)u,$$

which is solved as

$$u=\frac{\exp\left(\int_{x_H}^{1}\frac{dx_H}{x_{H(a)}-x_H}\right)}{x_H(1-x_H)}\left\{\int_{x_H}^{1}\frac{x_{H(a)}(1-x_{H(a)})}{x_H-x_{H(a)}}\cdot\exp\left(\int_{x_H}^{1}\frac{dx_H}{x_H-x_{H(a)}}\right)dx_H+C\right\};$$

the integration constant, C, is determined by substituting u from eq (12.29) into the above equation thus

$$\frac{N_{1HD}}{2N_H}=\exp\left(\int_{x_H}^{1}\frac{dx_H}{x_{H(a)}-x_H}\right)\left\{\int_{x_H}^{1}\frac{x_{H(a)}(1-x_{H(a)})}{x_H-x_{H(a)}}\cdot\exp\left(\int_{x_H}^{1}\frac{dx_H}{x_H-x_{H(a)}}\right)dx_H+C\right\}.$$

Since $N_{1HD}=0$ for $x_H=1$, we have $C=0$, hence eq (14.12) above.

Equation (14.12) leads to the following limiting values of u as x_H tends to unity or to $x_{H(a)}$, respectively:

$$\lim_{x_H\to 1}u=x_{H(a)}, \qquad \lim_{x_H\to x_{H(a)}}u=1. \qquad (14.13.a),\ (14.13.b)$$

Equation (14.13) applies in the case of deuteration of ethylene with pure deuterium, as in the experiment of Twigg and Rideal [68] reviewed in 5.1.2; part (a) shows that u starts from the initial value of $x_{H(a)}$, while part (b) indicates the situation, which is finally arrived at along with the progress of reaction.

It is now required to find $x_{H(a)}$ as a function of x_H in order to determine the relation between u and x_H by eq (14.12). The relation is given for a equimolar mixture of reactants as

$$x_H-x_{H(a)}=F\exp\left\{\int_{P_0}^{P}(F/V_s)(v_+I_b)/2+v_-(I_b)\,d\ln P\right\}, \qquad (14.14.x)$$

where

$$F=v_-(II)(v_-(II)+3v_+(I_b))^{-1} \qquad (14.14.F)$$

and P and P_0 are the current and the initial partial pressures of either reactant. The fraction x_H is given as a function of P, as

$$1-x_H=\int_{P}^{P_0}(Fv_-(I_b)/V_s)\exp\left\{-\int_{P}^{P_0}(F/V_s)\cdot(v_+(I_b)/2+v_-(I_b))d\ln P\right\}d\ln P. \qquad (14.15)$$

Equations (14.14) and (14.15) are derived as follows.

Equation (12.25.x_E) is written, replacing $v_-(I_a)$ with $v_+(I_a)$ according to equations (12.16.I_a) and (13.1), as

$$n_E\dot{x}_E=4(x_{E(a)}-x_E)v_+(I_a).$$

Eliminating $(x_E-x_{E(a)})v_+(I_a)$ and $(x_{E(a)}-x_{H(a)})v_-(II)$ from the above equation, eq. (12.23.a) and (12.23.c), we have

$$N\dot{x}_E=1/2\cdot(x_H-x_{H(a)})v_+(I_b), \qquad (14.16)$$

where $N=n_E/4=n_H/2$ is the number of molecules of either reactant. The fraction, $x_{H(a)}$, is substituted from eq (13.15) into eq (14.16) with reference to eq (14.14.F) as

$$N\dot{x}_E=1/2\cdot(x_H-x_E)Fv_+(I_b). \tag{14.17}$$

We have, on the other hand, from equations (12.25.H) and (12.26.H)

$$N\dot{x}_H=(x_{H(a)}-x_H)v_-(I_b) \tag{14.18}$$

or, substituting $x_{H(a)}$ from eq (13.15) with reference to eq (14.14.F),

$$N\dot{x}_H=(x_E-x_H)Fv_-(I_b). \tag{14.19}$$

Equations (14.17) and (14.19) lead to the differential equation

$$-(\dot{x}_E-\dot{x}_H)/(x_E-x_H)=(F/N)(v_+(I_b)/2+v_-(I_b)),$$

or by integration to the equation

$$x_E-x_H=C\exp\left\{-\int(F/N)(v_+(I_b)/2+v_-(I_b))dt\right\},$$

where C is the integration constant as determined for the initial conditions, i.e., $x_E=0$ and $x_H=1$ at $t=0$, as

$$-1=C\exp\left\{-\int^0(F/N)(v_+(I_b)/2+v_-(I_b))dt\right\},$$

hence

$$x_H-x_E=\exp\left\{-\int_0^t(F/N)(v_+(I_b)/2+v_-(I_b))dt\right\}.$$

The value x_H-x_E thus obtained is substituted into eq (14.19) as

$$\dot{x}_H=-(F/N)v_-(I_b)\exp\left\{-\int_0^t(F/N)(v_+(I_b)/2+v_-(I_b))dt\right\}.$$

On integration we have

$$1-x_H=\int_0^t(F/N)v_-(I_b)\exp\left\{-\int_0^t(F/N)(v_+(I_b)/2+v_-(I_b))dt\right\}dt,$$

determining the integration constant by the initial condition that $x_H=1$ at $t=0$.

The last two equations are written, changing the variable of integration for an expedient calculation according to the identity,

$$\frac{dt}{N}=\frac{d\ln P/dt}{d\ln N/dt}\frac{dt}{N}=\frac{-d\ln P}{-dN/dt}=-\frac{d\ln P}{V_s}$$

based on the proportionality between P and N and the relation, $V_s=-dN/dt$, as

$$\dot{x}_H=-(F/N)v_-(I_b)\exp\left\{-\int_P^{P_0}(F/V_s)(v_+(I_b)/2+v_-(I_b))d\ln P\right\}$$

and as eq (14.15) above respectively; eq (14.14.x) is obtained by substituting $\dot{x}_H$ from the above equation into eq (14.18).

Figure 29 shows the relation between $1-u$ and x_H calculated by eqs (14.12), (14.14), and (14.15) for $P_{E,0}=P_{H,0}\doteqdot 10$ mm Hg, which roughly reproduces the experimental results of Twigg and Rideal [68] in figure 16 on the one hand and predicts [8, 9, 10, 137] the rapid run down of the curves at lower temperatures, on the other hand, which has been verified by Matsuzaki [115] as shown in figure 17.

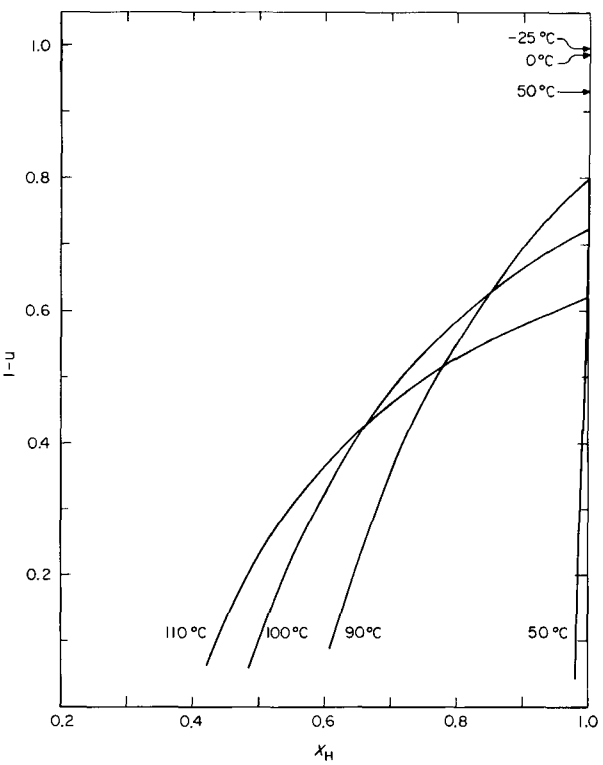

FIGURE 29. *Theoretical relation between* $1-u$ *and* x_H *in course of deuteration of light ethylene over nickel.*

$P_{E,0}=P_{H,0}=10$ mm Hg, $1-u$: nonequilibrium fraction, $u=[^1HD]/[^1HD]_{eq}$, x_H: atom fraction of deuterium in hydrogen gas.

The curves at 0 °C and −25 °C almost coincide with the vertical through $x_H=1$. The starting points of curves are $\lim_{x_H\to 1}(1-u)=1-x_{H(a)}$ according to eq (14.3.a) in the text, and are indicated with horizontal arrows where not clearly recognizable.

14.5. Changes in V_{A_n}'s With Temperature and Partial Pressures of the Reactants

We have from eq (13.5)

$$V_{A_0}:V_{A_1}:V_{A_2}:V_{A_{n>2}}=(1-x_{H(a)})^2$$

$$:2x_{H(a)}(1-x_{H(a)}):x_{H(a)}^2:0, \tag{14.20}$$

which shows that the relative magnitudes of V_{An} depend solely on $x_{H(a)}$. The fraction $x_{H(a)}$ is now uniquely defined, according to eq (13.7.a), by the ratio $v_+(I_b)/v_-(II)\equiv\kappa$ as

$$\frac{x_{H(a)}}{3(1-x_{H(a)})}=\frac{v_+(I_b)}{v_-(II)}\equiv\kappa, \tag{14.21.a}$$

while κ is expressed by eqs (12.16) as

$$\kappa=k(I_b)/\gamma(C_2H_5)k(II). \tag{14.21.b}$$

TABLE 28. *Theoretical values of initial evolution rates,* V_{E_n} *and* V_{A_n}, *of ethylenes-*$d_n \equiv E_n$ *and ethanes-*$d_n \equiv A_n$ *in the deuteration product of light ethylene over nickel*[a]

Temp. °C	Initial partial pressures mm Hg		κ	$x_{H(a)}$	V_{E_1}	$V_{E_{n>1}}$	V_{A_0}	V_{A_1}	V_{A_2}	$V_{A_{n>2}}$
	$P_{E,0}$	$P_{H,0}$								
90	10	20	0.121	0.264	69.9(76)	0	16.2(13)	11.7(9)	2.2(2)	0
90	10	100	0.287	0.463	63.8	0	10.4	18.0	7.8	0
90	10	600	0.819	0.711	56.0	0	4.2	20.0	25.0	0
120	10	20	0.486	0.593	86.1	0	2.3	6.7	4.9	0
150	10	20	2.13	0.865	93.5	0	0.1	1.5	4.9	0

[a] Parenthesized figures show experimental result of Turkevich et al. [117]

The function κ is determined by the values of $k(s)$ for the specified conditions according to eqs (13.14) and $\gamma(C_2H_5)$ derived from $k(s)$ by eq (12.19). The relative rates of eq (14.20) are thus calculated for different values of P_E, P_H and temperature as shown in table 28. The values at $P_E = 10$ mm Hg, $P_H = 20$ mm Hg and 90 °C closely reproduce the observations, shown in parentheses, by Turkevich et al. [117], under the same conditions.

We see from table 28 that the maximum yield of ethanes-d_n is shifted from A_0 through A_1 to A_2 by either increasing P_H/P_E or raising the temperature. These conclusions have been experimentally verified semiquantitatively by Miyahara and Narumi [114] as shown in tables 15 and 16.

The dominating factor κ is discussed in what follows. In case where I_b determines the rate, we have $\gamma(C_2H_5) = \gamma(H) = \sqrt{k(I_b)/k(III)}$ from eq (14.2) and (14.3), hence by eq (14.21.b)

$$\kappa = \sqrt{k(I_b)k(III)}/k(II) \qquad (14.22.a)$$

or, according to eqs (12.9) and (14.22.a),

$$\kappa \propto \sqrt{P_H/P_E}. \qquad (14.22.b)$$

Equations (14.21.a) and (14.22.b) indicate that $x_{H(a)}$ increases to shift the maximum yield of ethanes-d_n toward A_2 by increasing P_H/P_E in accordance with table 28.

When the rate is determined by step III, at higher temperatures, we have from eqs (14.21.b) and (14.6.a) $\kappa = k(I_b)/k(II)$. The factor κ increases with temperature, since $\Delta^{\ddagger}H(I_b) > \Delta^{\ddagger}H(II)$ as seen from eqs (13.3) and (13.12.II), so that at sufficiently high a temperature $x_{H(a)}$ tends to unity and the maximum yield shifts to A_2; there must, however, be a range of temperatures, as seen in figure 28, where step III determines the rate but $k(I_b) \ll k(II)$, hence A_0 predominate.

14.6. "Random Distribution" of Deuterium in Ethylene and Ethane in the Deuteration of Light Ethylene

Kemball [76] has observed the initial evolution rates of ethylenes-d_n and ethanes-d_n in deuteration of light ethylene over evaporated nickel film as referred to in 5.2.3. It is shown next that his results follow necessarily from the present theory for the associative mechanism.

The values of $\log_{10}(k(s)/\rho)$ are calculated for the specified experimental conditions, i.e., -100 °C, $P_E = 2.7$ mm Hg and $P_H = 8.1$ mm Hg by eqs (13.14) as

$$\log_{10}(k(I_b)/\rho) = \bar{1}6.9543,\ \log_{10}(k(II)/\rho) = \bar{2}.1552,$$

$$\log_{10}(k(III)/\rho) = \bar{1}.8604$$

from which $\gamma(C_2H_4)$, $\gamma(H)$ and $\gamma(C_2H_5)$ are evaluated by eq (12.19), ignoring $\gamma(C_2H_6)$ [31] and referring to eq (13.1), as

$$\gamma(C_2H_4) = 1, \qquad \gamma(H) = \gamma(C_2H_5) = 3.52 \times 10^{-8}.$$

The forward and backward rates, $v_+(s)$'s and $v_-(s)$'s, of steps s are calculated from the above values of $k(s)$'s and $\gamma(H)$ etc. according to eqs (12.16) as

$$v_+(II) = v_-(II) = 5.038 \times 10^{-11}\rho,\ v_+(I_b) = v_+(III)$$

$$= 9.002 \times 10^{-16}\rho,\ \ v_-(I_b) = 1.118 \times 10^{-29}\rho,$$

as given in the order of their magnitudes. Step II as well as step I_a, in accordance with 13.1, are thus occuring in both directions with rates far exceeding those of other steps, so that an isotopic exchange equilibrium is brought about among C_2H_4, $C_2H_4(a)$ and $H(a)$ according to the associative mechanism; the deuterium atoms in $C_2H_4(a)$ and H(a) are in

[31] $\gamma(C_2H_6) = 4.5 \times 10^{-30}$ was obtained as described in footnote 25 to 12.5 under the specified experimental conditions, equating the partial pressure P_A of ethane with P_E: $\gamma(C_2H_6)$ vanishes for $P_A = 0$ by definition.

consequence in random distribution, hence as well those in C_2H_6, which is composed of C_2H_4(a) and H(a) according to the mechanism. It follows that ethylenes-d_n are evolved with the relative rates given by eqs (12.31.E) and (12.32), and ethane-d_n by eq (12.33.c).

The above conclusion is compared with the experimental results of Kemball [76] in table 29 in terms of the percentages of ethylenes-d_n, $(100-36.7)\cdot\binom{4}{n}x_{H(a)}^n(1-x_{H(a)})^{4-n}\Big/\sum_{n=1}^{4}\binom{4}{n}x_{H(a)}^n(1-x_{H(a)})^{4-n}$, and of ethanes-$d_n$, $36.7\binom{6}{n}x_{H(a)}^n(1-x_{H(a)})^{6-n}$, among the total ethanes, and excellent agreement is found; 36.7 in the above expressions is the percentage of ethane in the entire hydrocarbons excluding light ethylene, and $\binom{4}{n}x_{H(a)}^n(1-x_{H(a)})^{4-n}\Big/\sum_{n=1}^{4}\binom{4}{n}x_{H(a)}^n(1-x_{H(a)})^{4-n}$ is the fraction of the amount of ethylene-d_n in the total amount of ethylene excluding light ethylene. The value of $x_{H(a)}$ was taken to be 0.222.

Wagner et al. [126], conducted an experiment, as referred to in 7.1.3, on the catalyzed deuteration of light ethylene in the presence of nickel on kieselguhr and observed the distribution of ethanes-d_n in the product of the catalyzed deuteration. They tried to account for the experimental results assuming a random distribution of deuterium in ethane, i.e., in accordance with eq (12.33.c); the maximum yield of ethanes-d_n was thus located at $n=2$ for -50 °C but at $n=3$ for 50 °C, whereas the maximum was observed at $n=2$ in both cases [126]. Wagner et al., calculated x_A to be 0.35 and 0.50 at -50 °C and 50 °C, respectively, as the fraction of the total number of deuterium atoms lost from hydrogen gas over the total number of hydrogen atoms in ethane evolved. Since no deuterium entered ethylene, this process of calculation would be correct, provided only that the supported catalyst did not exchange deuterium with reactants. Without relying on the assumption x_A is straightforwardly and necessarily given as $x_A=\sum_{n=1}^{6}nX_{A_n}/6$. The fraction, x_A, is thus calculated as 0.331 and 0.422, respectively, at -50 and 50 °C. With these values, the observed peaks at $n=2$ are reproduced at both temperatures.

TABLE 29. *Relative rates of evolution,* V_{E_n} *and* V_{A_n}, *of ethylenes-*$d_n \equiv E_n$ *and ethanes-*$d_n \equiv A_n$ *in the initial deuteration product of light ethylene over evaporated nickel film*

$P_{E,0}=2.7$ mm Hg, $P_{H,0}=8.1$ mm Hg, -100 °C

	$x_{H(a)}$	V_{E_1}	V_{E_2}	V_{E_3}	V_{E_4}	V_{A_0}	V_{A_1}	V_{A_2}	V_{A_3}	V_{A_4}	V_{A_5}	V_{A_6}
Obs. [76][a]		46.7	13.2	2.7	0.7	7.8	12.5	9.5	4.0	2.0	0.8	0.2
Calc.[b]	0.222	41.8	17.9	3.4	0.3	8.1	13.9	9.9	3.7	0.8	0.1	0.0

[a] Reproduced from table 12.

[b] The percentages are calculated according to eqs (12.31.E), (12.32) and (12.33.c), and the experimental result that the total ethanes amounts to 36.7 percent of the total hydrocarbons except E_0, as

$$V_{E_n}=(100-36.7)\binom{4}{n}x_{E(a)}^n(1-x_{E(a)})^{4-n}\Big/\sum_{n=1}^{4}\binom{4}{n}x_{E(a)}^n(1-x_{E(a)})^{4-n}$$

and $V_{A_n}=36.7\binom{6}{n}x_A^n(1-x_A)^{6-n}$, assuming $x_{E(a)}=x_A=x_{H(a)}$.

14.7. Isotopic Effect on Hydrogenation Rate

We have seen in section 6 that the hydrogenation rate of light ethylene with light hydrogen exceeds the deuteration rate of light ethylene under similar conditions by a factor of 2 to 3 at temperatures below the optimum; the factor decreases down to unity around the optimum temperature but exhibits a tendency to increase again at higher temperatures as seen in figures 19, 22, and 23 or in table 20. The experimental results are accounted for by the present theory as follows.

We see from figure 28 that step I_b governs the rate below the optimum, hence the appropriate isotopic difference in rate. Above the optimum, the rate is governed by step III, hence an isotopic difference in rate depending on $x_{H(a)}$, while the fraction $x_{E(a)}$ is kept equal to $x_E=0$ as inferred in 13.1. The fraction $x_{H(a)}$ for $x_E=0$ is now given according to eq (14.11), which is written for temperatures above the optimum according to eq (14.6.b) as $x_{H(a)}=\{3k(I_b)/(k(II)+3k(I_b))\}\,x_H$. There are two phases, one at lower and one at higher temperatures in the region of rate-determining step III, where $k(I_b)<k(II)$ and $k(I_b)>k(II)$, respectively, as seen from figure 28. The above equation states that at the lower temperatures in this region, $x_{H(a)}$ is small even in the case of deuteration, and affects little the rate-determining step III isotopically, whereas at higher temperatures $x_{H(a)}$ approaches $x_H=1$ and hence makes an isotopic difference through the rate-determining step III in accordance with experimental results.

15. Application of the Theory of Absolute Rates

Laidler [138] applied the theory of absolute rates to the rate-determining step III of the associative mechanism and to a step

$$2C_2H_5(a) \rightarrow C_2H_4(a) + C_2H_6, \qquad (15.1)$$

concluding that a tolerable agreement with experimental results is obtained in both cases. His procedure and conclusion are commented upon on the basis of the present theory.

15.1. Laidler expressed the concentration C_{s_2} of dual sites, i.e., the number of pairs of adjacent bare sites per unit area of catalyst as

$$C_{s_2} = sC_s^2/2L,$$

where C_s is the concentration of bare single sites, s the number of sites adjacent to a single site and L the concentration of single sites when the surface is completely bare. This equation is derived expressing the probability that one of adjacent single sites to a bare single site is also bare, by $1-\theta$, where θ is given by $2C_a/L$ in terms of the concentration C_a of adsorbed ethylene. This procedure would be exact, if $C_2H_4(a)$ were dissociated into adsorbed methylene radicals, $CH_2(a)$, and distributed over single sites independent of each other. Let 1 and 2 be the adjacent single sites, of which the above probability is in question. The probability that site 2 is occupied under the premised bareness of site 1 is $\left(\frac{s-1}{s}\right)\theta$, since the premised bareness of site 1 excludes one of s cases where site 2 is occupied by an $C_2H_4(a)$ lying across sites 1 and 2. The probability in question is thus $1-\frac{s-1}{s}\theta$ rather than $1-\theta$. The approximation associated with the revised expression is that the probability of the remaining $s-1$ cases of site 2 being occupied is assumed unchanged by premising the bareness of site 1 thus excluding the one of s cases. This correction changes, however, hardly the order of magnitude of the numerical factor in question below. We will remain, on that account, with Laidler's approximation in this regard.

15.2. A rather serious difficulty is associated with this treatment in the temperature change of rate. Laidler arrives at rate equations of step III of the associative mechanism and of step (15.1) respectively determining the rate, which contain numerical factors, AB^2 and A^2B^2, respectively, where

$$A = \frac{1+x-(1+2x)^{1/2}}{2x}, \qquad B = \frac{(1+2x)^{1/2}-1}{x}, \qquad (15.3.A), (15.3.B)$$

$$x = 2sKC_g \qquad (15.4)$$

and

$$K = C_a/C_gC_{s_2}; \qquad (15.5)$$

K is the equilibrium constant of adsorption and C_g is the concentration of ethylene in gas here given in terms of its partial pressure in mm Hg.

The procedure of Laidler to be questioned is this. He took arbitrarily the maxima of AB^2 and A^2B^2 with respect to x for the calculation of reaction rates. Since K varies with temperature, x will too, so that the numerical factors necessarily slip off the maximum at a particular temperature, when varying the temperature. The result is that the temperature change of the numerical factor is superimposed upon that due to the Boltzmann factor of a constant energy increment included in the rate equation.

This superimposition is illustrated with the observation of Farkas, Farkas, and Rideal [2] at 120 °C and $P_E = 12$ mm Hg with which Laidler compares his calculated rates. The last mentioned energy increment is taken to be 4.7 kcal/mole by Laidler. AB^2 and A^2B^2 have maximum values at around $x=2$ according to eqs (15.3). These maxima are taken to be numerical factors in calculating the rates in the respective case. The K value for $x=2$ and $s=4$ is according to eq (15.4)

$$K = 1/(4\times 12)\ (\text{mm Hg})^{-1}.$$

K can be written, on the other hand, in terms of the heat of adsorption, ϵ_E, and of the partition function of ethylene, $Q_{E,0}$, as done by Laidler with the adsorption of hydrogen, as

$$K = Q_{E,0}^{-1}\exp(\epsilon_E/RT). \qquad (15.6)$$

We have from the above equations and the numerical value of $Q_{E,0}$ of eq (12.5.E)

$$\epsilon_E = 23.2 \text{ kcal/mole}. \qquad (15.7)$$

It follows from eqs (15.6) and (15.7) that K and in consequence x decrease according to eq (15.4) monotonously with increase of temperature.

It is readily deduced from eqs (15.3) that extreme values of the numerical factors are

$$AB^2 = x^{-1},\ A^2B^2 = (2x)^{-1} \quad \text{for } x \gg 1 \qquad (15.8.a)$$

and

$$AB^2 = x/4,\ A^2B^2 = x^2/16 \quad \text{for } x \ll 1. \qquad (15.8.b)$$

We have from eqs (15.4), (15.6), (15.7), and (15.8) that

$$RT^2\partial \ln (AB^2)/\partial T = RT^2\partial \ln (A^2B^2)/\partial T = 23.2 \text{ kcal/mole}$$

in the extreme of low temperature and

$$RT^2\partial \ln (AB^2)/\partial T = -23.2 \text{ kcal/mole},$$

$$RT^2\partial \ln (A^2B^2)/\partial T = -46.4 \text{ kcal/mole}$$

in the extreme of high temperature. These amazing values are inevitably superimposed upon the constant energy increment mentioned above. The activation heat thus decreases from the low extreme of temperature to the high extreme by 46.4 kcal/mole in case of the rate determined by step III and by 69.6 kcal/mole in case of the rate determined by step (15.1).

Such a superimposition occurs, however, over not very wide a range of temperature; we have for example

$$RT^2\partial \ln (AB^2)/\partial T = 16.5 \text{ kcal/mole},$$

$$RT^2\partial \ln (A^2B^2)/\partial T = 13.1 \text{ kcal/mole}$$

at 90 °C and

$$RT^2\partial \ln (AB^2)/\partial T = -14.9 \text{ kcal/mole},$$

$$RT^2\partial \ln (A^2B^2)/\partial T = -33.9 \text{ kcal/mole}$$

at 150 °C as calculated by eqs (15.3), (15.4), (15.6), and (15.7) assuming $x=2$ at 120 °C. This amounts to saying that nearly 70 percent of the overall decreases of activation heat mentioned above are got through within the temperature range of ± 30 °C, which is far from being true.

15.3. One might try to elude the extravagant superimposition inherent to the Laidler's procedure by localizing the phase of the numerical factor either to that of (15.8.a) or (15.8.b). In the former case we have according to eqs (15.4) and (15.6)

$$AB^2 = \frac{Q_{E,0}}{2sC_g} \exp(-\epsilon_E/RT),$$

$$A^2B^2 = \frac{Q_{E,0}}{4sC_g} \exp(-\epsilon_E/RT).$$

Incorporating the exponential factor in the above equation in that of the activation heat as did by Laidler with the adsorption heat of hydrogen, the numerical factor is now $(1/2s)(Q_{E,0}/C_g)$ or $(1/4s)(Q_{E,0}/C_g)$, which amounts to 4.1×10^{12} or 21×10^{12} respectively for $s=4$ and $P_E=12$ mm Hg. In the latter case of eq (15.8.b), the numerical factor is

$$AB^2 = \frac{sC_g}{2Q_{E,0}} = 6.1\times10^{-14} \qquad (15.9.a),$$

or

$$A^2B^2 = \left(\frac{sC_g}{2Q_{E,0}}\right)^2 = 3.7\times10^{-27} \qquad (15.9.b)$$

respectively for step III or (15.1) determining the rate in place of the maximum value, 0.074 or 0.0156 used by Laidler. The agreement with experimental results is thus quite out of question.

One might see that the numerical factors are secured in the order of magnitude of unity by confining them to the intermediate phase, say to their maxima, where we encounter the difficulty described in 15.3.

15.4. The rate equation in case of step III determining the rate for $x \ll 1$ is given[32] according to eq (15.9.a) as

$$v = (kT/h)N_{\ddagger}(C_g/Q_{E,0})(C_{g'}/Q_{H,0}) \cdot \exp(-\Delta^{\ddagger}H(r)/RT), \qquad (15.10)$$

where $N_{\ddagger}$ represents $(s/2)L$ i.e., the concentration of dual sites in case of a practically bare surface, $Q_{E,0}$ or $Q_{H,0}$ the partition function of ethylene or hydrogen and $\Delta^{\ddagger}H(r)$ the activation heat. The difficulty, in particular, with eq (15.10) is that v is smaller than that observed by a factor ca. 10^{13} provided that $\Delta^{\ddagger}H(r)$ is fixed at 4.7 kcal/mole as assigned by Laidler. This difficulty is got over by excluding ethylene from $I(r)_r$ of eq (12.13), which reduces the rate remarkably by decreasing $\Delta^{\ddagger}S(r)$ as seen from eqs (12.14) and (12.15). We are thus just in line with the association mechanism, in which the rate is determined by the dissociative adsorption of hydrogen molecules, i.e., by step I_b, under the activation heat of the above magnitude.

The $\Delta^{\ddagger}S(III)$ is lower than $\Delta^{\ddagger}S(I_b)$ on account of an ethylene molecule comprised in $I(III)_r$ in excess over $I(I_b)_r$. Since $k(III)$ must, however, be greater than $k(I_b)$ in the temperature range, where I_b governs the rate according to 12.5.1.(iii), step III should have an activation heat sufficiently lower than step I_b in accordance with eq (12.14). Along with rise of temperature, however, the effect of the lower activation heat is reduced and sooner or later $k(III)$ becomes lower than $k(I_b)$ so that III governs the rate in place of I_b at higher temperature according to 12.5.1.(iii), hence the switchover in the rate-determining step described in 14.1.

[32] We have an extra factor s^2 by a direct substitution of AB^2 from eq (15.9.a) into eq (91) of the article of Laidler [138]. He identified the partition functions, $f_{a'a''}$ and $f_{aa'}$, in the last-mentioned equation of him respectively with unity, which is not correct, since the appropriate states are respectively s-fold degenerated. Equation (15.10) is obtained without the extra factor by identifying partition functions $f_{a'a''}$ and $f_{aa'}$ respectively with s instead on this account. Detailed account will not be given on this point since the factor in question does not affect the conclusion.

16. Concluding Remark

As developed in the foregoing sections, the present theory based on scheme (9.5) accounts systematically for the experimental results on the catalyzed hydrogenation of ethylene in the presence of metallic catalysts especially nickel. But it may be mentioned in concluding this review that the present theory accounts for the experimental results of other olefines as well, e.g., the optimum temperatures observed in the catalyzed hydrogenation of propylene [139, 140] and butylene [141], the distribution of deuterium in their deuteration products [139], the migration of double bonds [141] etc.

17. References

[1] P. Sabatier and J. B. Senderens, Compt. rend. **124,** 1358 (1897).
[2] A. Farkas, L. Farkas and E. K. Rideal, Proc. Roy. Soc. **A146,** 630 (1934).
[3] A. Farkas and H. W. Melville, Experimental Methods in Gas Reactions, p. 190 (Macmillan & Co. 1939).
[4] D. D. Eley and J. L. Tuck, Trans. Faraday Soc. **32,** 1425 (1936).
[5] E. S. Gilfillan and M. Ploanyi, Z. Phisik. Chem. **A166,** 254 (1933).
[6] O. Beeck, Rev. Mod. Phys. **17,** 61 (1945).
[7] J. Horiuti and M. Polanyi, Trans. Faraday Soc. **30,** 1164 (1934).
[8] J. Horiuti, Actes du Deuxieme Congres International du Catalyse, Paris 1960, **1,** 1191 (1961).
[9] J. Horiuti, "Shokubai" (Catalyst) **2,** 1 (1947).
[10] J. Horiuti, J. Res. Inst. Catalysis, Hokkaido Univ. **6,** 250 (1958).
[11] J. Horiuti, J. Res. Inst. Catalysis, Hokkaido Univ. **7,** 163 (1959).
[12] O. Toyama, Rev. Phys. Chem. Japan **9,** 123 (1935).
[13] G. I. Jenkins and E. K. Rideal, J. Chem. Soc. 2490, 2496 (1955).
[14] O. Beeck, Discuss. Faraday Soc. **8,** 118 (1950).
[15] S. J. Stephens, J. Phys. Chem. **63,** 512 (1959).
[16] B. M. W. Trapnell, Trans. Faraday Soc. **48,** 160 (1952).
[17] R. W. Roberts, J. Phys. Chem. **67,** 2035 (1963).
[18] G. C. Bond, Catalysis by Metals, p. 230 (Acad. Press Inc. London and New York 1962).
[19] D. W. Mckee, J. Amer. Chem. Soc. **84,** 1109 (1962).
[20] S. J. Thomson and J. L. Wishlade, Trans. Faraday Soc. **58,** 1170 (1962).
[21] D. Cormack, S. J. Thomson and G. Webb, J. Catalysis **5,** 224 (1 66).
[22] K. Miyahara, J. Res. Inst. Catalysis, Hokkaido Univ. **11,** 1 (1963).
[23] G. K. T. Conn and G. H. Twigg, Proc. Roy. Soc. **A171,** 70 (1939).
[24] T. B. Flanagan and B. S. Rabinovitch, J. Phys. Chem. **60,** 724, 730 (1956).
[25] K. C. Campbell and S. J. Thomson, Trans. Faraday Soc. **55,** 306, 985 (1959).
[26] K. Miyahara, J. Res. Inst. Catalysis, Hokkaido Univ. **14,** 134 (1966).
[27] J. G. Foss and H. Eyring, J. Phys. Chem. **62,** 103 (1958).
[28] K. Hirota and S. Teratani, Sci. Papers Inst. Phys. Chem. Res. Tokyo, Japan **57,** 206 (1963); "Shokubai" (Catalyst) **7,** 286 (1965).
[29] E. Crawford, M. W. Roberts, and C. Kemball, Trans. Faraday Soc. **58,** 1761 (1962).
[30] K. C. Campbell and D. T. Duthie, Trans. Faraday Soc. **61,** 558 (1965).
[31] K. Miyahara and K. Harada, to be published.
[32] R. E. Cunningham and A. T. Gwathmey, Advances in Catalysis **9,** 25 (1957).
[33] H. E. Farnsworth and R. F. Woodcock, Advances in Catalysis **9,** 123 (1957).
[34] S. Z. Roginskii, Theoretical Foundations of Isotopic Methods for Study of Chemical Reactions (Akad. Nauk Press Moscow 1959).
[35] G. C. A. Schuit, Discuss. Faraday Soc. **8,** 126, 205 (1950).
[36] L. Pauling, Proc. Roy. Soc. **A196,** 343 (1949).
[37] G. H. Twigg and E. K. Rideal, Trans. Faraday Soc. **36,** 533 (1940).
[38] J. Horiuti, K. Miyahara, and I. Toyoshima, Trans. Symposium Physical Chemistry of Processes on Solid Surfaces, Libreria Cientifica Mendinaceli Madride, 1965, p. 143; J. Res. Inst. Catalysis, Hokkaido Univ. **14,** 59 (1966).
[39] T. Toya, J. Res. Inst. Catalysis, Hokkaido Univ. **6,** 308 (1958); **8,** 209 (1960).
[40] Y. Mizushima, J. Phys. Soc. Japan **15,** 1614 (1960; R. Suhrmann et al., Z. Physik. Chem. (N. F.) **17,** 350 (1958); **12,** 128 (1957); **20,** 332 (1959).
[41] J. C. P. Mignolet, Bull. Soc. Chim. Belg. **64,** 126 (1955).
[42] F. C. Tompkins et al., Trans. Faraday Soc. **52,** 1609 (1956); **53,** 218 (1957).
[43] T. Toya, J. Res. Inst. Catalysis, Hokkaido Univ. **6,** 308 (1958); J. Horiuti and T. Toya, Chapter "Chemisorbed Hydrogen" in "Solid State Surface Science" (Marcel Bekker Inc. New York 1966); cf. J. Happel, Chem. & Eng. News **80,** May 30 (1966).
[44] R. Gomer, R. Wortman, and R. Lundy, J. Chem. Phys. **26,** 1147 (1957).
[45] T. Takeuchi and T. Asano, Z. Physik. Chem. (N. F.) **36,** 118 (1962).
[46] D. A. Dowden, J. Chem. Soc. 242 (1950); Ind. Eng. Chem. **44,** 97 (1951).
[47] G. Rienäcker and E. A. Bommer, Z. anorg. allgem. Chem. **242,** 302 (1939).
[48] G. Rienäcker, E. Müller, and R. Burmann, Z. anorg. allgem. Chem. **251,** 55 (1943).
[49] G. Rienäcker and E. A. Bommer, Z. anorg. allgem. Chem. **236,** 263 (1938).
[50] G. Rienäcker and B. Sarry, Z. anorg. allgem. Chem. **257,** 41 (1948).
[51] G. Rienäcker and G. Vormum, Z. anorg. allgem. Chem. **283,** 287 (1956).
[52] M. Kowaka, J. Japan Inst. Metals **23,** 655 (1959).
[53] R. J. Best and W. W. Russell, J. Amer. Chem. Soc. **76,** 838 (1954).
[54] T. Yamashina and H. E. Farnsworth, Shokubai (Catalyst) **4,** 312 (1962).
[55] J. Tuul and H. E. Farnsworth, J. Amer. Chem. Soc. **83,** 2247 (1961).
[56] R. J. Kokes, H. Tobin, Jr., and P. H. Emmett, J. Amer. Chem. Soc. **77,** 5800 (1955).
[57] W. K. Hall and J. A. Hassel, J. Phys. Chem. **67,** 636 (1963).
[58] W. K. Hall and P. H. Emmett, J. Phys. Chem. **63,** 1102 (1959).
[59] W. K. Hall, F. E. Lutinski and J. A. Hassel, Trans. Faraday Soc. **60,** 1823 (1964).
[60] G. C. Bond and D. E. Webster, Platinum Metals Rev. **9,** 12 (1965).

[61] K. Miyahara, S. Teratani and A. Tsumura, J. Res. Inst. Catalysis, Hokkaido Univ. **12,** 98 (1965).
[62] R. N. Pease, J. Amer. Chem. Soc. **54,** 1876 (1932).
[63] E. K. Rideal, J. Chem. Soc. **121,** 309 (1922).
[64] H. zur.Strassen, Z. Physik. Chem. **A169,** 81 (1934).
[65] J. Tuul and H. E. Farnsworth, J. Amer. Chem. Soc. **83,** 2253 (1961).
[66] I. Matsuzaki, A. Tada and T. Nakajima, Shokubai (Catalyst) **8,** 5 (1966).
[67] T. Tucholski and E. K. Rideal, J. Chem. Soc. 1701 (1935).
[68] G. H. Twigg and E. K. Rideal, Proc. Roy. Soc. **A171,** 55 (1939).
[69] G. H. Twigg, Trans. Faraday Soc. **35,** 934 (1939).
[70] M. Masuda, J. Res. Inst. Catalysis, Hokkaido Univ. **12,** 67 (1964).
[71] O. Toyama, Rev. Phys. Chem. Japan **12,** 115 (1938).
[72] H. W. Melville, J. Chem. Soc. 797 (1934).
[73] G.-M. Schwab, W. Schmaltz and H. Noller, Z. Physik Chem. (N. F.) **29,** 356 (1961).
[74] O. Toyama, Rev. Phys. Chem. Japan **11,** 353 (1937).
[75] G.-M. Schwab and H. Zorn, Z. Physik. Chem. **B32,** 169 (1936).
[76] C. Kemball, J. Chem. Soc. **146,** 735 (1956).
[77] K. J. Laidler and R. E. Townshend, Trans. Faraday Soc. **57,** 1590 (1961).
[78] M. K. Gharpurey and P. H. Emmett, J. Phys. Chem. **65,** 1182 (1961).
[79] E. G. Alexander and W. W. Russell, J. Catalysis **4,** 184 (1965).
[80] S. Sato and K. Miyahara, J. Res. Inst. Catalysis, Hokkaido Univ. **13,** 10 (1965).
[81] G. C. A. Schuit and L. L. van Reijen, Advances in Catalysis **10,** 298 (1958).
[82] A. C. Pauls, E. W. Comings and J. M. Smith, Am. Ind. chem. Eng. J. **5,** 453 (1959).
[83] L. A. Wanninger and J. M. Smith, Chem. Weekblad **56,** 273 (1960).
[84] A. Y. Rozovskii, V. V. Shchekin, and E. G. Pokrovskaya, Kinetika i Kataliz **1,** 464 (1960).
[85] A. Farkas and L. Farkas, J. Amer. Chem. Soc. **60,** 22 (1938).
[86] G. C. Bond, Quart. Rev. **8,** 279 (1954).
[87] V. B. Kazanskii and V. P. Strunin, Kinetika i Kataliz **1,** 553 (1960).
[88] G. C. Bond, Trans. Faraday Soc. **52,** 1235 (1956).
[89] G. C. Bond, J. J. Phillipson, P. B. Wells and J. M. Winterbottom, Trans. Faraday Soc. **60,** 1847 (1964).
[90] J. H. Sinfelt, J. Phys. Chem. **68,** 856 (1964).
[91] L. O. Apel'baum and M. I. Temkin, Zh. Fiz. Khim. **35,** 2060 (1961).
[92] M. Kowaka and M. J. Joncich, Mem. Inst. Sci. Res., Osaka Univ. **16,** 107 (1959).
[93] T. Yamaguchi, S. Teranishi and K. Tarama, J. Japan Chem. Soc. **78,** 759 (1957).
[94] G. C. Bond, J. J. Phillipson, P. B. Wells and J. M. Winterbottom, Trans. Faraday Soc. **62,** 443 (1966).
[95] G. C. Bond, G. Webb and P. B. Wells, Trans. Faraday Soc. **61,** 999 (1965).
[96] U. Grassi, Nuovo Cimento **11,** 147 (1916).
[97] R. N. Pease, J. Amer. Chem. Soc. **45,** 1196 (1923).
[98] R. N. Pease, J. Amer. Chem. Soc. **45,** 2235 (1923).
[99] R. Wynkoop and R. H. Wilhelm, Chem. Eng. Progress **46,** 300 (1950).
[100] R. N. Pease and C. A. Harris, J. Amer. Chem. Soc. **49,** 2503 (1927).
[101] J. P. Leinroth and T. K. Sherwood, Am. Ind. chem. Eng. J. **10,** 524 (1964).
[102] Y. Amenomiya, Shokubai (Catalyst) **12,** 39 (1956).
[103] G. Joris, H. S. Taylor and J. C. Jungers, J. Amer. Chem. Soc. **60,** 1982 (1938).
[104] R. Klar, Z. Physik. Chem. **B27,** 319 (1934).
[105] R. C. Hansford and P. H. Emmett, J. Amer. Chem. Soc. **60,** 1185 (1938).
[106] P. H. Emmett and J. B. Gray, J. Amer. Chem. Soc. **66,** 1338 (1944).
[107] R. N. Pease and L. Stewart, J. Amer. Chem. Soc. **47,** 1235 (1925).
[108] S. E. Voltz, J. Phys. Chem. **61,** 756 (1957).
[109] K. Tarama, I. Teranishi, M. Kumada, and M. Yamaguchi, Shokubai (Catalyst) **2,** 203 (1960).
[110] K. Tarama, S. Wada, M. Yamaguchi and Y. Hiraki, Shokubai (Catalyst) **8,** 58 (1966).
[111] O. A. Hougen and K. M. Watson, Chemical Process Principles, p. 942 (John Wiley & Sons Inc. New York, N.Y., 1950).
[112] O. A. Hougen and K. M. Watson, ibid., p. 958.
[113] G.-M. Schwab, Discuss. Faraday Soc. **8,** 79 (1950).
[114] K. Miyahara and H. Narumi, J. Res. Inst. Catalysis, Hokkaido Univ. **13,** 20 (1965).
[115] I. Matsuzaki, J. Res. Inst. Catalysis, Hokkaido Univ. **7,** 210 (1959).
[116] G. H. Twigg, Discuss. Faraday Soc. **8,** 152 (1950).
[117] J. Turkevich, F. Bonner, D. O. Schissler, and P. Irsa, Discuss. Faraday Soc. **8,** 352 (1950); J. Turkevich, D. O. Schissler, and P. Irsa, J. Phys. Colloid. Chem. **55,** 1078 (1951).
[118] K. Miyahara, J. Res. Inst. Catalysis, Hokkaido Univ. **14,** 144 (1966).
[119] V. B. Kazanskii and V. V. Voevodskii, Dokl. Akad. Nauk **111,** 125 (1956).
[120] I. Matsuzaki and T. Nakajima, J. Res. Inst. Catalysis, Hokkaido Univ. **13,** 44 (1965).
[121] M. Kowaka, J. Japan Chem. Soc. **81,** 1366 (1960).
[122] K. H. Geib, Handbuch der Katalyse **6** (3), 46 (1943).
[123] R. N. Pease and A. Wheeler, J. Amer. Chem. Soc. **57,** 1144 (1935); A. Wheeler and R. N. Pease, J. Amer. Chem. Soc. **58,** 1665 (1936).
[124] T. Titani and M. Koizumi, Shokubai (Catalyst) **3,** 105 (1948).
[125] J. E. Douglas and B. S. Rabinovitch, J. Amer. Chem. Soc. **74,** 2486 (1952).
[126] J. N. Wilson, J. W. Otvos, D. P. Stevenson, and C. D. Wagner, Ind. Eng. Chem. **45,** 1180 (1953); J. Chem. Phys. **20,** 338, 1331 (1952).
[127] J. Horiuti, Chemical Kinetics Iwanami Series, Physics X.C.2,(1940); J. Res. Inst. Catalysis, Hokkaido Univ. **5,** 1 (1957); J. Catalysis **1,** 199 (1962).
[128] K. F. Bonhoeffer and A. Farkas, Z. Physik. Chem. **B12,** 231 (1931).
[129] A. F. Benton and T. A. White, J. Amer. Chem. Soc. **50,** 2325 (1930).
[130] W. A. Pliskin and R. P. Eischens, J. Chem. Phys. **24,** 482 (1956); Advances in Catalysis **10,** 1 (1958); Z. Elektrochem. **60,** 872 (1956).
[131] N. N. Semenov, Some Problems of Chemical Kinetics and Reactivity (Akad. Nauk Press Moscow 1958), sec. 7, ch. 6.
[132] J. J. Rooney, J. Catalysis **2,** 53 (1963); J. L. Garnett and W. A. Sollich-Baumgartner, J. Catalysis **5,** 244 (1966); G. C. Bond, Platinum Metals Rev. **8,** 92 (1964); G. Webbs and P. B. Wells, Trans. Faraday Soc. **61,** 1232 (1965).
[133] G.-M. Schwab, Z. Physik. Chem **A171,** 421 (1934).
[134] J. Horiuti and T. Nakamura, Advances in Catalysis **17,** (1966) in press.
[135] J. Horiuti, J. Res. Inst. Catalysis, Hokkaido Univ. **1,** 8 (1948–51).
[136] R. H. Fowler and E. A. Guggenheim, Statistical Thermodynamics, p. 66 (Cambridge Univ. Press 1939).
[137] J. Horiuti and I. Matsuzaki, J. Res. Inst. Catalysis, Hokkaido Univ. **7,** 187 (1959).
[138] K. J. Laidler, Discuss. Faraday Soc. **8,** 47 (1950); Catalysis edited by Emmett (Reinhold Publ. Corp. New York) **1,** 219 (1954).
[139] G. C. Bond and J. Turkevich, Trans. Faraday Soc. **49,** 281 (1953).
[140] K. Miyahara and H. Narumi, to be published.
[141] Y. Amenomiya, J. Res. Inst. Catalysis, Hokkaido Univ. **9,** 1 (1961).

U.S. GOVERNMENT PRINTING OFFICE : 1968 OL—273-052